ORTA DOĞU TEKNİK ÜNİVERSİTESİ
FEN BİLİMLERİ ENSTİTÜSÜ MÜDÜRLÜĞÜ

TEZ ŞABLONU ONAY FORMU
THESIS TEMPLATE CONFIRMATION FORM

1. Şablonda verilen yerleşim ve boşluklar değiştirilmemelidir.
2. **Jüri tarihi** Başlık Sayfası, İmza Sayfası, Abstract ve Öz'de ilgili yerlere yazılmalıdır.
3. İmza sayfasında jüri üyelerinin unvanları doğru olarak yazılmalıdır. Tüm imzalar **mavi pilot kalemle** atılmalıdır.
4. **Disiplinlerarası** programlarda görevlendirilen öğretim üyeleri için jüri üyeleri kısmında tam zamanlı olarak çalıştıkları anabilim dalı başkanlığının ismi yazılmalıdır. Örneğin: bir öğretim üyesi Biyoteknoloji programında görev yapıyor ve biyoloji bölümünde tam zamanlı çalışıyorsa, İmza sayfasına biyoloji bölümü yazılmalıdır. İstisnai olarak, disiplinler arası program başkanı ve tez danışmanı için disiplinlerarası program adı yazılmalıdır.
5. Tezin **son sayfasının sayfa** numarası Abstract ve Öz'de ilgili yerlere yazılmalıdır.
6. Bütün chapterlar, referanslar, ekler ve CV sağ sayfada başlamalıdır. Bunun için **kesmeler** kullanılmıştır. **Kesmelerin kayması** fazladan boş sayfaların oluşmasına sebep olabilir. Bu gibi durumlarda paragraf (¶) işaretine tıklayarak kesmeleri görünür hale getirin ve yerlerini **kontrol edin**.
7. Figürler ve tablolar kenar boşluklarına taşmamalıdır.
8. Şablonda yorum olarak eklenen uyarılar dikkatle okunmalı ve uygulanmalıdır.
9. Tez yazdırılmadan önce PDF olarak kaydedilmelidir. Şablonda yorum olarak eklenen uyarılar PDF dokümanında yer almamalıdır.
10. Tez taslaklarının kontrol işlemleri tamamlandığında, bu durum öğrencilere METU uzantılı öğrenci e-posta adresleri aracılığıyla duyurulacaktır.
11. Tez yazım süreci ile ilgili herhangi bir sıkıntı yaşarsanız, Sıkça Sorulan Sorular (SSS) sayfamızı ziyaret ederek yaşadığınız sıkıntıyla ilgili bir çözüm bulabilirsiniz.

1. Do not change the spacing and placement in the template.
2. Write **defense date** to the related places given on Title page, Approval page, Abstract and Öz.
3. Write the titles of the examining committee members correctly on Approval Page. **Blue ink** must be used for all signatures.
4. For faculty members working in **interdisciplinary programs**, the name of the department that they work full-time should be written on the Approval page. For example, if a faculty member staffs in the biotechnology program and works full-time in the biology department, the department of biology should be written on the approval page. Exceptionally, for the interdisciplinary program chair and your thesis supervisor, the interdisciplinary program name should be written.
5. Write **the page number of the last page** in the related places given on Abstract and Öz pages.
6. All chapters, references, appendices and CV must be started on the right page. **Section Breaks** were used for this. **Change in the placement** of section breaks can result in extra blank pages. In such cases, make the section breaks visible by clicking paragraph (¶) mark and **check their position.**
7. All figures and tables must be given inside the page. Nothing must appear in the margins.
8. All the warnings given on the comments section through the thesis template must be read and applied.
9. Save your thesis as pdf and Disable all the comments before taking the printout.
10. This will be announced to the students via their METU students e-mail addresses when the control of the thesis drafts has been completed.
11. If you have any problems with the thesis writing process, you may visit our Frequently Asked Questions (FAQ) page and find a solution to your problem.

☒ **Yukarıda bulunan tüm maddeleri okudum, anladım ve kabul ediyorum. / I have read, understand and accept all of the items above.**

Name : Utku
Surname : Deniz
E-Mail : deniz.utku@metu.edu.tr
Date : 03.06.2024
Signature : _____

GENOME-WIDE ASSOCIATION STUDY IN DURUM WHEAT UNDER IRON DEFICIENCY

A THESIS SUBMITTED TO
THE GRADUATE SCHOOL OF NATURAL AND APPLIED SCIENCES
OF
MIDDLE EAST TECHNICAL UNIVERSITY

BY

UTKU DENİZ

IN PARTIAL FULFILLMENT OF THE REQUIREMENTS
FOR
THE DEGREE OF MASTER OF SCIENCE
IN
MOLECULAR BIOLOGY AND GENETICS

JUNE 2024

Approval of the thesis:

GENOME-WIDE ASSOCIATION STUDY IN DURUM WHEAT UNDER IRON DEFICIENCY

submitted by **UTKU DENİZ** in partial fulfillment of the requirements for the degree of **Master of Science in Molecular Biology and Genetics, Middle East Technical University** by,

Prof. Dr. Naci Emre Altun
Dean, **Graduate School of Natural and Applied Sciences** _____

Prof. Dr. Mesut Muyan
Head of the Department, **Biological Sciences, METU** _____

Assist. Prof. Dr. Emre Aksoy
Supervisor, **Biological Sciences, METU** _____

Examining Committee Members:

Prof. Dr. Sertaç Önde
Biological Sciences, METU _____

Assist. Prof. Dr. Emre Aksoy
Biological Sciences, METU _____

Assoc. Prof. Dr. Ceyhun Kayıhan
Molecular Biology and Genetics, Başkent University _____

Date: 03.06.2024

I hereby declare that all information in this document has been obtained and presented in accordance with academic rules and ethical conduct. I also declare that, as required by these rules and conduct, I have fully cited and referenced all material and results that are not original to this work.

Name Last Name : Utku Deniz

Signature :

ABSTRACT

GENOME-WIDE ASSOCIATION STUDY IN DURUM WHEAT UNDER IRON DEFICIENCY

Deniz, Utku
Master of Science, Molecular Biology and Genetics
Supervisor: Assist. Prof. Dr. Emre Aksoy

June 2024, 98 pages

Durum wheat faces significant challenges due to iron deficiency, which hampers its growth and reduces yield. To develop varieties tolerant to iron deficiency, it is essential to first examine the traits related to iron deficiency in a plant panel with broad variation. Therefore, this study investigates iron deficiency tolerance in 123 durum wheat genotypes and aims to identify genetic markers associated with this trait through genome-wide association mapping. The genotypes were subjected to iron deficiency for 21 days in a controlled greenhouse and analyzed for various biochemical and physiological traits. In general, chlorophyll contents and leaf and root biomasses significantly decreased while FCR enzyme activity and rhizosphere acidification significantly increased. These findings are consistent with known iron deficiency responses in plants and indicate that durum wheat utilizes a combination of two different iron uptake strategies. Notably, strong correlations were observed between FCR activity and rhizosphere acidification, supporting non-gramineous iron uptake strategy utilization. The genome-wide association study identified seven significant markers associated with observed traits. A total of 63 candidate genes were identified, and their Arabidopsis orthologs were investigated for their gene ontologies. The study also revealed significant differences in iron deficiency

responses between Turkish cultivars and landraces, with landraces showing greater tolerance. Candidate genotypes and genes for iron deficiency tolerance were identified, providing valuable resources for breeding programs to enhance iron deficiency tolerance. These findings contribute to understanding the genetic and physiological mechanisms of iron deficiency tolerance in durum wheat and offer insights for developing more resilient wheat varieties to optimize agricultural productivity.

Keywords: GWAS, Iron deficiency chlorosis, Biochemical responses, Physiological responses, *Triticum durum*

ÖZ

DEMİR EKSİKLİĞİNDE MAKARNALIK BUĞDAYDA GENOM ÇAPINDA İLİŞKİLENDİRME ÇALIŞMASI

Deniz, Utku
Yüksek Lisans, Moleküler Biyoloji ve Genetik
Tez Yöneticisi: Dr. Öğr. Üyesi Emre Aksoy

Haziran 2024, 98 sayfa

Makarnalık buğday, büyümesini engelleyen ve verimi düşüren demir eksikliği nedeniyle önemli zorluklarla karşı karşıyadır. Demir eksikliğine dayanıklı çeşitler geliştirebilmek için öncelikle geniş varyasyona sahip bir bitki panelinin demir eksikliğiyle ilgili özelliklerinin incelenmesi gerekmektedir. Bu nedenle, bu çalışma, 123 makarnalık buğday genotipinde demir eksikliği toleransını araştırmakta ve bu özellik ile ilişkili genetik belirteçleri genom çapında ilişkilendirme haritalaması (GWAS) yoluyla tanımlamayı amaçlamaktadır. Genotipler kontrollü bir sera ortamında 21 gün boyunca demir eksikliğine maruz bırakılmış ve çeşitli biyokimyasal ve fizyolojik özellikler analiz edilmiştir. Genel olarak, klorofil içeriği ve kök ile yaprak biyokütleleri önemli ölçüde azalırken, FCR enzim aktivitesi ve rizosfer asitleşmesi önemli ölçüde artmıştır. Bu bulgular, bitkilerde bilinen demir eksikliği tepkileriyle tutarlıdır ve makarnalık buğdayın iki farklı demir alım stratejisini birleştirerek kullandığını göstermektedir. Özellikle, FCR aktivitesi ile rizosfer asitleşmesi arasında güçlü korelasyonlar gözlenmiş ve bu da Gramine olmayan demir alım stratejisinin kullanımını desteklemektedir. Genom çapında ilişkilendirme çalışmasıyla gözlemlenen özelliklerle ilişkili yedi önemli belirteç tanımlanmıştır. Toplamda 63 aday gen belirlenmiş ve bu genlerin Arabidopsis

ortologları için gen ontolojileri incelenmiştir. Çalışma ayrıca Türk çeşitleri ile yerel çeşitler arasında demir eksikliği tepkilerinde önemli farklılıklar olduğunu ortaya koymuş ve yerel çeşitlerin daha yüksek toleransa sahip olduğunu göstermiştir. Demir eksikliği toleransı için aday genotipler ve genler belirlenmiş ve ıslah programları için değerli kaynaklar sunulmuştur. Bu bulgular, makarnalık buğdayda demir eksikliği toleransının genetik ve fizyolojik mekanizmalarının anlaşılmasına katkıda bulunmakta ve tarımsal verimi optimize etmek için daha dayanıklı buğday çeşitlerinin geliştirilmesine yönelik içgörüler sunmaktadır.

Anahtar Kelimeler: GWAS, Demir eksikliği klorozu, Biyokimyasal tepkiler, Fizyolojik tepkiler, *Triticum durum*

With the whispering winds through durum wheat's golden fields,
this thesis finds its voice.

ACKNOWLEDGMENTS

I want to express my heartfelt gratitude to my mentor, Assist. Prof. Dr. Emre Aksoy. His guidance and support have been instrumental in shaping the direction of my study. Throughout this journey, he has consistently treated me as a colleague rather than just a student, which made me feel valued and motivated. This approach not only inspired me but also made the entire process much easier. Thank you for being an outstanding mentor and making this experience memorable. I look forward to building upon the foundation you've helped me create.

Besides my advisor, I would like to thank the rest of my thesis committee: Prof. Dr. Sertaç Önde and Assoc. Prof. Dr. Ceyhun Kayıhan for their insightful suggestions and comments.

I am also grateful to all my fellow lab members who helped with the laborious experiments, created perfect playlists, and supported me during challenging times. Special thanks are extended to my two invaluable friends, Fatih Kaya and Berfin Kalali, whose devoted care for my beloved cats not only made it possible for me to take vacations with peace of mind, knowing my companions were in loving hands.

I am deeply grateful to my beloved family for their boundless love, patience, and encouragement. My mother, Selma Parlar, and my father, Ahmet Cemal Sarak, have been my constant sources of strength, guiding me with their wisdom and standing by me through every challenge. I am thankful for our delightful pets -our playful cats, Hermes and Iris, and our loyal dogs, Maya and Sakız- whose joyful presence has brought so much happiness and comfort to my life. Without my family's unwavering support and care, this journey would have been much more difficult.

Lastly, I would like to thank my fiancée Selime Çelik, who has been my best friend for the past nine years, my hardworking colleague, and the loving mother of our cats Nohut and Karamel. Every day, you brightened my day and shared the burden of this

process with me. I also want to thank our cats for their purrs of encouragement and the occasional keyboard interruptions that kept us sane over the last two years. Thank you for reminding me that life is more than deadlines.

I want to thank TÜBİTAK BİDEB (Bilim İnsanı Destek Programları Başkanlığı), where I was a 2210-A scholarship recipient, for their financial support during the study.

This work was supported by Research Fund of the Middle East Technical University. Project Number: TEZ-YL-108-2023-11142.

TABLE OF CONTENTS

LIST OF TABLES

TABLES

LIST OF FIGURES

FIGURES

LIST OF ABBREVIATIONS

ABBREVIATIONS

GWAS	Genome-wide association study
TR-CV	Turkish cultivars
For-CV	Foreign cultivars
TR-LD	Turkish landrace
Pop-LD	Popular landrace
SNP	Single nucleotide polymorphism
DArT	Diversity arrays technology
FCR	FERRIC CHELATE REDUCTASE or FCR activity in the roots
RFCR	Relative change in FCR enzyme activity in the roots
CHL	Total chlorophyll concentration
RCHL	Relative change in total chlorophyll concentration
RA	Rhizosphere acidification
RRA	Relative change in rhizosphere acidification
LA	Leaf area
RLA	Relative change in leaf area
LFW	Leaf fresh weight
RLFW	Relative change in leaf fresh weight
RFW	Root fresh weight
RRFW	Relative change in root fresh weight

FWR	Root fresh weight/second leaf fresh weight ratio
RFWR	Relative change in root fresh weight/second leaf fresh weight ratio
RDW	Root dry weight
RRDW	Relative change in root dry weight
LDW	Leaf dry weight
RLDW	Relative change in leaf dry weight
DWR	Root dry weight/second leaf dry weight ratio
RDWR	Relative change in root dry weight/second leaf dry weight ratio
MRN	Maximum root number
RMRN	Relative change in maximum root number
RTN	Root tip number
RRTN	Relative change in root tip number
TRL	Total root length
RTRL	Relative change in total root length
MRL	Maximum root length
RMRL	Relative change in maximum root length
TRA	Total root area
RTRA	Relative change in total root area
TRV	Total root volume
RTRV	Relative change in total root volume

CHAPTER 1

INTRODUCTION

1.1 Origin, Importance, and Production of Wheat in Türkiye and the World

Wheat cultivation, which began in the Fertile Crescent (encompassing Southeastern Türkiye, Syria, Iraq, Iran, Palestine, Jordan, and Israel) about 10.000 to 12.000 years ago, played a significant role in the transition from hunter-gatherer societies to settled lifestyles and the development of numerous civilizations and kingdoms worldwide (Peng et al., 2011). Wheat and its close relatives belong to the Poaceae (Gramineae) family and are classified within the *Triticum* genus, which includes approximately 300 species (Matsuoka, 2011). Wheat is categorized into two main groups for trade purposes: bread wheat (*Triticum aestivum* L.), which is hexaploid with a chromosome structure of 2n=42 (AAABBD), and durum wheat (*Triticum durum* Desf.), which is tetraploid with a chromosome structure of 2n=28 (AABB). Additionally, there is some cultivation of diploid einkorn wheat (*Triticum monococcum* L.) with 2n=14 (AA) chromosomes and tetraploid emmer wheat (*Triticum dicoccum* Schrank.) with 2n=28 (AABB) chromosomes (Levy et al., 1988).

According to the United Nations projections, the global population exceeded 8 billion on November 15, 2022. The world's population is expected to expand by approximately one-fifth, nearing 10 billion by around 2050. Of this total, about 6.6 billion individuals reside in developing nations. Notably, although the world's population is proliferating, the progress in increasing global food production and improving the distribution of food resources among countries has not met the expected UN targets (UNCTAD, 2022). Wheat is the most widely cultivated and produced crop globally among staple crops used in human nutrition. This is mainly due to its wide adaptability to different environments, ranging from high altitudes to

tropical and subtropical regions, reaching as far north as 67° degrees in Scandinavia and as far south as 45° degrees in Argentina, making it unparalleled in its adaptability (Shewry, 2009). Moreover, wheat grains have good nutritional value and are easy to store and process, making them a staple food in approximately 50 countries. Wheat provides about 22% of the total calories from plant-based foods for the global population, but in Türkiye, this percentage is as high as 40% (FAO, 2023). Therefore, ensuring sustainable wheat production as a primary food source is crucial for the national economy and food security. Despite having fertile lands suitable for wheat cultivation, Türkiye's wheat yield is significantly below the world average. For instance, the average wheat yields in the world were approximately 3540, 3470, and 3490 kg per hectare, whereas 2780, 2960, and 2660 kilograms per hectare in Türkiye in 2019, 2020, and 2021, respectively (FAO, 2023). Additionally, according to Turkish Statistical Institute, in Türkiye, wheat was cultivated on approximately 6.6 million hectares of land, where 5.4 million hectares were dedicated to bread wheat and 1.2 million hectares to durum wheat; wheat production was totaled around 19.8 million tons, with 16 million tons of it being bread wheat and 3.8 million tons being durum wheat; and the yield was approximately 2950 kg per hectare for bread wheat and 3110 kg per hectare for durum wheat in 2023 (TÜİK, 2023a). While Southeastern Anatolia fulfills a significant portion of Türkiye's durum wheat demand, Central Anatolia and Thrace-Marmara regions have ideal climatic conditions for durum wheat production (Karaman et al., 2012). In Türkiye, Southeastern Anatolia (39%) and Central Anatolia (34%) are the top two producers of durum wheat, with the Aegean region ranking third with a 13% share of production (TÜİK, 2023b). Durum wheat, a crucial raw material for pasta, semolina, and bulgur industries, has more selective ecological requirements than bread wheat and poses challenges for cultivation in various regions (Kılıç H. et al., 2014).

1.2 Importance of Iron for Plants and Impacts of Iron Deficiency

Iron (Fe) is one of the essential micronutrients for plants, and iron deficiency is among the most common nutritional deficiencies. Iron is a cofactor for metalloproteins and is found in the active sites of iron-sulfur proteins involved in photosynthesis and respiration. Additionally, it plays crucial roles in DNA and hormone biosynthesis, nitrogen fixation, sulfate assimilation, and chlorophyll biosynthesis (Hell & Stephan, 2003). However, due to its high reactivity, excessive accumulation of Fe within cells can trigger the production of reactive oxygen species through Fenton reactions, leading to cell death (Møller et al., 2007).

Even though iron (Fe) is one of the most abundant elements in the soil, it is primarily found in the insoluble ferric (Fe^{3+}) form, especially in aerobic environments (Palmer & Guerinot, 2009). The soil pH must be low to reduce the insoluble iron form, Fe^{3+}, to the soluble ferrous, Fe^{2+}, form. Iron deficiency is frequently observed in plants growing in well-aerated, calcareous soils due to the low acidity of such soils. Unfortunately, since one-third of the world's arable land and 70% of Turkish soils are covered by calcareous soils, agriculturally important plants are constantly exposed to iron deficiency (White & Brown, 2010). Plant iron deficiency leads to a chlorosis condition known as "iron deficiency chlorosis" (IDC), which occurs between leaf veins due to decreased chlorophyll biosynthesis. One of the most significant effects of IDC is stunted growth, which directly affects plant yields. Therefore, genotypes that cannot tolerate Fe deficiency show stunted growth and lower yields.

1.3 Iron Uptake Strategies

1.3.1 Strategy I

Dicots take up the insoluble ferric iron (Fe3+) in soil via a reduction strategy known as "Strategy I," which involves three consecutive activities facilitating its

transport into root cells (Thomine & Vert, 2013). The first of these activities consists of the acidification of the rhizosphere, which is facilitated by proton transport through H^+-ATPases (AHA) in the root cell membrane (Li et al., 2022). Following rhizosphere acidification, ferric iron is reduced to soluble ferrous iron (Fe^{2+}) through an oxidoreductase known as FERRIC CHELATE REDUCTASE (FCR) (Connolly et al., 2003; Jeong & Connolly, 2009; Robinson et al., 1999). Finally, Fe^{2+} ions are transported into root cells through a metal transporter called IRON-REGULATED TRANSPORTER-1 (IRT1) belonging to the ZINC (Zn)–Fe-REGULATED TRANSPORTER (ZIP) family (Connolly et al., 2002; Eide et al., 1996; Vert et al., 2002). While FCR enzyme activity and gene expression levels increase in plant roots under Fe deficiency conditions (Blair et al., 2010), studies in pea and *Arabidopsis thaliana* have identified FCR as the primary regulator of Fe uptake (Satbhai et al., 2017). The constitutive expression of a gene encoding the ferric reductase oxidase enzyme from *A. thaliana* (*AtFRO2*) in soybean leads to increased tolerance to IDC due to high FCR enzyme activity (Vasconcelos et al., 2006).

Once inside the root, a portion of the absorbed Fe is stored in root vacuoles, while the rest is transported to the shoot through the xylem. Loading of Fe from the root to the xylem occurs through the ferric chelator citrate transporter, FERRIC REDUCTASE DEFECTIVE-3 (FRD3), belonging to the MULTIDRUG AND TOXIC COMPOUND EXTRUSION (MATE) family (Roschzttardtz et al., 2011). *FRD3* is among the genes with increased expression under Fe-deficient conditions, like *IRT1* and *FRO2* (Kobayashi & Nishizawa, 2012). Iron is transported between different tissues by binding to another chelator called nicotianamine through the phloem. During this transport, the role of OLIGOPEPTID TRANSPORTER-2 (OPT2) and OLIGOPEPTID TRANSPORTER-3 (OPT3), a member of the Oligopeptide transporter family, has been elucidated in previous studies (Zhai et al., 2014; Z. Zhang et al., 2016).

1.3.2 Strategy II

Phytosiderophores (PSs) released from the roots of grass-like plants such as wheat, rice, and corn (belonging to the Gramineae family) form complexes by binding to insoluble Fe^{3+} ions in the soil, called chelation strategy. The Fe^{3+}-PS complex is taken up into root cells with the help of a transporter protein family called YELLOW STRIPE (YS), with *ZmYS1* first discovered in maize (Curie et al., 2001, 2009; Kim & Guerinot, 2007; Kobayashi & Nishizawa, 2012; Takagi, 1976; Takagi et al., 1984). Phytosiderophores like mugineic acids (MAs) are synthesized from L-methionine through four consecutive enzymatic reactions (Bashir et al., 2006; Ma et al., 1999; Mori et al., 1987; Shojima et al., 1990; Ueno et al., 2007) whereas L-methionine is produced as the final product of the sulfur assimilation pathway (Amir et al., 2002; Anjum et al., 2008; Ravanel et al., 1995). SAM (S-adenosyl-L-methionine) synthase converts L-methionine into SAM. The three molecules of SAM are subsequently converted into nicotianamine by an enzyme called NICOTIANAMINE SYNTHASE (NAS), followed by conversion to 3'-keto acid by NICOTIANAMINE AMINOTRANSFERASE (NAAT), and finally to 2'-deoxymugineic acid (DMA) by DEOXYMUGINEIC ACID SYNTHASE (DMAS) (Bashir & Nishizawa, 2006; Suzuki et al., 1999; Takahashi et al., 1999). DMA serves as the precursor for nine characterized types of MAs so far. In barley and wheat, two different dioxygenase mugineic acids, called IRON DEFICIENCY–SPECIFIC CLONE2 (IDS2) and IDS3, add hydroxyl groups to DMA to produce various forms of mugineic acids (Kobayashi et al., 2001; Nakanishi et al., 2000).

In rice, there are three *NAS* genes (*OsNAS1-3*), and in *Arabidopsis*, four *NAS* genes (*AtNAS1-4*), each with distinct roles in Fe uptake and distribution (Inoue et al., 2003; Klatte et al., 2009). Nicotianamine (NA), a non-protein amino acid, is found in the roots, leaves, and phloem sap of plants, and it can move within the plant through the phloem (Schmiedeberg et al., 2003; Scholz et al., 1992). The expression of *NAS* genes involved in MA production is induced under Fe deficiency in Gramineae roots (Higuchi et al., 2001; Inoue et al., 2003; Mizuno et al., 2003). In

rice, there are six *NAAT* genes (*OsNAAT1-6*), but only the expression of *OsNAAT1* is induced under Fe deficiency. Therefore, it is believed that *OsNAAT1* is the only gene producing a functional protein with NAAT activity.

DMA produced in rice roots is transferred to the rhizosphere through a transporter called TRANSPORTER OF MUGINEIC ACID1 (OsTOM1) (Nozoye et al., 2011). The OsTOM1 transporter localizes to the plasma membrane of root epidermal cells and is significantly induced under Fe deficiency. Rice has six *TOM* (TOM transporter) genes, and *OsTOM2*, like its homolog, contributes to the movement of DMA outside of the cells (Nozoye et al., 2015). A similar protein called HvTOM1 has been identified in barley (Nozoye et al., 2011). Among the five *TOM* genes in rice, *OsTOM1-3* and *OsTOM4-6* are arranged in tandem on the 11th and 12th chromosomes, indicating the importance of DMA transport in rice and the duplication of the *TOM* gene. Interestingly, *OsTOM2* is expressed in the tissues responsible for metal transport during seed development and germination in rice (Nozoye et al., 2015). Overexpression of *OsTOM1* and *HvTOM1* in plants makes them tolerant to Fe deficiency. TOM proteins belong to the Major Facilitator Superfamily (MFS) transporter family (Pao et al., 1998).

In a rice study, it was found that the protocatechuic acid (PCA) transporter PHENOLICS EFFLUX ZERO1 (PEZ1) assists in Fe uptake into the root (Ishimaru et al., 2011). Under Fe deficiency, PEZ1 was found to be responsible for transporting phenolics such as PCA and caffeic acid to the rhizosphere. Interestingly, PEZ1 localizes to the root vascular tissue, and plants that produce high levels of PEZ1 accumulate excess Fe, leading to some physiological changes due to Fe toxicity (Kobayashi et al., 2014). Conversely, silencing *PEZ1* reduces Fe concentration in plants.

The *YELLOW STRIPE1* (*YS1*) gene encoding Fe^{3+}-MA transporters was first identified in maize. The *ysl1* mutant of maize exhibits symptoms of interveinal chlorosis due to Fe deficiency (Inoue et al., 2009). In studies conducted over the past decade, the expression levels of rice ZmYS1-like genes (YS1-LIKE – OsYSL) are

induced in both roots and shoots under Fe-deficient conditions. In *Arabidopsis*, there are eight orthologs (*AtYSL1-8*), and in rice, there are 18 orthologs (*OsYSL1-18*) of *ZmYS1* (Curie et al., 2009; Koike et al., 2004; Murata et al., 2006). The YSL family is responsible for transporting various DMA-bound metals, including Fe^{3+}, Zn^{2+}, Cu^{2+}, and Ni^{2+}, and NA-chelated Ni^{2+}, Fe^{2+}, and Fe^{3+} complexes. For example, YS1 transports various metals bound to DMA and NA-chelated Ni^{2+}, Fe^{2+}, and Fe^{3+} complexes (Schaaf et al., 2004). OsYSL15 and OsYSL18 transport Fe^{3+}-DMA (Aoyama et al., 2009; Inoue et al., 2009), OsYSL2 transports Fe^{2+}-NA and Mn^{2+}-NA (Koike et al., 2004), and *OsYSL16* transports Fe^{3+}-DMA and Cu^{2+}-NA (Kakei et al., 2012; C. Zhang et al., 2018). Moreover, OsYSL transporters play a role in Fe relocalization within rice plants (Kakei et al., 2012; Koike et al., 2004). After entering the cytosol, Fe^{3+}-DMA can be reduced to Fe^{2+}-NA by ascorbate. Therefore, NA is an essential intermediate for MA biosynthesis and a significant metal chelator that can participate in Fe relocalization within plants (Inoue et al., 2003). The expression of *YS1*, *OsYSL2*, *OsYSL15*, and *OsYSL16* increases in both roots and shoots under Fe-deficient conditions, while the expression of *OsYSL18* remains unchanged depending on the Fe level. YSL family transporters play a crucial role in internal metal homeostasis by transporting metal-MA and metal-NA complexes.

Similar to Strategy I plants, some gramineous plants can also acquire Fe^{2+} from the rhizosphere in addition to the Fe^{3+}-PS complex through the help of Fe^{2+} transporters. IRT1 (OsIRT1) protein in rice functions in Fe^{2+} uptake similar to its counterpart in *Arabidopsis* (Nakanishi et al., 2006). Even when the rice *NAAT* gene is mutated, preventing plants from synthesizing PS, plant growth remains unaffected as long as external Fe^{2+} is supplied (Cheng et al., 2007). This demonstrates that rice employs both Strategy II and Strategy I for Fe acquisition. A similar strategy was also observed in maize (*Zea maize*), which does not grow in oxygen-deprived environments such as swamps (S. Li et al., 2018). Genome analysis identified nine *ZmZIP* genes, and their relationship with iron uptake was elucidated through cloning and yeast experiments (S. Li et al., 2016). Furthermore, it has been demonstrated that the transporters *ZmIRT1* and *ZmZIP3* can transport Fe^{2+} in plants (S. Li et al., 2015).

1.4 Transcription Factors in Strategy II

In gramineous plants that utilize Strategy II to uptake Fe from the rhizosphere, the acquisition is regulated by basic helix–loop–helix (bHLH) transcription factors. The iron-related bHLH transcription factor 2 (IRO2) was found to be the key regulator of this strategy in rice, even though its mode of action or subcellular localization has not yet been studied (Ogo, 2006). Under Fe deficient conditions, the OsFIT-OsIRO2 complex controls the strategy II genes, namely *OsNAS1, OsNAS2, OsNAAT1, OsDMAS1, OsTOM1*, and *OsYSL15* in rice (Liang et al., 2020). Besides IRO2, there are two constitutively expressed Fe deficiency-responsive element (IDE) binding factors called OsIDEF1 and OsIDEF2, which positively regulate many genes in rice by binding to iron deficiency-responsive cis-acting elements 1 (IDE1) and 2 (IDE2). Additionally, OsIDEF1 positively regulates the expression of *IRO2,* and OsIDEF2 binds to *OsYSL2* promoters and downstream genes of *IRO2* (Kobayashi et al., 2007; Ogo et al., 2008). Lately, OsbHLH156 has been identified as a new positive regulator of Fe deficiency-responsive genes and facilitated the localization of IRO2 in rice under Fe deficiency (S. Wang et al., 2020).

1.5 Iron Distribution and Storage

After being taken up by the roots, Fe is transported to the sink tissues. IRT1 appears predominantly located on the exterior surface of epidermal cells, implying it serves as the initial point for Fe transfer into the symplastic pathway, facilitating cellular connectivity through plasmodesmata (Barberon et al., 2014). Efflux transporters are anticipated to be situated within the inner membrane domain of root epidermal cells (Dubeaux et al., 2015). Nutrients, including Fe, traverse through the apoplastic space amid the cell walls of the epidermis and cortex cells, making their way to the endodermis. Once Fe encounters the Casparian strip, it obliges all iron to traverse into the symplast. The endodermis operates as a decisive checkpoint, governing the movement of Fe into the plant (Barberon, 2017).

Because of its potential toxicity and minimal solubility, Fe necessitates chelators to facilitate safe and efficient translocation without inducing harmful redox reactions. Fe is believed to be conveyed within the symplast in the guise of Fe^{2+}–NA complexes (Bonneau et al., 2016; Inoue et al., 2003; Klatte et al., 2009).

Following its transit through the endodermis, Fe is loaded into the xylem for eventual translocation to the shoots. The pericycle, positioned within the endodermis, regulates Fe loading into the xylem via YSL2 and ferroportin (DiDonato et al., 2004; Morrissey et al., 2009). In the xylem, Fe is transported in the form of Fe^{3+}–citrate complex, necessitating the oxidation of Fe^{2+} to Fe^{3+}. Essential for the translocation of iron is the efflux of citrate, a process primarily facilitated by the efflux transporter FERRIC REDUCTASE DEFECTIVE-3 (FRD3) in *Arabidopsis* (Green & Rogers, 2004; Rellán-Álvarez et al., 2010).

The leaves are a crucial site for Fe storage because they are vital for photosynthesis. Within this context, Fe re-enters the symplast, primarily reduced to Fe^{2+} through the action of FCR proteins, and predominantly observed in the Fe^{2+}–NA form. Iron from leaf tissues is redistributed to other sink organs via the phloem. In *Arabidopsis*, the participation of the oligopeptide transporter family protein OPT3 is observed in this Fe remobilization. Mutants lacking *OPT3* display higher Fe accumulation in the leaves and limited translocation to other storage organs, such as the seed (Mendoza-Cózatl et al., 2014; Zhai et al., 2014). While Fe is distributed across various tissues, its ultimate destination is commonly deemed to be the seed. Iron reserves in the seed are crucial during germination, especially before the seedling develops roots to extract nutrients from the soil. The involvement of YSL transporters in seed loading has been shown in a previous study (Jean et al., 2005).

Two primary storage mechanisms for Fe have been suggested in the cell: sequestration into vacuoles and ferritin. Notably, the Vacuolar Iron Transporter1 (VIT1), identified in *Arabidopsis* as similar to the yeast Fe transporter CCC1, plays a vital role in this process. In *vit1* mutants, while the Fe content in embryos remains similar to that in the wild type, the characteristic accumulation of Fe in the vacuoles

of the root endodermis and veins is disrupted (Kim et al., 2006; Roschzttardtz et al., 2009). During germination, Fe is released into the cytosol through the action of the efflux transporters NRAMP3 and NRAMP4 (Lanquar et al., 2005). A screening study conducted on *nramp3-nramp4* mutants revealed mutations in *VIT1*, rescuing their susceptibility to low Fe conditions (Mary et al., 2015).

Ferritins, crucial Fe storage proteins found throughout various biological kingdoms, consist of a shell formed by twenty-four subunits capable of accommodating a maximum of 4500 Fe^{3+} ions. The percentage of overall Fe stored in ferritin within seeds varies across species, representing around 60% in peas but less than 5% in *Arabidopsis* seeds (Zielińska-Dawidziak, 2015). In plants, ferritin is primarily situated within the plastids. In cereal grains like wheat and rice, most Fe exists in the vacuoles within the aleurone layer, a part of the grain that is frequently eliminated during grain processing (Kyriacou et al., 2014).

1.6 Iron Deficiency Studies in Wheat

While molecular analyses regarding Fe deficiency tolerance have been conducted in Gramineae, such as rice and maize (Bocchini et al., 2015; Kawakami & Bhullar, 2021), studies in a high-ploidy plant like wheat are limited. In the first study aimed at determining the molecular responses of wheat to Fe deficiency, hexaploid bread wheat was subjected to Fe deficiency for 5, 10, 15, and 20 days, and transcriptomic changes in the roots were determined using RNA sequencing (Singh et al., 2019). The study showed that the expression levels of genes involved in both Strategy I and II were significantly affected, as well as essential genes involved in sulfur metabolism. Those encoding various metal transporter families, such as NAS, YSL, and ABC transporters, were identified among the upregulated genes. In another transcriptomic study, it was found that the expression levels of genes responsible for phytosiderophore production and transport were significantly affected by iron deficiency at different growth stages of the plants (Wang et al., 2019). The induction of *NAS* and *DMAS* genes, especially in the flag leaves and grains of plants subjected

to Fe deficiency may suggest the crucial roles of NA and DMA in Fe accumulation in grains. Additionally, it has been suggested that YSL and NRAMP transporters responsible for intercellular iron transport and bHLH transcription factors may also play essential roles in Fe-deficient bread wheat. In another study by the same group, the expression levels of 337 and 665 transporter-encoding genes significantly altered in the roots and flag leaves, respectively, of bread wheat under Fe deficiency (Wang et al., 2020). Among these genes, the ones that encode the MSF, ABC, NRAMP, and OPT transporters are noteworthy.

The *NAS* genes responsible for nicotianamine synthesis in bread wheat were identified through bioinformatic analyses (Bonneau et al., 2016; Pearce et al., 2014). It was shown in these studies that a significant portion of the total 21 *TaNAS* genes had increased expression levels in wheat roots under Fe deficiency (Bonneau et al., 2016).

Another study discovered that 6 and 3 genes encode NAAT and DMAS in the bread wheat genome, respectively. *TaNAAT1*, *TaNAAT2*, and *TaDMAS1* expression levels increased in wheat roots after five days of Fe deficiency (Beasley et al., 2017). In another study, the expression level of *TaIDS3*, the ortholog of *HvIDS3* in bread wheat, reached its highest level on the 15th day of Fe deficiency, and then the expression level declined (Mathpal et al., 2018). A genome-wide analysis for identifying *YSL* genes in bread wheat revealed 67 genomic regions (A. Kumar et al., 2019). Among these, *TaYS1A* was selected, and its expression level was shown to increase 60-fold after 15 days of Fe deficiency, while *TaYSL3* expression increased up to 200-fold under 12 hours of Fe deficiency. Regarding the genome-wide identification and expression analyses of the ZINC-INDUCED FACILITATOR-LIKE (ZIFL) family of proteins responsible for Fe transport in bread wheat under Fe deficiency. Fifteen identified genes are distributed on chromosomes 3, 4, and 5. It was shown that the expression levels of some of these genes increased in the roots or shoots after six days of Fe deficiency (Jose et al., 2019). In addition, another study identified 8 *VACUOLAR IRON TRANSPORTER (VIT)* and 23 *VIT–LIKE (VTL)* genes in the bread wheat genome, with most of these

genes showing decreased expression levels in wheat roots under Fe deficiency (Sharma et al., 2020). Furthermore, 20 protein-coding sequences belonging to the Metal Tolerance Protein (MTP) family were identified in the wheat genome (Vatansever et al., 2017). However, their expression levels were not reported under Fe deficiency.

1.7 Genome-Wide Association Studies

A genome-wide association study (GWAS) is a research approach used to screen the entire genome of a population to identify associations of genotypes with phenotypes. Quantitative traits being influenced by environmental conditions can make traditional breeding methods challenging. Therefore, combining conventional and molecular methods is essential to overcome these challenges (Garcia-Oliveira et al., 2018). DNA markers can be categorized into sequence-based (SNP, DArT), hybridization-based (RFLP), and PCR-based markers (RAPD, AFLP, SSR). With the assistance of molecular markers, Marker-Assisted Selection (MAS) is widely used for the selection of desired traits (Yorgancılar et al., 2016), genetic linkage mapping (Alsaleh et al., 2015; Nachit et al., 2001), genetic mapping and quantitative trait locus (QTL) identification studies (Poland et al., 2012). Single Nucleotide Polymorphisms (SNPs) are point nucleotide variations within the same DNA sequence, with each SNP potentially considered a molecular marker (Ganal et al., 2009). SNPs are the most common polymorphisms in plant and animal genomes (Hiremath et al., 2012). Their wide distribution, codominant nature, chromosome-specific locations, and high repeatability make SNPs preferred markers in genetic analyses (Kujur et al., 2015; Trebbi et al., 2019). Ren et al. (2013) used 946 SNP markers to scan the genetic structure of 150 durum wheat genotypes from different locations worldwide. They reported an average of 79.9% polymorphism among 53 locations and an average of 98.6% polymorphism for 97 varieties.

Diversity Array Technology (DArT), based on DNA sequence and chip (microarray) technologies, is a high-throughput genomic analysis method. DArT

technology, initially developed by A. Kilian and D. Jaccoud (Jaccoud, 2001), was first applied to wheat by Akbari et al. (2006). This technology measures the presence or quantity of a unique DNA fragment originating from a population or an organism's genomic DNA. DArT is more economical than other DNA sequence-based marker types like SNPs. It applies to most species as it does not require prior knowledge of DNA sequence information for genotyping, and a small amount of DNA is sufficient for its use (Khan et al., 2014). In recent years, DArTseq markers based on Next-Generation Sequencing (NGS) have replaced traditional DArT markers. DArTseq and SNP markers based on Next-Generation Sequencing (NGS) technology have been successfully applied in linkage, association, and whole-genome association mapping studies (Baloch et al., 2017).

1.8 GWAS in Wheat

Many Genome-Wide Association Studies on durum wheat have been published in recent years. Studies generally focused on key agronomic traits such as drought tolerance, grain shape, and color (Alemu et al., 2020; S. Wang et al., 2019) by using SNP markers, yield potential, drought, heat, and disease tolerance, heading date, flag leaf width (Ahmed et al., 2021; Akram et al., 2021; Liu et al., 2017; Sukumaran et al., 2018; Tadesse et al., 2015; Tyrka et al., 2023) by using DArT markers. In our study, both SNP and DArT markers were used to investigate four different populations, Turkish cultivars, Turkish landraces, foreign cultivars, and popular landraces, for 16 agronomic traits related to iron deficiency. Since Türkiye is the original habitat of Turkish landraces, unique genetic traits will likely be found by studying them. Our research uses these landraces, which are valuable because of their unique connection to Türkiye's genetic heritage.

1.9 Aim of the Study

Iron deficiency is one of the most significant abiotic stress factors for plants worldwide, and as Fe deficiency significantly affects yield, the underlying molecular mechanisms for Fe deficiency tolerance must be enlightened. This GWAS study examined the association between the durum wheat genome and the phenotypes of 123 different genotypes by investigating sixteen traits, including above-soil and root properties, under iron-deficient conditions to identify loci and candidate genes related to iron deficiency. Moreover, the most tolerant and sensitive varieties among the population were aimed to be identified for further Fe deficiency studies.

CHAPTER 2

MATERIALS AND METHODS

2.1 Plant Material

123 genotypes of durum wheat (*Triticum turgidum* L. *durum*) collected from various regions of Türkiye were used as plant materials (Appendix A). In a previous study, the structure and principal coordinate analysis was performed for the population, and four subgroups were observed (Alsaleh et al., 2022). The four subgroups include 48 Turkish cultivars (TR-CVs) registered in Türkiye from 1964 to 2012, 20 foreign cultivars (For-CVs) registered in foreign countries from 1974 to 2011, 42 Turkish landraces (TR-LDs) obtained from the National Genebank located in Aegean Agricultural Research Institute in İzmir, Türkiye and collected from different regions of Türkiye, and 13 popular landraces (Pop-LDs), widely produced by farmers, collected from local villages in southeastern Türkiye.

2.2 Growth Conditions and Stress Application

In the study, a hydroponic culture system with ten 26-liter rectangular opaque plastic boxes (measuring 35 x 50 x 15 cm) was designed. Five boxes were used for each system, iron deficient and sufficient. As shown in Figure 2.1, five boxes were interconnected using 22 mm in diameter pipes. These pipes facilitated the flow of nutrient solution among the boxes, with the final box linked to a central 50-liter main tank. Positioned midway along the height of the main tank, an aquarium pump ensured adequate aeration of the solution, pumping it through another 22 mm diameter pipe to the initial box. To allow the plants to float on the nutrient solution, insulation foams (measuring 33 x 48 cm) were placed within each box, and holes with a diameter of 15 mm were drilled into insulation foams. Within these holes,

seedlings were wrapped in black lightproof sponges (measuring 25 x 25 x 40 mm). One plantlet was placed per hole. Each foam panel accommodated a total of 135 holes, arranged with 15 holes on one side and 9 on the other. The holes were spaced 3 cm apart from each other, with an additional 3 cm gap from the foam's edges.

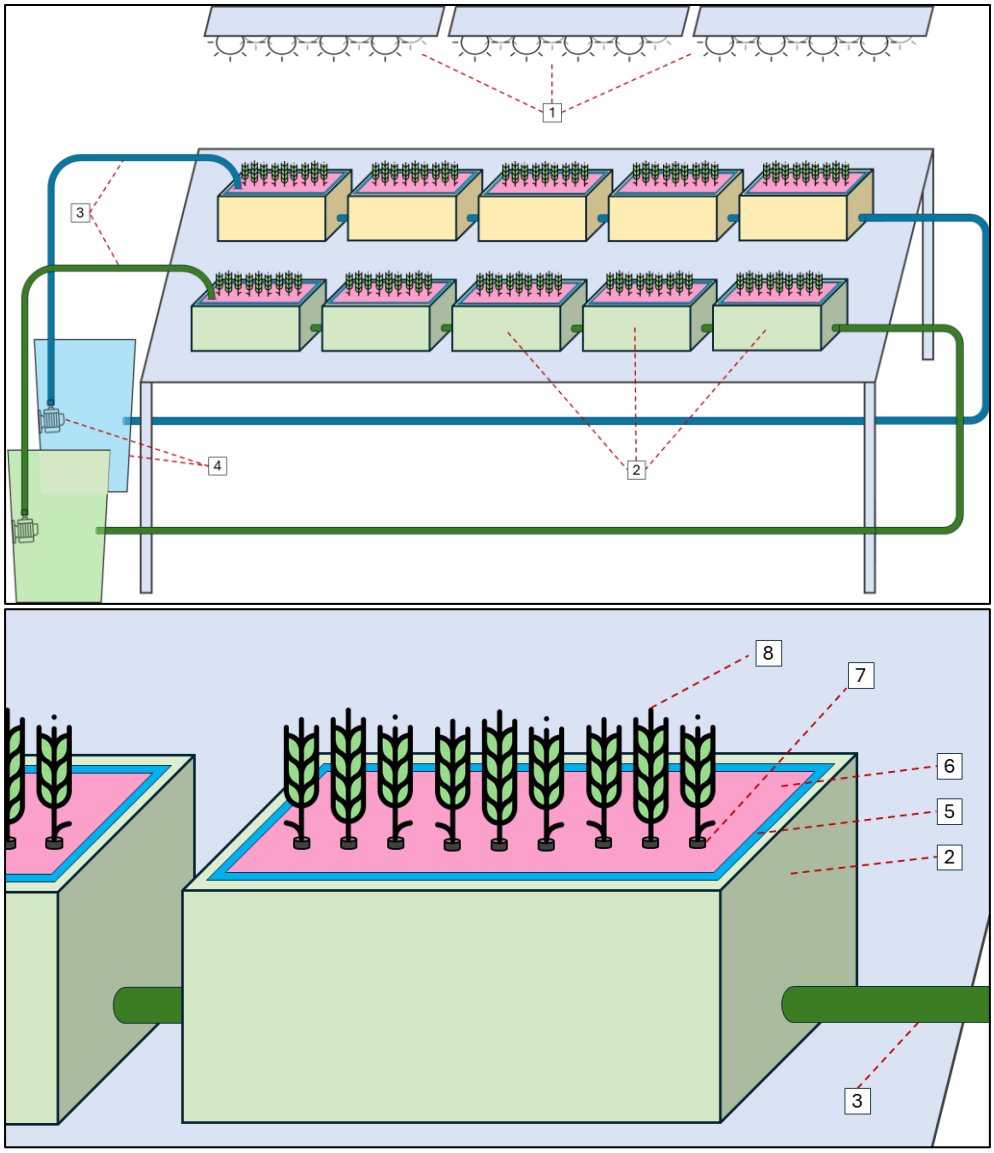

Figure 2.1. Hydroponic system scheme of the study. 1) Lightning panel, 2) containers, 3) circulatory pipes, 4) water pump and main tank, 5) nutrient solution, 6) floating insulation foam, 7) sponge in a hole, and 8) seedling can be seen on the scheme.

On Day 0, the stratification process of the seeds was achieved by incubating them at -20°C for 24 hours. Then, on Day 1, seeds were placed between two wet paper towels, covered with opaque black bags, and put in the dark at 23°C. On Day 3, the black bags were replaced with transparent bags and placed in the light at 23°C. On Day 6, seedlings with similar root lengths and no necrosis (darkening) at the root tips were carefully transferred to the hydroponic system by wrapping them with sponges where the stem meets the root and placing them into the holes in the insulation foams. The transfer was done in boxes containing nutrient solutions to prevent root drying. Half of the plants were placed under control, and the other half were placed under Fe deficiency conditions. After 21 days of stress application, on Day 27, physiological and biochemical measurements were taken from both groups of plants. From Day 1 to Day 27, the plants were grown under a long-day cycle with the help of high-pressure sodium lamps in a controlled greenhouse under 1200 μmoles photons $m^{-2}s^{-1}$. The hydroponics experiment was set up with a randomized block design with 15 biological replicates per genotype in control and stress conditions.

In the study, half-strength (1/2) Hoagland's solution (Hoagland & Arnon, 1950) was used as the nutrient medium, with the following mineral element concentrations: 2 mM KNO_3, 2 mM $Ca(NO_3)$, 1 mM NH_4HCO_3, 0.5 mM $MgSO_4$, 0.25 mM KH_2PO_4, 50 μM KCl, 25 μM H_3BO_3, 2 μM $MnSO_4$, 2 μM $ZnCl_2$, 0.5 μM $CuSO_4$, , and 0.15 μM $CoCl_2$, 0.075 μM $(NH_4)_6Mo_7O_{24}$ and 10 μM Fe-EDTA. The concentration of Fe-EDTA was reduced by $1/10^{th}$ of the control treatment (to 1 μM) for Fe deficiency treatment. Before the transfer of plants, the pH of the nutrient solutions was adjusted to 5.7. As the amount of nutrient solution in the boxes decreased, fresh Hoagland's solution was added to the main tank. Likewise, as the pH of the solution changed, it was readjusted to 5.7.

The study was completed in three sets in a greenhouse in Ankara, Türkiye. The same three genotypes were repeatedly planted as controls in each set, and no significant differences were observed among their measurements. The greenhouse conditions were 22°C/18°C (±3°C) with a 16-h light/8-h dark cycle, 60% humidity,

and 1200 μmol $m^{-2}s^{-1}$ photosynthetic active radiation. Light sources provided by high-pressure sodium lamps were delivered from above the plant canopy to prevent excess light and reduce photoinhibition on the photosystem (Evans et al., 1993). To prevent algae formation in the nutrient solution, 4 mL of ReeFlowers Rem Algae were added to the nutrient solution in the main tank every three days.

2.3 Biochemical Analyses

2.3.1 Total Chlorophyll Concentration Measurement

The second leaf of the plant was detached; its fresh weight was measured and crushed using mortar and pestle in 7 mL of 80% (v/v) acetone. Then, a 1 mL sample was taken in an Eppendorf tube and placed at 4°C for 48 hours. Subsequently, this solution was centrifuged at 13,000 g for 5 minutes at 4°C, and the supernatant was taken for absorbance reading at 470, 646.8, and 663.2 nm relative to 80% (v/v) acetone. Total chlorophyll concentration (chlorophyll a + b) was calculated using the formula below, in the unit of mg total chlorophyll/g leaf FW (Lichtenthaler & Wellburn, 1983).

$$\frac{((A_{663,2}x7{,}15) + (A_{646,8}x18{,}71))(\mu g/ml)\ x\ Volume\ (ml)}{1000\ x\ Leaf\ FW\ (g)}$$

2.3.2 FCR Enzyme Activity

The plants' root was detached; its fresh weight was measured and transferred into 15 ml falcon tubes containing 8 mL of assay solution of 0.33mM Fe^{3+}-EDTA and 1mM ferrozine (Aksoy & Koiwa, 2013). They were incubated for 20-22 hours in darkness at room temperature. At the end of the incubation, the samples were taken for absorbance reading at 562 nm relative to an identical assay solution without a sample. The formula below calculated the FCR enzyme activity level in the unit of μmol Fe^{2+}/g root FW/h.

$$\frac{(A_{562}/28{,}6)\ x\ Volume\ (ml)\ x\ 1000}{Root\ FW\ (g)\ x\ incubation\ time\ (h)}$$

2.3.3 Rhizosphere Acidification Assay

The roots of the plants were dipped in water and subsequently rinsed. Then, they were placed in 50 mL falcon tubes containing 25 mL of Hoagland solution with a known pH. Iron deficient and sufficient ½ Hoagland solutions were used for the plants grown initially in iron deficient and sufficient ½ Hoagland solutions, respectively. They were kept in their growth conditions for 48 hours, with the tubes being the only part kept in the dark. Then, the roots were taken to measure their fresh weights and the incubated solution's pH. The secreted [H^+] (in mole/L) in the samples was calculated by the equation below, and the number of H^+ moles in 25 mL incubation solution (in mole/25 mL) was calculated. Lastly, the secreted [H^+] (in mole/25mL) was normalized by dividing the root fresh weight (Pizzio et al., 2015).

$$pH\ change = -\log[H^+]$$

2.4 Physiological Analyses

2.4.1 Leaf Area Measurement

The second leaf of the plant was detached and placed on the scanner with its entire surface exposed, tightly stretched, and then scanned at a resolution of 300 dpi in 24-bit color on an Epson Perfection V850 Pro Scanner. The Easy Leaf Area software (Easlon & Bloom, 2014) was used to calculate the surface of the scanned leaves in the unit of cm^2. An example input and output image of a root scanning in the software can be seen in Figure 2.2.

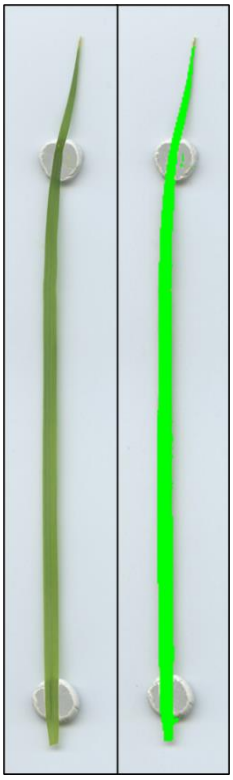

Figure 2.2 An example of the input and output of leaf scanning in the Easy Leaf Area.

2.4.2 Root Structure Profiling

The plant's root was detached and placed on the scanner with its entire surface exposed, tightly stretched, and then scanned at a resolution of 300 dpi in 16-bit grayscale on an Epson Perfection V850 Pro Scanner. The RhizoVision Explorer software (Seethepalli et al., 2021) was used to calculate the total root length (TRL), maximum root length (MRL), maximum root number (MRN), root tip number (RTN), total root area (TRA), and total root volume (TRV). The crucial settings in the software were as follows: root type option was whole root, image threshold level was 215, keep largest component option was true, edge smoothing option was enabled and threshold level was 2, root pruning option was enabled, and threshold level was 2, convert pixels to physical unit option was enabled and dots per inch was

300. An example input and output image of a root scanning in the software can be seen in Figure 2.3.

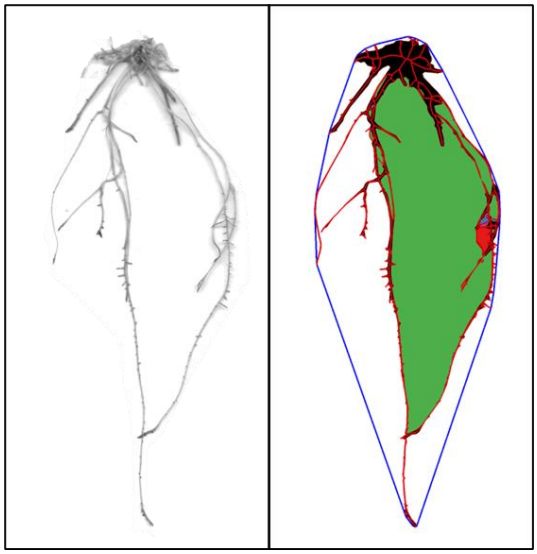

Figure 2.3 An example of the input and output of root scanning in the RhizoVision Explorer.

2.4.3 Root and Leaf Weight Measurement

After the scanning, the detached roots and second leaves were weighed separately and recorded as fresh weight. Subsequently, the samples were sandwiched between two sheets of paper and subjected to drying in an oven at 60°C for 24 hours. After drying, the samples were reweighed and recorded as dry weight.

2.5 Genotyping-by-sequencing Analysis

Genotyping-by-sequencing analysis was performed in a previous study by Alsaleh et al. (2022). Briefly, genomic DNA was extracted from the leaf samples by CTAB protocol, and the samples were run on a 0.8% agarose gel to check the quality. Then, DNA samples were sent to Diversity Array Technology (Australia) for sequencing on Illumina's next-generation sequencer, and 30,376 SNPs and 34,130

Silico-DArT markers were produced. Finally, the markers were filtered and refined to 14,255 high-quality markers with their genetic information, which was kindly provided by Prof. Dr. Hakan Özkan (Çukurova University) for this study.

2.6 Association Mapping Analysis

GWAS was conducted by the GAPIT package in R (version 3) using the BLINK model with default settings (Huang et al., 2019; J. Wang & Zhang, 2021). The associated markers are selected and optimized for Bayesian information content and reexamined across multiple tests to reduce false negatives. The threshold level to identify a marker as significant was determined as -log(p)=7.00. The region investigated to identify candidate genes for the significantly associated markers was determined to be 500kb before and after the start position of the markers in the *Triticum turgidum* genome (Svevo.v1). Later, the genome browser of GrainGenes was used to visualize the investigated regions for each marker (Yao et al., 2022). The *Arabidopsis thaliana* orthologs of the candidate genes were identified via NCBI's Blast tool (Altschul et al., 1990). Gene ontology analysis was performed using the Ensembl database platform's BioMart tool (Kinsella et al., 2011).

2.7 Statistical Analysis of Biochemical and Physiological Data

Descriptive statistics, analysis of variance (ANOVA) tests, and Pearson's correlation tests (at a significance level of 5%) of the data generated in the study were performed in XLSTAT software (XLSTAT, 2021). Fisher's LSD test was conducted following two-way ANOVA (analysis of variance) for investigated traits (Table 3.2) according to the randomized block design model at a significance level of 5%. Shapire-Wilk normality tests were applied for relative changes of each trait at a significance level of 5%. The formula below calculated relative trait values, where C is the measurement from control, and S is the measurement from stress application.

$$\%Relative\ measurement = \frac{S - C}{C} \times 100$$

CHAPTER 3

RESULTS

3.1 Phenotypic Evaluations of the Traits

The durum wheat panel of 123 genotypes was evaluated for various physiological and biochemical traits in a hydroponic system under iron deficiency. Descriptive statistics for all investigated traits over two environments were summarized in Table 3.1. In control conditions, the total chlorophyll concentration (CHL) (in mg/g LFW) had minimum, maximum, and average values of 0.07, 1.83, and 0.76, respectively, while under iron deficiency, these values were 0.05, 1.45, and 0.58, resulting in a significant 23.7% decrease. Ferric chelate reductase activity (FCR) (in μmol Fe (II)/g RFW/h) ranged from 2.39 to 81.89 with an average of 28.61 under control conditions, and under iron deficiency, it ranged from 3.55 to 106.51 with an average of 35.72, indicating a significant 24.9% increase. Rhizosphere acidification (RA) (in mmol H+/g RFW) ranged from 8.75 to 319.51 with an average of 69.33 under control conditions, while under iron deficiency, it ranged from 13.47 to 364.56 with an average of 90.35, showing a significant 30.3% increase. Leaf area (LA) (in cm^2) ranged from 1.91 to 5.03 with an average of 3.67 under control conditions, and under iron deficiency, it ranged from 1.94 to 4.83 with an average of 3.41, indicating a significant 7.1% decrease. Leaf fresh weight (LFW) (in mg) ranged from 36.03 to 102.22 with an average of 69.83 under control conditions, and under iron deficiency, it ranged from 28.83 to 108.10 with an average of 65.8, resulting in a significant 5.8% decrease. Root fresh weight (RFW) (in mg) ranged from 81.00 to 233.15 with an average of 147.00 under control conditions, while under iron deficiency, it ranged from 53.66 to 189.90 with an average of 111.25, showing a significant 24.3% decrease. Fresh weight ratio (FWR) ranged from 1.45 to 5.31 with an average of 2.32 under control conditions, and under iron deficiency, it ranged

from 1.04 to 4.68 with an average of 1.92, indicating a significant 17.2% decrease. Root dry weight (RDW) (in mg) ranged from 7.90 to 29.68 with an average of 18.32 under control conditions, while under iron deficiency, it ranged from 7.57 to 22.76 with an average of 15.41, showing a significant 15.9% decrease. Leaf dry weight (LDW) (in mg) ranged from 5.23 to 17.45 with an average of 10.86 under control conditions, and under iron deficiency, it ranged from 5.65 to 17.06 with an average of 10.05, resulting in a significant 7.5% decrease. Dry weight ratio (DWR) ranged from 1.18 to 2.62 with an average of 1.74 under control conditions, and under iron deficiency, it ranged from 0.78 to 2.26 with an average of 1.54, indicating a significant 11.5% decrease. Maximum root number (MRN) ranged from 5.00 to 14.00 with an average of 8.46 under control conditions, while under iron deficiency, it ranged from 4.75 to 14.33 with an average of 8.74, showing a significant 3.3% increase. Root tip number (RTN) ranged from 16.50 to 162.00 with an average of 47.99 under control conditions, and under iron deficiency, it ranged from 13.80 to 145.00 with an average of 47.15, resulting in a non-significant 1.8% decrease. Total root length (TRL) (in cm) ranged from 16.86 to 101.78 with an average of 46.95 under control conditions, and under iron deficiency, it ranged from 16.78 to 100.84 with an average of 41.40, indicating a significant 11.8% decrease. Maximum root length (MRL) (in cm) ranged from 2.60 to 15.94 with an average of 7.21 under control conditions, and under iron deficiency, it ranged from 2.60 to 14.70 with an average of 6.24, showing a significant 13.5% decrease. Total root area (TRA) (in cm^2) ranged from 1.09 to 8.79 with an average of 2.81 under control conditions, while under iron deficiency, it ranged from 0.90 to 7.20 with an average of 2.29, indicating a significant 18.5% decrease. Total root volume (TRV) (in cm^3) ranged from 0.48 to 5.41 with an average of 1.40 under control conditions, and under iron deficiency, it ranged from 0.32 to 4.26 with an average of 1.01, showing a significant 27.9% decrease. Additionally, the Shapiro-Wilk test did not show a significant departure from normality for all investigated traits: p-value of 0.0824 for CHL, p-value of 0.0700 for FCR, p-value of 0.0689 for RA, p-value of 0.0815 for LA, p-value of 0.0598 for LFW, p-value of 0.0642 for RFW, p-value of 0.1279 for FWR,

p-value of 0.0743 for RDW, p-value of 0.2342 for LDW, p-value of 0.2891 for DWR, p-value of 0.2107 for MRN, p-value of 0.1243 for RTN, p-value of 0.1325 for TRL, p-value of 0.2274 for MRL, p-value of 0.1075 for TRA and p-value of 0.0897 for TRV (Appendix D).

Analysis of variance (ANOVA) reported significant ($p<0.0001$) genetic diversity for all the studied traits among the wheat genotypes under iron deficiency. Highly significant ($p<0.0001$) differences were observed among all the investigated traits between the conditions (control and iron deficient) except for RTN with a p-value of 0.416 (Table 3.2). Moreover, MRN had a p-value of 0.003 but was also accepted as significant. The condition x genotype interaction was significant among all the investigated traits, except for LA, with a p-value of 0.486. In other words, all the relative changes in Table 3.1 were found to be significant with a p-value of less than 0.0001, except MRN with a p-value of 0.003, but RTN was accepted as insignificant due to a p-value of 0.416.

In Figure 3.1, the violin plots of each studied trait can be seen, including a box plot and a dot plot inside. In detail, for CHR, the control group's violin plot showed a bimodal distribution, suggesting there were two distinct subpopulations with different chlorophyll concentrations; one was around 1.25 mg/g LFW, while the other was around 0.25 mg/g LFW. In the Fe deficient group, the bimodal pattern was less pronounced, with the majority of values clustering between 0.0-0.4 mg/g LFW since the measurements mostly aggregated towards the lower end. In the FCR trait, the control group's violin plot was more spread out with a median of around 30 μmol Fe(II)/g RFW/h. There was a clear increase in FCR activity under iron-deficient conditions, with most values clustering between 20-70 μmol Fe(II)/g RFW/h. The control group of RA exhibited a wide range of values, with a peak around 150 nmol H+/g RFW, while in the Fe deficient group, there was a noticeable shift towards higher acidification values, peaking around 200 nmol H+/g RFW, except for the outliers with higher values. There was a similar trend in the LA, LFW, RFW, FWR, LDW, and DWR traits. In the control groups, there was a wide range of values around the mean values of each trait, and under Fe-deficient conditions,

there was a clear shift toward lower values. The control group of RDW showed a slight bimodal distribution, which shifted lower and became clear under Fe-deficient conditions. The MRN trait increased as the Fe deficiency was applied, and the violin plots showed a clearer bimodal distribution in Fe deficient condition like in violin plots of RDW. The violin plots of the RTN, TRL, MRL, TRA and TRV traits showed a wider distribution in both conditions. They mostly aggregated around the mean values but also have outliers with higher values. As the Fe deficiency applied, they all shifted toward lower values, except RTN, which showed an insignificant change. Only TRL and TRA showed clearer bimodal distribution among these five traits as the treatment was applied. In summary, the violin plots (Figure 3.1) and the ANOVA test results (Table 3.2) showed that there were significant decreases in all traits, except increases in FCR, RA, and MRN, and no significant difference in RTN in iron-deficient conditions compared to control.

Pearson's correlation test revealed many correlations between the studied traits (Table 3.3). Significantly strong positive linear relationships (between 0.50 and 0.75) were observed between RCHL and RLA (0.621), RLFW (0.564); RLA and RTRL (0.608), RMRL (0.612), RTRA (0.581), TRV (0.561); RLFW and RLDW (0.537), RTRL (0.578), RMRL (0.529), RTRA (0.574), TRV (0.523); RMRN and RRTN (0.714); and a significantly strong negative linear relationship (between (-0.50) and (-0.75)) was observed between RCHL and RFCR (-0.650). Significantly stronger positive linear relationships (≥0.75) were observed between RFCR and RRA (0.902); RLA and RLFW (0.859); RRFW and RRDW (0.799); RFWR and RDWR (0.843); RTRL and RMRL (0.869), RTRA (0.897), and RTRV (0.859); RMRL and RTRA (0.906), RTRV (0.872); and RTRA and RTRV (0.940). The correlations between the other variables fall within the range of -0.50 to 0.50, indicating a negligible relationship between them.

Table 3.1 Basic statistics of the traits related to Fe deficiency.

Traits	Control					Iron Deficiency					RL. (%)
	Min.	Max.	Mean	SD	CV%	Min.	Max.	Mean	SD	CV%	
CHL (mg/g LFW)	0.07	1.83	0.76	0.50	66.3	0.05	1.45	0.58	0.38	65.3	-23.7
FCR (μmol Fe(II)/g RFW/h)	2.39	81.89	28.61	17.20	60.1	3.55	106.51	35.72	18.82	52.7	24.9
RA (mmol H^+/g RFW)	8.75	319.51	69.33	54.92	79.2	13.47	364.56	90.35	65.33	72.3	30.3
LA (cm^2)	1.91	5.03	3.67	0.58	15.7	1.94	4.83	3.41	0.57	16.7	-7.1
LFW (mg)	36.03	102.22	69.83	12.25	17.5	28.83	108.10	65.8	13.42	20.4	-5.8
RFW (mg)	81.00	233.15	147	31.19	21.2	53.66	189.90	111.25	30.12	27.1	-24.3
FWR	1.45	5.31	2.32	0.64	27.6	1.04	4.68	1.92	0.64	33.1	-17.2
RDW (mg)	7.90	29.68	18.32	3.76	20.5	7.57	22.76	15.41	3.58	23.2	-15.9
LDW (mg)	5.23	17.45	10.86	2.13	19.6	5.65	17.06	10.05	1.96	19.5	-7.5
DWR	1.18	2.62	1.74	0.28	16.3	0.78	2.26	1.54	0.31	19.8	-11.5
MRN	5.00	14.00	8.46	1.73	20.5	4.75	14.33	8.74	1.83	20.9	3.3
RTN	16.50	162.00	47.99	28.49	59.4	13.80	145.00	47.15	26.21	55.6	-1.8
TRL (cm)	16.86	101.78	46.95	19.23	40.9	16.78	100.84	41.40	16.11	38.9	-11.8
MRL (cm)	2.60	15.94	7.21	3.19	44.3	2.60	14.70	6.24	2.50	40.1	-13.5
TRA (cm^2)	1.09	8.79	2.81	1.64	58.3	0.90	7.20	2.29	1.25	54.5	-18.5
TRV (cm^3)	0.48	5.41	1.40	1.12	80.4	0.32	4.26	1.01	0.73	72.7	-27.9

CHL, total chlorophyll concentration; FCR, ferric chelate reductase enzyme activity; RA, rhizosphere acidification; LA, leaf area; LFW, second leaf fresh weight; RFW, root fresh weight; LFW, second leaf dry weight; FWR, root fresh weight/second leaf fresh weight ratio; RDW, root dry weight; LDW, second leaf dry weight; DWR, root dry weight/second leaf dry weight ratio; MRN, maximum root number; RTN, root tip number; TRL, total root length; MRL, maximum root length; TRA, total root area; TRV, total root volume; SD, standard deviation; CV, coefficient of variation; RL, relative change.

Table 3.2 ANOVA of the traits under control and Fe-deficient conditions.

Trait	Source	dF	Mean Square	F value	Pr > F
CHL	Condition	1	7.73	146.96	<0.0001
	Genotype	122	1.39	26.35	<0.0001
	Condition x Genotype	122	0.19	3.60	<0.0001
FCR	Condition	1	8625.91	43.83	<0.0001
	Genotype	122	2415.02	12.27	<0.0001
	Condition x Genotype	122	506.53	2.57	<0.0001
RA	Condition	1	55797.33	18.88	<0.0001
	Genotype	122	13077.22	4.43	<0.0001
	Condition x Genotype	122	7108.17	2.41	<0.0001
LA	Condition	1	16.01	41.12	<0.0001
	Genotype	122	2.38	6.12	<0.0001
	Condition x Genotype	122	0.39	1.00	0.486
LFW	Condition	1	4227.98	22.72	<0.0001
	Genotype	122	1125.57	6.05	<0.0001
	Condition x Genotype	122	312.36	1.68	<0.0001
RFW	Condition	1	333610.10	428.60	<0.0001
	Genotype	122	6218.37	7.99	<0.0001
	Condition x Genotype	122	1614.96	2.08	<0.0001
FWR	Condition	1	41.91	104.18	<0.0001
	Genotype	122	5.55	13.79	<0.0001
	Condition x Genotype	122	0.68	1.70	<0.0001
RDW	Condition	1	2196.31	169.54	<0.0001
	Genotype	122	89.16	6.88	<0.0001
	Condition x Genotype	122	23.22	1.79	<0.0001
LDW	Condition	1	166.26	41.99	<0.0001
	Genotype	122	27.70	7.00	<0.0001
	Condition x Genotype	122	6.88	1.74	<0.0001
DWR	Condition	1	8.51	88.70	<0.0001
	Genotype	122	0.52	5.38	<0.0001
	Condition x Genotype	122	0.16	1.69	<0.0001
MRN	Condition	1	19.02	8.59	0.003
	Genotype	122	19.89	8.98	<0.0001
	Condition x Genotype	122	4.20	1.90	<0.0001

Table 3.2 Cont'd

RTN	Condition	1	155.63	0.66	0.416
	Genotype	122	4489.65	19.08	<0.0001
	Condition x Genotype	122	619.79	2.63	<0.0001
TRL	Condition	1	9004.87	60.02	<0.0001
	Genotype	122	2438.79	16.25	<0.0001
	Condition x Genotype	122	419.88	2.80	<0.0001
MRL	Condition	1	257.15	47.38	<0.0001
	Genotype	122	44.20	8.14	<0.0001
	Condition x Genotype	122	11.39	2.10	<0.0001
TRA	Condition	1	50.42	78.07	<0.0001
	Genotype	122	13.03	20.17	<0.0001
	Condition x Genotype	122	1.95	3.02	<0.0001
TRV	Condition	1	26.88	66.78	<0.0001
	Genotype	122	7.19	17.87	<0.0001
	Condition x Genotype	122	0.74	1.85	<0.0001

CHL, total chlorophyll concentration; FCR, ferric chelate reductase enzyme activity; RA, rhizosphere acidification; LA, leaf area; LFW, second leaf fresh weight; RFW, root fresh weight; FWR, root fresh weight/second leaf fresh weight ratio; RDW, root dry weight; LDW, second leaf dry weight; DWR, root dry weight/second leaf dry weight ratio; MRN, maximum root number; RTN, root tip number; TRL, total root length; MRL, maximum root length; TRA, total root area; TRV, total root volume; dF, degree of freedom. Pr >F, p-value associated with the F statistic of a given effect.

Table 3.3 Pearson's correlation coefficient values of the traits.

Traits	RCHL	RFCR	RRA	RLA	RLFW	RRFW	RFWR	RLDW	RRDW	RDWR	RMRN	RRTN	RTRL	RMRL	RTRA
RFCR	**-0.650***														
RRA	-0.123	**0.902***													
RLA	**0.621***	0.125	0.059												
RLFW	**0.564***	0.175	0.104	**0.859***											
RRFW	-0.160	0.183	0.018	0.146	0.218										
RFWR	-0.095	-0.100	-0.219	0.120	0.078	0.343									
RLDW	0.037	0.008	-0.083	0.135	**0.537***	0.307	-0.118								
RRDW	-0.233	0.157	-0.008	0.100	0.047	**0.799***	0.289	0.455							
RDWR	-0.237	0.135	0.053	0.009	-0.030	0.363	**0.843***	-0.264	0.366						
RMRN	0.030	0.081	0.071	0.189	0.133	0.191	0.167	-0.045	0.088	0.232					
RRTN	-0.008	0.141	0.119	0.400	0.333	0.104	-0.033	-0.052	0.026	0.057	**0.714***				
RTRL	0.269	0.249	-0.008	**0.608***	**0.578***	0.185	0.068	0.089	0.128	0.124	0.135	0.196			
RMRL	0.289	0.151	0.010	**0.612***	**0.529***	0.123	0.156	0.112	0.159	0.091	0.048	0.128	**0.869***		
RTRA	0.321	0.098	-0.039	**0.581***	**0.574***	0.126	0.113	0.076	0.081	0.096	0.098	0.200	**0.897***	**0.906***	
RTRV	0.347	0.105	-0.009	**0.561***	**0.523***	0.180	0.067	0.091	0.158	0.081	0.087	0.267	**0.859***	**0.872***	**0.940***

RCHL, relative total chlorophyll concentration; RFCR, relative ferric chelate reductase enzyme activity; RRA, relative rhizosphere acidification; RLA, relative leaf area; RLFW, relative second leaf fresh weight; RRFW, relative root fresh weight; RFWR, relative root fresh weight/second leaf fresh weight ratio; RLDW, relative second leaf dry weight; RRDW, relative root dry weight; RDWR, relative root dry weight/second leaf dry weight ratio; RMRN, relative maximum root number; RRTN, relative root tip number; RTRL, relative total root length; RMRL, relative maximum root length; RTRA, relative total root area; RTRV, relative total root volume; *Significant level under 0.0001 for Pearson correlation test.

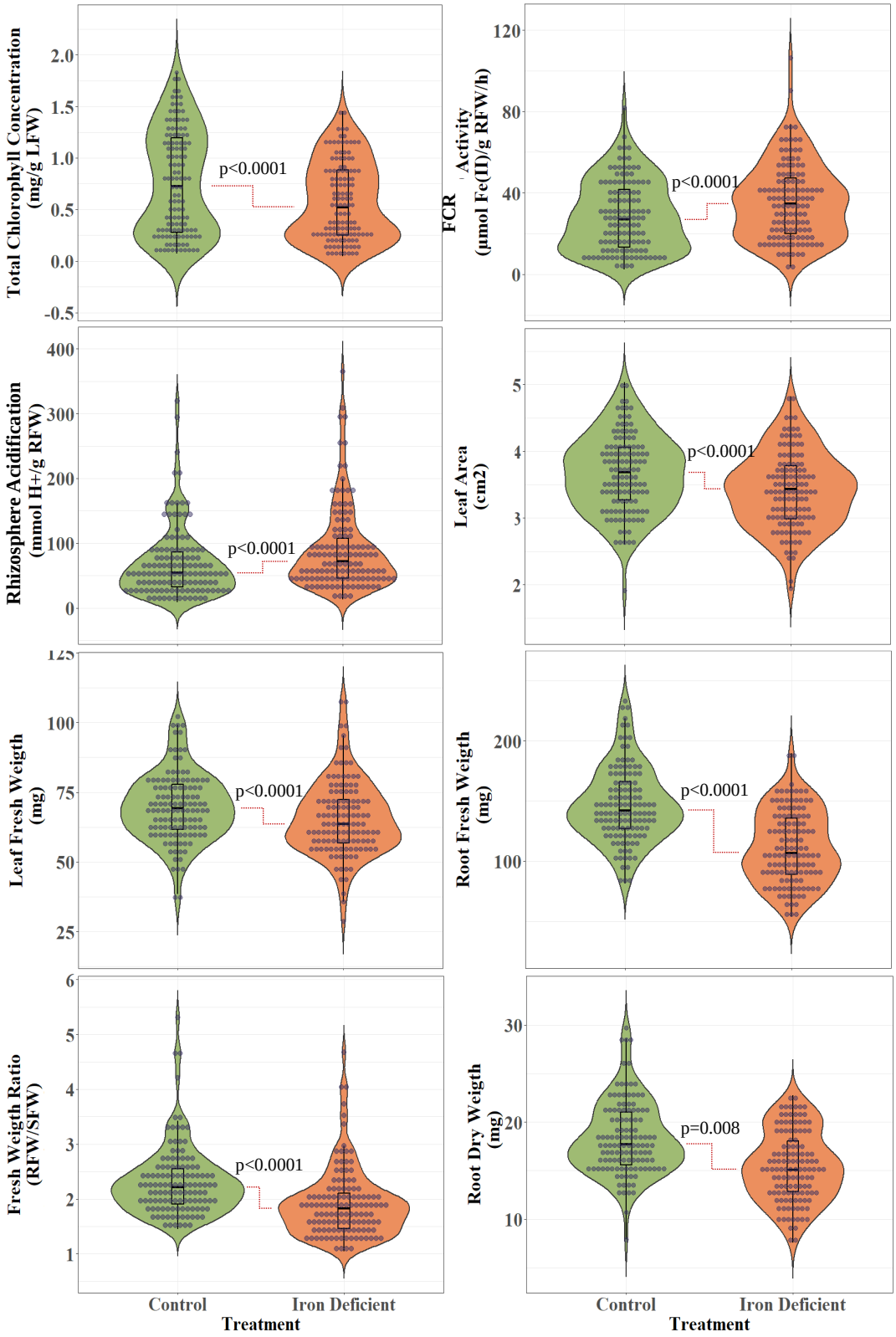
Total Chlorophyll Concentration (mg/g LFW)
p<0.0001
FCR Activity (µmol Fe(II)/g RFW/h)
p<0.0001
Rhizosphere Acidification (mmol H+/g RFW)
p<0.0001
Leaf Area (cm2)
p<0.0001
Leaf Fresh Weigth (mg)
p<0.0001
Root Fresh Weigth (mg)
p<0.0001
Fresh Weigth Ratio (RFW/SFW)
p<0.0001
Root Dry Weigth (mg)
p=0.008
Control
Iron Deficient
Treatment
Control
Iron Deficient
Treatment

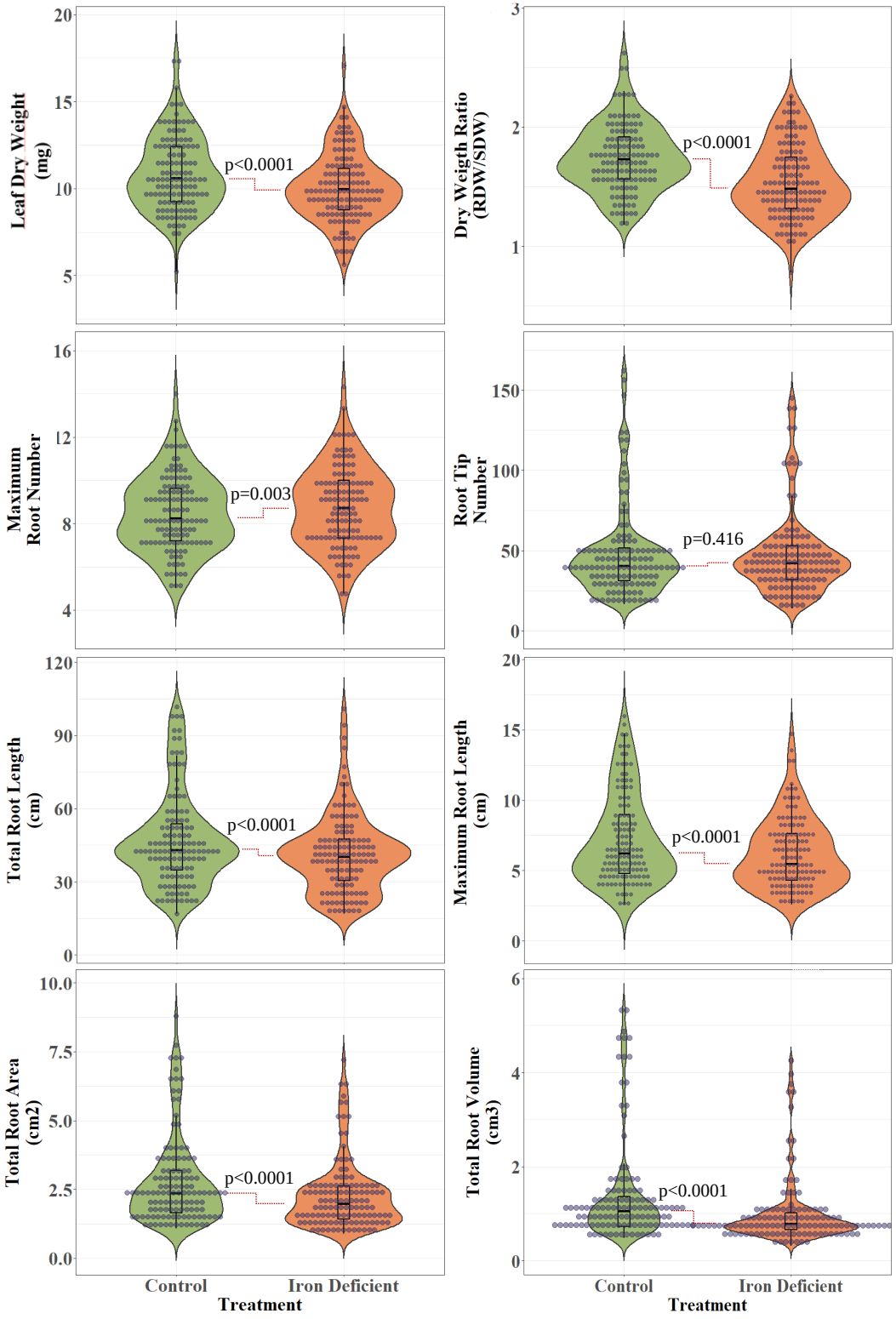

Figure 3.1. Plots of the studied traits under control and Fe-deficient conditions.

3.2 Selection of Sensitive and Tolerant Genotypes under Fe Deficiency

Iron deficiency-sensitive genotypes showed decreases in some traits, such as CHL; thus, the relative change of those traits was negative under Fe deficiency compared to the control condition. On the contrary, in tolerant genotypes, these relative changes were either positive or negative but were not as low as in the negative values of sensitive ones. Hence, in Table 3.4, genotypes were placed in descending order. Therefore, the genotypes in the top and bottom 10% rows were considered candidate tolerant and sensitive durum wheat genotypes, respectively. In this aspect, another table was generated to see the most sensitive and tolerant genotypes clearer among the candidates (Table 3.5). The threshold for classification as a candidate was adjusted to be in the top or bottom 10% of at least five traits among the traits of FCR, RA, CHL, LA, LFW, RFW, TRL, MRL, TRA and TRV (Table 3.4). Because the relative changes of these traits were significant, and in such studies, it can be determined whether the plant has been affected or not by looking at these traits. Later, the genotypes were further analyzed and put in order by their relative changes to determine the most sensitive and tolerant genotypes. As a result, in the studied population, "Gap" has been defined as the most sensitive genotype to Fe deficiency, followed by the genotypes Ceylan-95, Tunca-79, Aydın-93, Fatasel-185/1, Diyarbakır-81, Sham-1 and Özberk, respectively; whereas "TR56128-Eskişehir" has been determined as the most tolerant genotype, followed by the genotypes TR54977-Yozgat, TR56135-Eskişehir, TR53861-Yozgat, Artuklu, TR46881-Erzincan, and Beyaziye, respectively (Table 3.5). Among the candidate sensitive genotypes, the traits of CHL, LA, LFW, TRL, MRL, TRA, and TRV were found to be in the bottom 10%, whereas FCR and RA were in the Top 10%. There were a few exceptions to this ruling. For instance, Diyarbakır-81 and Özberk showed a great decrease in LA, LFW, TRL and MRL, and a non-significant 3 and 12% increase in CHL, respectively. Similarly, among the candidate tolerant genotypes, LA, LFW, TRL, MRL, TRA, and TRV were found in the top 10%, which is an opposite trend compared to the other group, whereas FCR and RA were found in both columns.

In Appendix B, IDC is shown in the leaf scans of the top four candidate tolerant and sensitive genotypes, while Appendix C presents the root architectures of these top four candidate genotypes.

Table 3.4 Top and bottom 10% tails of the relative change of the studied traits. Numbers correspond to the genotype numbers in Appendix A.

Traits		RFCR	RRA	RCHL	RLA	RLFW	RRFW	RTRL	RMRL	RTRA	RTRV
Top 10%	←	20	47	40	113	12	4	88	87	91	87
		6	35	64	28	70	68	52	96	87	91
		5	17	39	91	64	74	24	88	88	96
		24	20	84	87	95	3	87	91	70	70
		12	11	101	70	68	51	91	70	96	88
		69	15	38	95	107	69	57	20	20	20
		16	33	46	52	52	29	92	27	79	1
		22	26	63	85	87	80	79	75	6	9
		80	19	23	24	28	56	20	79	16	79
		115	12	28	120	20	15	96	120	50	16
		11	16	92	80	91	75	70	102	92	120
		23	3	13	88	80	109	64	1	120	17
		...									
Bottom 10%	→	120	95	42	71	23	48	15	15	114	90
		57	99	47	32	4	26	40	26	37	93
		51	43	29	23	3	117	23	40	4	33
		29	94	45	104	83	28	99	4	14	18
		98	93	73	115	81	8	26	14	15	35
		99	51	15	40	44	82	5	23	48	48
		61	79	26	83	14	23	22	38	26	26
		110	108	50	47	40	90	47	22	47	5
		84	90	1	42	41	123	38	47	38	14
		122	69	44	41	60	63	48	42	22	22
		88	88	21	44	65	122	44	106	44	44
		113	105	22	60	47	101	42	44	42	42

Yellow, green, orange, and red color-filled cells correspond to genotypes belonging to TR-CVs (Turkish cultivars), For-CVs (Foreign cultivars), TR-LDs (Turkish landraces), and Pop-LDs (Popular landraces), respectively.

Table 3.5 The most sensitive and tolerant genotypes.

Genotype No - Name	Top 10%	Bottom 10%
44 - Gap	-	CHL, LA, LFW, TRL, MRL, TRA, TRV
42 - Ceylan-95	-	CHL, LA, TRL, MRL, TRA, TRV
47 - Tunca-79	RA	CHL, LA, LFW, TRL, MRL, TRA
22 - Aydın-93	FCR	CHL, TRL, MRL, TRA, TRV
26 - Fatasel-185/1	RA	CHL, RFW, TRL, MRL, TRA, TRV
23 - Diyarbakır-81	CHL, FCR	LA, LFW, RFW, TRL, MRL
15 - Sham-1	RA, RFW	CHL, TRL, MRL, TRA
40 - Özberk	CHL	LA, LFW, TRL, MRL
Genotype No - Name	**Top 10%**	**Bottom 10%**
87 - TR56128-Eskişehir	LA, LFW, TRL, MRL, TRA, TRV	-
88 - TR54977-Yozgat	LA, TRL, MRL, TRA, TRV	FCR, RA
91 - TR56135-Eskişehir	LA, LFW, TRL, MRL, TRA, TRV	-
70 - TR53861-Yozgat	LA, LFW, TRL, MRL, TRA, TRV	-
20 - Artuklu	FCR, RA, LFW, TRL, MRL, TRA, TRV	-
79 - TR46881-Erzincan	TRL, MRL, TRA, TRV	RA
120 - Beyaziye	LA, MRL, TRA, TRV	FCR

Yellow, orange, and red color-filled cells correspond to genotypes belonging to TR-CVs, TR-LDs, and Pop-LDs, respectively.

3.3 Genome-Wide Association Analysis

A genome-wide association study resulted in a Manhattan plot with a threshold level of -log(p)=7.00, and in total, significantly associated 8 SNPs ($-\log_{10}(p) \geq 7$) were identified. Table 3.6 and Figure 3.2 provide information about the significant markers associated with various traits in a wheat genome study. For the CHL trait, one significant marker was identified: DArT3384738 on chromosome 1A at position 548,633,743 bp with a -log(p) value of 10.88. In the case of the FCR trait, two notable markers were identified: DArT1318188 on chromosome 4A at 690,787,802 bp with a -log(p) value of 7.58 and SNP-3937683 on chromosome 4B at 54,293,590 bp with a -log(p) value of 12.74. For the RFW trait, DArT1262476 on chromosome 7A at position 14,674,804 bp is significant with a -log(p) value of 9.04. Regarding the RDW trait, SNP-3064513 on chromosome 2B at 578,621,680 bp shows a -log(p) value of 9.77. The MRL trait is marked by a significant marker, DArT4408556, on chromosome 7A at position 108,024,120 bp with a remarkable -log(p) value of 17.00. For the TRA and TRV traits, the same marker, DArT1108111, on chromosome 6A at position 601,941,734 bp was found to be significantly associated with -log(p) values of 18.70 and 12.03, respectively.

Table 3.6 Detected SNP markers for studied traits in the population.

Trait	Marker	Chr.	Position (bp)	p-value	-log(p)	MAF	Effect
CHL	DArT3384738	1A	548,633,743	1.31E-11	10.88	0.118	-9.63
FCR	DArT1318188	4A	690,787,802	2.64E-08	7.58	0.354	-82.84
	SNP-3937683	4B	54,293,590	1.82E-13	12.74	0.150	119.32
RFW	DArT1262476	7A	14,674,804	9.15E-10	9.04	0.260	-9.48
RDW	SNP-3064513	2B	578,621,680	1.72E-10	9.77	0.045	-10.20
MRL	DArT4408556	7A	108,024,120	1.00E-17	17.00	0.225	-16.25
TRA	DArT1108111	6A	601,941,734	2.00E-19	18.70	0.061	-14.14
TRV	DArT1108111	6A	601,941,734	9.40E-13	12.03	0.061	-16.17

MAF, Minor Allele Frequency.

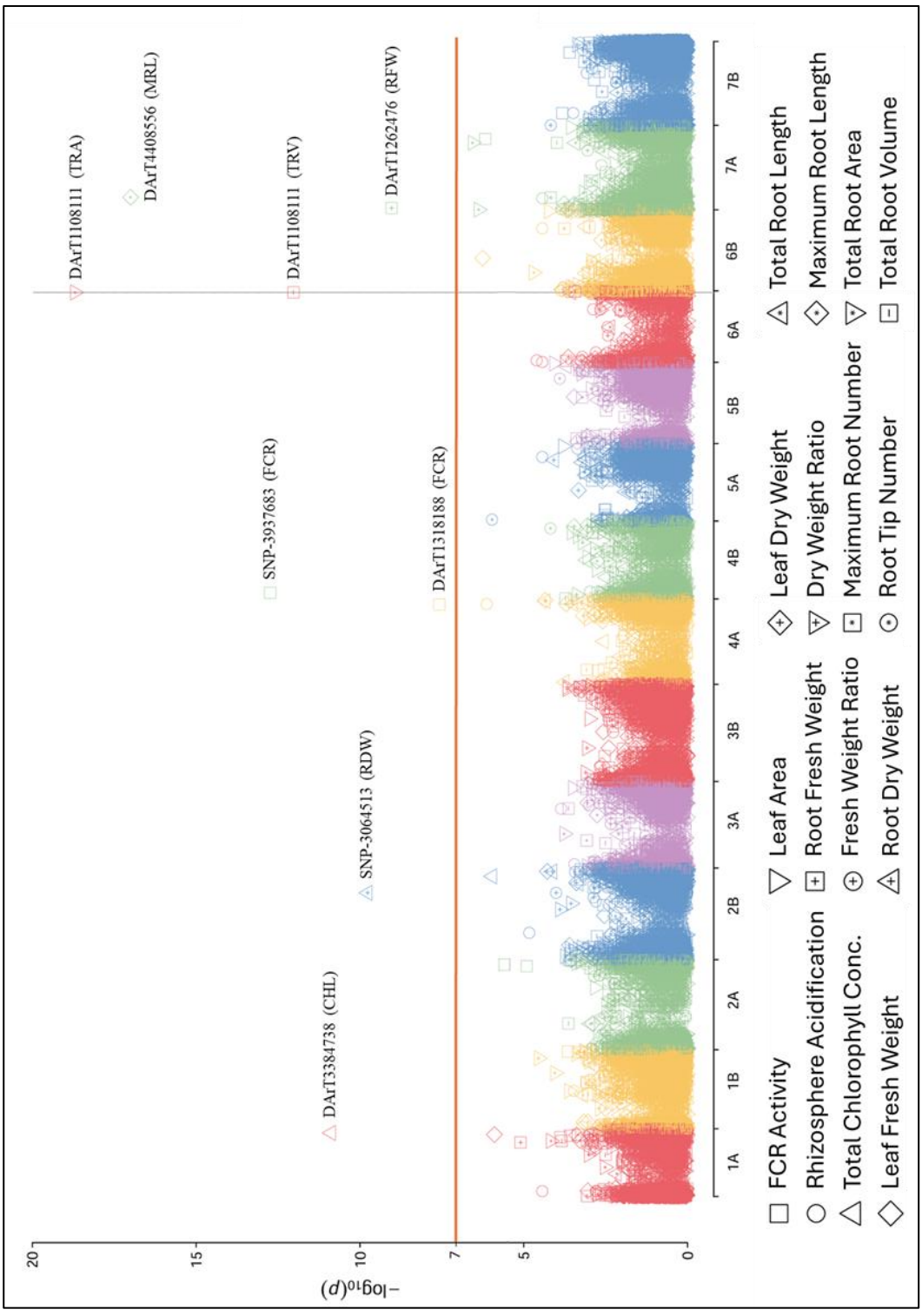

Figure 3.2. The Manhattan plot of the GWAS results for all studied traits. The names of the markers and the related associated traits were stated.

The candidate genes of each marker in Table 3.6 were listed with their *Arabidopsis thaliana* orthologs in Table 3.7 to Table 3.12. The gene description was added in the tables if the gene name was unavailable. The investigated regions for each marker can be seen in Figure 3.3. For the marker DArT3384738 (associated with CHL trait), 23 candidate genes; for the marker SNP-3064513 (associated with RDW trait), 2 candidate genes; for the marker SNP-3937683 (associated with FCR trait), 8 candidate genes; for the marker DArT1108111 (associated with TRA and TRV trait), 16 candidate genes; for the marker DArT1262476 (associated with RFW trait), 9 candidate genes; and lastly for the marker DArT4408556 (associated with MRL trait), 5 candidate genes were identified. However, no candidate genes were identified for the marker DArT1318188 (associated with FCR trait).

Table 3.7 The candidate genes near marker DArT3384738 (associated with CHL trait) and their orthologs in *Arabidopsis thaliana*.

Triticum durum **Gene ID**	***Arabidopsis thaliana*** **Ortholog**		
	Gene ID	**Gene Abbreviation**	**Gene Name**
TRITD1Av1G210610	AT4G22060	*FDB29*	*F-BOX/DUF295 BRASSICEAE-SPECIFIC 29*
TRITD1Av1G210640; TRITD1Av1G210700	AT2G26160	*FDA16*	*F-BOX/DUF295 ANCESTRAL 16*
TRITD1Av1G210650	AT1G10110	*FDB1*	*F-BOX/DUF295 BRASSICEAE-SPECIFIC 1*
TRITD1Av1G210660	AT2G17030	*FDA11; SKIP23*	*F-BOX/DUF295 ANCESTRAL 11; SKP1/ASK-INTERACTING PROTEIN 23*
TRITD1Av1G210670	AT1G31880	*BRX; NLM9*	*BREVIS RADIX*
TRITD1Av1G210690	AT1G44080	*FDA1*	*F-BOX/DUF295 ANCESTRAL 1*
TRITD1Av1G210710	AT5G60860	*RABA1F*	*RAB GTPASE HOMOLOG A1F*
TRITD1Av1G210720	AT3G15070	*TEAR2; CTL02*	*TIE1-ASSOCIATED 33 RING-TYPE E3 LIGASE 2*
TRITD1Av1G210730; TRITD1Av1G210740; TRITD1Av1G210750	AT5G36910	*THI2.2*	*THIONIN 2.2*
TRITD1Av1G210830	AT5G45540	N/A	Transmembrane protein, putative
TRITD1Av1G210860	AT2G24490	*ROR1; RPA2; RPA32A*	*SUPPRESSOR OF ROS1; REPLICON PROTEIN A2*
TRITD1Av1G210870	N/A	N/A	N/A
TRITD1Av1G210950	AT2G19960	N/A	hAT family dimerization domain-containing protein
TRITD1Av1G210960	AT4G05050	*UBQ11*	*UBIQUITIN 11*
TRITD1Av1G210990	AT1G27650	*C3H8; U2AF35A*	N/A
TRITD1Av1G211190; TRITD1Av1G211240	AT1G28480	*GRX480; GRXC9; ROXY19*	N/A
TRITD1Av1G211210	AT5G44170	N/A	S-adenosyl-L-methionine-dependent methyltransferases superfamily protein
TRITD1Av1G211220	AT5G44150	*CER16; RIPR*	*ECERIFERUM 16; R RST1 INTERACTING PROTEIN*
TRITD1Av1G211270	AT2G20520	*FLA6*	*FASCICLIN-LIKE ARABINOGALACTAN 6*

N/A: Not available.

Table 3.8 The candidate genes near marker SNP-3064513 (associated with RDW trait) and their orthologs in *Arabidopsis thaliana*.

Triticum durum **Gene ID**	***Arabidopsis thaliana*** **Ortholog**		
	Gene ID	**Gene Abbreviation**	**Gene Name**
TRITD2Bv1G195190	AT2G46870	*NGA1*	*NGATHA1*
TRITD2Bv1G195240	AT4G10500	*DLO1*	*DMR6-LIKE OXYGENASE 1*

Table 3.9 The candidate genes near marker SNP-3937683 (associated with FCR trait) and their orthologs in *Arabidopsis thaliana*.

Triticum durum **Gene ID**	***Arabidopsis thaliana*** **Ortholog**		
	Gene ID	**Gene Abbreviation**	**Gene Name**
TRITD4Bv1G020650	AT2G23760	*BLH4; SAW2*	*BEL1-LIKE HOMEODOMAIN 4; SAWTOOTH 2*
TRITD4Bv1G020670	AT5G14105	N/A	Hypothetical protein
TRITD4Bv1G020800	AT1G76610	*DUF617*	*MIZU-KUSSEI-like protein*
TRITD4Bv1G020840	AT5G10530	*LECRK-IX.1*	*L-TYPE LECTIN RECEPTOR KINASE IX.1*
TRITD4Bv1G020920	AT5G66590	N/A	Cysteine-rich secretory proteins, Antigen 5, and Pathogenesis-related 1 protein, superfamily protein
TRITD4Bv1G020940; TRITD4Bv1G020960	AT3G42170	*DAYSLEEPER*	N/A
TRITD4Bv1G020950	AT5G47635	N/A	Pollen Ole e 1 allergen and extensin family protein

N/A: Not available.

Table 3.10 The candidate genes near marker DArT1108111 (associated with TRA and TRV trait) and their orthologs in *Arabidopsis thaliana*.

Triticum durum **Gene ID**	***Arabidopsis thaliana*** **Ortholog**		
	Gene ID	**Gene Abbreviation**	**Gene Name**
TRITD6Av1G219960	AT1G31800	*CYP97A3; LUT5*	*CYTOCHROME P450, FAMILY 97, SUBFAMILY A, POLYPEPTIDE 3; LUTEIN DEFICIENT 5*
TRITD6Av1G219970	AT4G36910	*CBSX1; CDCP2; LEJ2;*	*CBS DOMAIN CONTAINING PROTEIN 1; CYSTATHIONE [BETA]-SYNTHASE DOMAIN-CONTAINING PROTEIN 2; LOSS OF THE TIMING OF ET AND JA BIOSYNTHESIS 2*
TRITD6Av1G219990	N/A	N/A	N/A
TRITD6Av1G220060	AT1G07540	*TRFL2*	*TRF-LIKE 2*
TRITD6Av1G220070	AT2G33150	*KAT2; PKT3; PED1*	*3-KETOACYL-COA THIOLASE 2; PEROXISOMAL 3-KETOACYL-COA THIOLASE 3; PEROXISOME DEFECTIVE 1*
TRITD6Av1G220080	AT4G23180	*CRK10; RLK4*	*CYSTEINE-RICH RLK (RECEPTOR-LIKE PROTEIN KINASE) 10*
TRITD6Av1G220090	AT2G33310	*IAA13*	*AUXIN-INDUCED PROTEIN 13*
TRITD6Av1G220100	AT1G04690	*KAB1; KV-BETA1*	*POTASSIUM CHANNEL BETA SUBUNIT 1*
TRITD6Av1G220110	AT3G47390	*PHS1; PYRR*	*PHOTOSENSITIVE 1; PYRIMIDINE REDUCTASE*
TRITD6Av1G220150	AT1G08125	N/A	S-adenosyl-L-methionine-dependent methyltransferases superfamily protein
TRITD6Av1G220160	AT2G29760	*OTP81; QED1*	*ORGANELLE TRANSCRIPT PROCESSING 81*
TRITD6Av1G220170	AT3G53530	*ATHMP30; NAKR3*	*HEAVY METAL ASSOCIATED PROTEIN 30; SODIUM POTASSIUM ROOT DEFECTIVE 3*
TRITD6Av1G220220	AT2G24960	N/A	Myb/SANT-like DNA-binding domain protein
TRITD6Av1G220250	N/A	N/A	N/A
TRITD6Av1G220280	AT5G03380	*ATHMP43*	*HEAVY METAL ASSOCIATED PROTEIN 43*
TRITD6Av1G220370	AT5G04270	*PAT15*	*PROTEIN ACYL TRANSFERASE 15*

N/A: Not available

Table 3.11 The candidate genes near marker DArT1262476 (associated with RFW trait) and their orthologs in *Arabidopsis thaliana*.

Triticum durum **Gene ID**	***Arabidopsis thaliana*** **Ortholog**		
	Gene ID	**Gene Abbreviation**	**Gene Name**
TRITD7Av1G008400	N/A	N/A	N/A
TRITD7Av1G008440	AT4G34020	*DJ1C*	*DJ-1 HOMOLOG C*
TRITD7Av1G008460	AT1G49010	*MYBL; MYBS1*	N/A
TRITD7Av1G008550	AT1G55490	*CPN60B; CPNB1; LEN1*	*CHAPERONIN 60 BETA; CHAPERONIN-60BETA1; LESION INITIATION 1*
TRITD7Av1G008680	N/A	N/A	N/A
TRITD7Av1G008710	AT4G19090	N/A	Transmembrane protein, putative
TRITD7Av1G008850; TRITD7Av1G008860	AT1G47890	*RLP7*	*RECEPTOR LIKE PROTEIN 7*
TRITD7Av1G008990	AT2G28370	*CASPL5A2*	*CASP-LIKE PROTEIN 5A2*

N/A: Not available.

Table 3.12 The candidate genes near marker DArT4408556 (associated with MRL trait) and their orthologs in *Arabidopsis thaliana*.

Triticum durum **Gene ID**	***Arabidopsis thaliana*** **Ortholog**		
	Gene ID	**Gene Abbreviation**	**Gene Name**
TRITD7Av1G049850	AT5G50430	*UBC33*	*UBIQUITIN-CONJUGATING ENZYME 33*
TRITD7Av1G049880	AT2G26440	*PME12*	*PECTIN METHYLESTERASE 12*
TRITD7Av1G049890	AT3G14280	N/A	LL-diaminopimelate aminotransferase
TRITD7Av1G049900	AT4G32110	N/A	Beta-1,3-N-Acetylglucosaminyltransferase family protein
TRITD7Av1G049970	AT5G58010	*DROP3; LRL3*	*DEFECTIVE REGION OF POLLEN 3; LJRHL1-LIKE 3*

N/A: Not available.

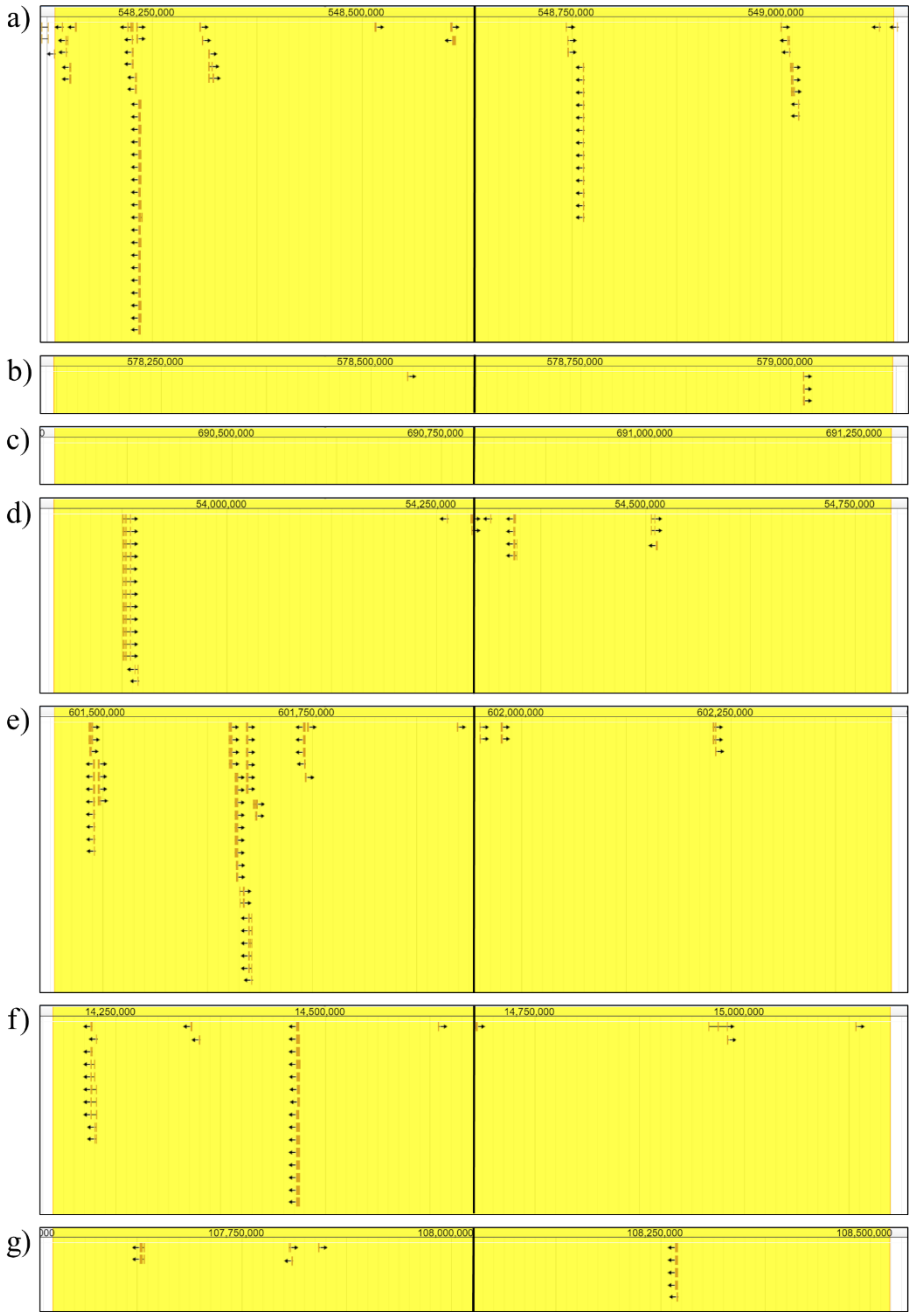

Figure 3.3. Investigated areas of each marker in the genome browser. The images belong to a) marker DArT3384738 (CHL trait), b) marker SNP-3064513 (RDW trait), c) marker DArT1318188 (FCR trait), d) marker SNP-3937683 (FCR trait), e) marker DArT1108111 (TRA and TRV traits), f) marker DArT1262476 (RFW trait) and g) marker DArT4408556 (MRL trait). Black line represents the start position of the investigated marker.

The gene ontology analysis was performed for the potential candidate genes in Tables 3.7 to 3.12. Tables 3.13 to 3.18 provided many significant enrichments in different biological processes of potential candidate genes associated with various traits. Each table lists the GO term accession numbers and the corresponding biological processes. The analysis reveals several key insights. For total chlorophyll content (CHL), the genes were involved in processes like RNA splicing, photoperiodism, salicylic and jasmonic acid signaling pathways, and various aspects of root development and hormone signaling (Table 3.13). Regarding root dry weight (RDW), the related genes were linked to leaf and flower development, responses to bacteria and fungi, and defense mechanisms, particularly involving salicylic acid pathways (Table 3.14). Ferric chelate reductase activity (FCR) was associated with genes implicated in hydrotropism, leaf morphogenesis, defense responses, and protein phosphorylation (Table 3.15). The total root area (TRA) and total root volume (TRV) were the traits associated with genes involved in ion transport, lipid metabolism, chloroplast organization, and various metabolic processes, including responses to high light intensity and hypoxia (Table 3.16). Genes linked to root fresh weight (RFW) were related to protein folding, response to cold, systemic acquired resistance, cell death, and glutamine metabolism (Table 3.17). Lastly, maximum root length (MRL) was associated with the genes involved in pectin catabolism, cell wall organization and modification, response to bacteria, protein ubiquitination, and water deprivation responses.

Table 3.13 Gene ontology analysis of potential candidate genes from the marker DArT3384738 (CHL).

GO term accession	GO term name
GO:0006397	mRNA processing
GO:0000398	mRNA splicing, via spliceosome
GO:0008380	RNA splicing
GO:0048573	photoperiodism, flowering
GO:0009751	response to salicylic acid
GO:0009867	jasmonic acid mediated signaling pathway
GO:0000122	negative regulation of transcription by RNA polymerase II
GO:0009863	salicylic acid mediated signaling pathway
GO:0030154	cell differentiation
GO:2000280	regulation of root development
GO:0048527	lateral root development
GO:0048364	root development
GO:0009736	cytokinin-activated signaling pathway
GO:0009734	auxin-activated signaling pathway
GO:0009737	response to abscisic acid
GO:0010078	maintenance of root meristem identity
GO:0048756	sieve cell differentiation
GO:0010088	phloem development
GO:0010315	auxin export across the plasma membrane
GO:0008150	biological process
GO:0016567	protein ubiquitination
GO:0006260	DNA replication
GO:0006281	DNA repair
GO:0006310	DNA recombination
GO:0006974	cellular response to DNA damage stimulus
GO:0006807	nitrogen compound metabolic process
GO:0044238	primary metabolic process
GO:0043170	macromolecule metabolic process
GO:0060776	simple leaf morphogenesis
GO:0006511	ubiquitin-dependent protein catabolic process
GO:0006952	defense response
GO:0035821	modulation of process of another organism
GO:0032259	methylation
GO:0015031	protein transport

Table 3.14 Gene ontology analysis of potential candidate genes from the marker SNP-3064513 (RDW).

GO term accession	GO term name
GO:0006355	regulation of DNA-templated transcription
GO:0048366	leaf development
GO:0009908	flower development
GO:1901371	regulation of leaf morphogenesis
GO:0006952	defense response
GO:0009617	response to bacterium
GO:0009620	response to fungus
GO:0009751	response to salicylic acid
GO:0002229	defense response to oomycetes
GO:0002239	response to oomycetes
GO:0010150	leaf senescence
GO:0046244	salicylic acid catabolic process

Table 3.15 Gene ontology analysis of potential candidate genes from the marker SNP-3937683 (FCR).

GO term accession	GO term name
GO:0010274	hydrotropism
GO:0006355	regulation of DNA-templated transcription
GO:0009965	leaf morphogenesis
GO:0048363	mucilage pectin metabolic process
GO:0009791	post-embryonic development
GO:0016310	phosphorylation
GO:0006952	defense response
GO:0050896	response to stimulus
GO:0009626	plant-type hypersensitive response
GO:0006468	protein phosphorylation
GO:0002229	defense response to oomycetes
GO:0008150	biological process

Table 3.16 Gene ontology analysis of potential candidate genes from the marker DArT1108111 (TRA and TRV).

GO term accession	GO term name
GO:0006811	monoatomic ion transport
GO:0006813	potassium ion transport
GO:0034220	monoatomic ion transmembrane transport
GO:0008150	biological_process
GO:0032259	methylation
GO:0016117	carotenoid biosynthetic process
GO:0016123	xanthophyll biosynthetic process
GO:0009451	RNA modification
GO:0031425	chloroplast RNA processing
GO:0006633	fatty acid biosynthetic process
GO:0006629	lipid metabolic process
GO:0006631	fatty acid metabolic process
GO:0031408	oxylipin biosynthetic process
GO:0009611	response to wounding
GO:0009789	positive regulation of abscisic acid-activated signaling pathway
GO:0009695	jasmonic acid biosynthetic process
GO:0006635	fatty acid beta-oxidation
GO:0010111	glyoxysome organization
GO:0006355	regulation of DNA-templated transcription
GO:0009734	auxin-activated signaling pathway
GO:0009733	response to auxin
GO:0008152	metabolic process
GO:0009231	riboflavin biosynthetic process
GO:0006807	nitrogen compound metabolic process
GO:0009644	response to high light intensity
GO:0009658	chloroplast organization
GO:0046443	FAD metabolic process
GO:1901135	carbohydrate derivative metabolic process
GO:0071704	organic substance metabolic process
GO:0016310	phosphorylation
GO:0006468	protein phosphorylation
GO:0045454	cell redox homeostasis
GO:0071456	cellular response to hypoxia

Table 3.17 Gene ontology analysis of potential candidate genes from the marker DArT1262476 (RFW).

GO term accession	GO term name
GO:0006355	regulation of DNA-templated transcription
GO:0006457	protein folding
GO:0042026	protein refolding
GO:0009409	response to cold
GO:0009627	systemic acquired resistance
GO:0008219	cell death
GO:0051085	chaperone cofactor-dependent protein refolding
GO:0006541	glutamine metabolic process
GO:0009658	chloroplast organization
GO:0006355	regulation of DNA-templated transcription
GO:0006457	protein folding
GO:0042026	protein refolding
GO:0009409	response to cold
GO:0009627	systemic acquired resistance
GO:0008219	cell death
GO:0051085	chaperone cofactor-dependent protein refolding
GO:0006541	glutamine metabolic process
GO:0009658	chloroplast organization

Table 3.18 Gene ontology analysis of potential candidate genes from the marker DArT4408556 (MRL).

GO term accession	GO term name
GO:0045490	pectin catabolic process
GO:0071555	cell wall organization
GO:0042545	cell wall modification
GO:0009617	response to bacterium
GO:0016567	protein ubiquitination
GO:0042631	cellular response to water deprivation
GO:1902457	negative regulation of stomatal opening
GO:0006355	regulation of DNA-templated transcription
GO:0080147	root hair cell development

CHAPTER 4

DISCUSSION

Like all other living organisms, plants require essential nutrients for their growth and development. These crucial nutrients are vital because they directly influence various physiological processes within the plant. Without these nutrients, plants may encounter growth deficiencies, reduced yields, or even display visible symptoms of nutrient deficiencies such as stunted growth, yellowing of leaves, or poor fruit development. Therefore, ensuring the availability of essential nutrients is crucial for promoting healthy plant growth and optimizing agricultural productivity.

The main iron deficiency symptom is iron deficiency chlorosis (IDC), which occurs between leaf veins and results in a delay in flowering, stunted growth, and reduced yield (Clark et al., 1988). Additionally, as mentioned in the Introduction chapter, the rhizosphere acidification process facilitated by proton transport in the root cell membrane, following the reduction of ferric iron to ferrous iron through FERRIC CHELATE REDUCTASE (FCR), are consecutive activities known as "Strategy I" to uptake ferric iron by dicots in soil. The findings of this study indicate that durum wheat, despite being a gramineous species, utilizes Strategy I to uptake insoluble iron from the soil in addition to Strategy II. Over the past two decades, certain gramineous plants may have adopted a combination of iron uptake strategies to enhance iron absorption. For example, the involvement of OsNAS1, OsNAS2, OsNAAT1, OsDMAS1, and OsYSL15 genes in Strategy II has been established in rice. Still, it was also revealed that *OsIRT1*, *OsIRT2*, and *OsFRO1* were induced in the roots of rice under Fe deficiency as a Strategy I pathway (Bashir et al., 2006; Higuchi et al., 2001; Inoue et al., 2003, 2008, 2009; Ishimaru et al., 2006; Walker & Connolly, 2008). On the other hand, maize, as a gramineous plant, utilizes Strategy II for iron uptake with *ZmYS1* and some *ZmNAS* genes. However, as observed in

rice, *ZmIRT1, ZmIRT2,* and many *ZmZIP* genes were also involved in iron uptake in maize roots as Strategy I (S. Li et al., 2013, 2022; Zhou et al., 2013). Lastly, in bread wheat (*Triticum aestivum*), another gramineous plant, *FRO2-2A* and *IRT1a-4A* were highly upregulated under iron deficiency (Hua et al., 2022). Our study showed that chlorophyll biosynthesis has disrupted and resulted in IDC in the leaves. Also, FCR enzyme activity in the roots and rhizosphere acidification levels increased, with 24.9% and 30.3% due to iron deficiency, respectively. The reduction in chlorophyll content, increased FCR enzyme activity, and rhizosphere acidification were expected and are well-known Fe deficiency responses studied previously (Guo et al., 2020; J. Li et al., 2021).

In our study, we aimed to measure phytosiderophore levels but encountered two main challenges that prevented us from doing so. Firstly, technical challenges arose due to unclear and outdated protocol instructions. Secondly, the high number of plants (450 plants/set) made it impossible to execute each step of the protocol within the same circadian rhythm. Since the phytosiderophore secretion varies throughout a plant's circadian cycle (Walter et al., 1995), it is important to finish the protocol for all samples to prevent undesired variation. Despite these obstacles, our findings provided sufficient data to identify candidate genotypes sensitive and tolerant to iron deficiency among the panel by examining traits associated with Strategy I, namely FCR and RA.

Leaf development also suffers from the overall deterioration in plant growth. The significant decreases in both leaf fresh weight (LFW) and leaf dry weight (LDW) were comparatively lower at 5.8% and 7.5%, respectively, than the decreases in root fresh weight (RFW) at 24.3% and root dry weight (RDW) at 15.9%. Consequently, the significant reduction in root-to-leaf fresh weight ratio (FWR) was more pronounced at 17.2% compared to the significant decrease in dry weight ratio (DWR) at 11.5%. These findings imply that iron deficiency primarily impacts root biomass over leaf biomass. Additionally, leaf area (LA), measured from the second oldest leaf of the plants, exhibited a significant 7.1% decrease, consistent with the reductions observed in LFW and LDW. This aligns with previous research on rice,

which also noted a greater decline in root biomass compared to leaf biomass, coupled with a reduction in leaf area (W. Wang et al., 2020).

Besides the negative effects of iron deficiency on above soil properties, it was also recognized that iron deficiency has a tremendous negative impact on root growth (M. R. Jiménez et al., 2019; Kobayashi et al., 2014; Zocchi et al., 2007). Many significant reductions in physiological traits in roots (RFW, RDW, TRL, MRL, TRA, and TRV) were observed and consistent with previous findings (W. Wang et al., 2020). These reductions suggest a general disruption in root growth. To adapt to limited iron availability, plants may increase the quantity of roots and root tips rather than enhancing primary root growth. Under standard conditions, fewer, longer, thicker roots are expected, accompanied by fewer root tips. Conversely, in iron-deficient conditions, roots tend to be shorter and thinner but more abundant, with numerous root tips. Studies using iron deficiency hypersensitive *iro3* mutant rice plants have shown decreases in root fresh weight, total root area, total root length, and total root tip number compared to WT plants under iron deficiency conditions (W. Wang et al., 2020). Similarly, another study found decreases in total root length, total root area, volume, and root tip number due to iron deficiency (Long et al., 2020). In our study, the significant decrease in TRL, MRL, TRA, and TRV supports the presence of shorter and thinner roots, while the significant increase in MRN indicates abundant roots in this adaptive strategy. However, no significant change was observed in RTN, which does not support the last part of the suggested strategy. The short duration of stress application may explain it. If the duration was extended, the effects would be more severe and clearer.

Basic statistics in Table 3.1, ANOVA in Table 3.2, and violin plots in Figure 3.1 collectively demonstrate that iron deficiency treatment significantly influenced almost every trait except for the root tip number. It shows that iron deficiency treatment has been successfully applied but showed no significant effect on root tip numbers in durum wheat under the specified study conditions. The bimodal distributions in the violin plots in Figure 3.1 suggest that there are two subpopulations that are tolerant and sensitive to Fe deficiency. However, some traits

showed wider distributions, making it harder to conclude the presence of the same subpopulations just by looking at the violin plots.

The ANOVA analysis revealed that the impact of genotype on the response variable varies depending on environmental conditions. However, the genotype*environment interaction was non-significant in the LA trait, which suggests that genetic effects do not vary across different environmental conditions. Furthermore, environmental influences appear to operate independently of the genotype on the observed outcome. Lastly, the consistent p values between the genotypes for the studied traits in ANOVA show that this panel of 123 durum wheat genotypes is appropriate for following GWAS.

The strongest correlation among all studied traits was between FCR and RA, with a positive r^2 value of 0.902. This ratio was valid due to strategy I of iron uptake in plants, where rhizosphere acidification and iron uptake through FCR are consecutive processes. It is also further supporting the utilization of strategy I for iron uptake by a gramineous species. A previous study showed that rhizosphere acidification and FCR activity act similarly under Fe deficiency and control conditions (Dong et al., 2019; Sun et al., 2023). Other strong correlations, such as between LFW and LDW, RFW and RDW, and FWR and DWR, were reasonable since the drying process generally decreased by around 90%. In previous studies, it was found that in peas, iron deficiency leads to a proportional reduction in these traits, with each trait decreasing by the same relative amount (Nenova, 2009). In another study, the observed decreases in LFW and LA under iron deficiency (in peach/pear), with reductions of 23/24% and 24/26%, align with the strong correlation between these traits found in our study (Fernández et al., 2008). In the physiological root traits, a strong correlation was observed between MRN and RTN, and much stronger correlations were found among TRL, MRL, TRA, and TRV. This was expected, as iron deficiency leads to significant disruptions in root growth, resulting in smaller and less abundant roots, thereby reducing the overall root length, area, and volume. Although earlier studies investigated these traits, they did not examine the correlations among them, yet they have reported that these traits decreased similarly

under iron deficiency (Long et al., 2020; Tamuk et al., 2024). Our findings suggest there might be an inherent correlation that was not previously explored. Lastly, a negative strong correlation between CHL and FCR was expected since iron deficiency symptoms are mainly involved in a mutual decrease in CHL and an increase in FCR. A previous study found that in two different peach rootstocks, CHL and FCR showed opposite trends under deficiency, which supports the negative correlation in this study (Molassiotis et al., 2006). On the contrary, another study showed a positive correlation between CHL and FCR in citrus rootstocks under iron deficiency (Llosa et al., 2009).

It was seen that the most sensitive genotypes in Table 3.5 belong to Turkish cultivars (TR-CVs), whereas tolerant genotypes were mostly Turkish landraces (Tr-LDs). These results were expected due to the nature of landraces and cultivars. Briefly, landraces have evolved naturally over a long time in a specific region without human intervention by adopting local conditions. For this reason, they are generally resistant to various biotic or abiotic conditions in their growing area. It was known that around 70% of the soil of Türkiye is classified as calcareous and alkaline, so iron availability is low. Therefore, Turkish landraces are expected to naturally tolerate iron deficiency, which was also supported by this study. On the other hand, cultivars have been cultivated through human intervention, and specific traits such as yield, flavor, and color are selected to be inherited. Even though resistance is also considered, it is not the primary concern. Therefore, susceptibility to iron deficiency among the cultivars was expected in our study. Moreover, as seen in Table 3.4, most of the genotypes in the Top 10% and Bottom 10% rows belonged to Turkish landraces and cultivars, respectively, except for the RFCR and RRA columns.

Although the other investigated traits have either significantly decreased in sensitive genotypes or a bit reduced or increased in tolerant genotypes in Table 3.5, FCR has a more complex trend. For example, sensitive genotypes have an increased FCR from 6 to 40%, where Aydın-93 and Diyarbakır-81 have 211% and 144% increase, respectively; tolerant genotypes have an increased FCR from 3 to 50%, where TR54977-Yozgat, Artuklu, and Beyaziye have 65% decrease, 600% increase,

and 30% decrease, respectively. FCR has an exceptional trend in these genotypes, which shows that its behavior is not as simple as other investigated traits. Two reasons may explain the increasing trend in FCR: it may be a symptom of Fe deficiency susceptibility or the reason for Fe deficiency tolerance. In detail, Fe deficiency-sensitive plants may significantly increase their FERRIC CHELATE REDUCTASE activity in roots in response to low Fe availability. In this way, roots can uptake as much iron as possible. On the other hand, Fe deficiency-tolerant plants may exhibit tolerance due to enhanced FCR activity in roots. As a third option, FCR may be increased because of susceptibility and increased more in the tolerant genotypes. This can connect the other two scenarios and is supported by previous findings (Aksoy et al., 2020; Connolly et al., 2003; S. Jiménez et al., 2008; Q. Tian et al., 2016).

In Appendix B, the significant reduction of chlorophyll concentrations in the leaves of candidate sensitive genotypes can be seen easily as yellowing. In iron-deficient conditions, the leaves were green to dark green, whereas under iron deficiency, the leaves suffered from chlorosis and even necrosis in the genotype Tunca-79 (genotype number 47). On the other hand, candidate-tolerant genotypes showed almost no yellowing in their leaves under both conditions.

Even though there has been no previous study on alkaline or iron deficient conditions in these durum wheat genotypes, a study investigates Fe content in the grain and thousands of kernel weights in some of the candidate genotypes of this study. Hocaoğlu et al. (2020) found that genotypes Ceyland-95, Aydın-93, Diyarbakır-81 and Özberk (Fe deficiency sensitive candidate genotypes in this study) was found to have 38.6, 35.3, 41.5 and 43.3 ppm Fe content in their grains and 44, 44, 43 and 49 grams of thousands kernel weight; whereas Artuklu (Fe deficiency tolerant candidate genotypes in this study) has 37.5 ppm Fe and 50 grams of thousands kernel weight. This study was done in Çanakkale province, located in the Marmara region of Türkiye, and phosphorus and nitrogen fertilizers during sowing. Even though the Fe content in the grains of these genotypes was analyzed, it is not sufficient to determine the Fe deficiency tolerant or sensitive genotypes. The

growing conditions and soil properties in this study significantly impact grain content. All the other micronutrients, such as zinc, manganese, etc., in the leaves and roots from our research are needed and will be investigated further. Moreover, in previous findings, only Aydın-93 was found to be tolerant to drought and heat (Barutçular et al., 2017; Budak et al., 2022). For durum wheat breeding against Fe deficiency, the tolerant candidate genotypes are an excellent resource as parental material. Therefore, as they were nominated, TR56128-Eskişehir, TR54977-Yozgat, TR56135-Eskişehir, TR53861-Yozgat, Artuklu, TR46881-Erzincan and Beyaziye genotypes can be used as parental material.

In the GWAS results, one striking feature is the repeated significance of the marker DArT1108111, which appears for both the TRA and TRV traits on chromosome 6A, positioned at 601,941,734 bp. This suggests a potential pleiotropic effect or a genome region that influences multiple characteristics. This situation is logical because the Pearson correlation test shows that root area and volume are correlated traits, resulting in a 0.940 coefficient value between them. Therefore, it is reasonable to expect that a genetic region influencing the root area would also affect root volume, as a larger root area typically allows for greater water and nutrient uptake, potentially leading to an increase in root volume. Therefore, the repeated significance of the same genetic marker for both traits may reflect this natural relationship between the two traits, suggesting that genetic variation in this region affects both traits.

The MAF values in Table 3.6 indicate the level of genetic variation at a particular SNP in the population. Higher MAF suggests minor alleles are relatively common, while lower MAF indicates rareness. The effect size indicates the strength of the association, as the larger absolute values of effect size mean a stronger influence of the marker on the trait. Additionally, positive effect sizes indicate that the minor allele increases the trait value, while negative effect sizes indicate a decrease. For example, the markers DArT1318188 on chromosome 4A and SNP-3937683 on chromosome 4B were associated with the FCR trait with large effect values. The results indicate that marker DArT1318188, with a large negative effect

size of -82.84, substantially decreases the FCR trait by 82.84 units by presenting at 15% frequency. Likewise, the marker SNP-3937683 has a large positive effect size of 119.32, substantially increasing the FCR trait by 119.32 units by presenting at 35% frequency. The other six markers have smaller negative effect sizes ranging from -16.25 to -9.48.

The lack of candidate genes for the marker DArT1318188 associated with the FCR trait at chromosome 4A and the low number of total identified genes, even though the 1Mb range of the markers was investigated, may be explained by a few reasons. Firstly, it must be known that the genome size of durum wheat is enormously bigger than other model organisms. For example, the genome size of model organisms and crops such as *Arabidopsis thaliana*, *Brassica rapa*, *Oryza sativa*, *Solanum lycopersicum*, and *Zea mays* is around 135 Mb, 455 Mb, 430 Mb, 950Mb and 2.4Gb, respectively, whereas durum wheat's genome size is 12Gb. Additionally, the durum wheat genome is not as well-known as other model organisms. As a result, the investigated 1Mb region in durum wheat (in Figure 3.3) may be in a non-coding, low-functional DNA or cis-regulatory region, or the genomic region has not been annotated or characterized in existing genomic databases. A comprehensive genome scan could have resulted in a more extensive list of potential genetic factors that could be linked with the traits under investigation. This could lead to a better understanding of the genetic basis underlying different phenotypes. For example, in a previous QTL mapping study for grain iron concentration in wheat revealed four QTLs with physical intervals of 1, 7, 30 and 58 Mb (Y. Wang et al., 2021). However, such intervals require enormous time and effort to identify candidate genes.

Some genome-wide association studies investigated the same traits in this study but in different organisms under no stress conditions. For instance, Beyer et al. (2019) conducted a GWAS on 215 soft red winter wheat genotypes, identifying two significant SNPs associated with root length on chromosome 5B among 20,881 SNPs. Similarly, Jin et al. (2023) investigated 378 maize genotypes and found numerous SNPs associated with chlorophyll content among 96,726 SNPs. Hoang et

al. (2019) explored rice genetics, identifying 11 QTLs associated with leaf fresh weight and 1 QTL associated with leaf dry weight among 21,623 SNPs. Babu et al. (2019) also uncovered two QTLs associated with leaf area in oil palm. Yan et al. (2004) delved into rhizosphere acidification, associating it with two QTLs in common bean. Lastly, Satbhai et al. (2017) investigated *Arabidopsis thaliana* under iron deficiency conditions, identifying an SNP associated with short roots, later revealing the FRO2, responsible for the reduction of iron at the root surface, was found to be the best candidate in the study. Even though the FCR activity was observed to be higher in the long root group than the short root group and had a positive correlation with the expression of *FRO2* in this study, no study investigates FCR activity in roots in a genome-wide association study.

Among the total of 63 candidate genes found for all the significant markers, some of them are important to mention. For total chlorophyll content trait, *BRX*, *BREVIS RADIX*, (AT1G31880) is known to be involved in root growth and development (Mouchel et al., 2006). Although it is directly related to root development, the *BRX* gene can influence overall plant growth and biomass accumulation, which can indirectly affect chlorophyll content as healthier, well-developed roots contribute to better nutrient uptake and chlorophyll biosynthesis in leaves. Another gene, *RABA1F, RAB GTPASE HOMOLOG A1F*, (AT5G60860) belongs to RAB GTPases, and it was known that they are involved in vesicle trafficking, which is essential for various cellular processes (Tripathy et al., 2021). These processes may include the transportation of chlorophyll biosynthetic enzymes and the distribution of chloroplast. Therefore, efficient vesicle trafficking is critical for the optimal functioning of chloroplasts and, hence, the chlorophyll content in leaves. For example, another RAB GTPase protein, CPRABA5e, was localized in chloroplast and thought to have a role in photosynthesis-related processes (Karim et al., 2014). Another gene, *THI2.2, THIONIN 2.2*, (AT5G36910) belongs to thionins, which are proteins that play a role in plant defense mechanisms. While their primary role is in response to biotic stress, they also contribute to maintaining cell integrity and function under stress conditions (Stec, 2006). For example, a previous study

showed that constitutive overexpression of *THI2.1* resulted in reduced loss of chlorophyll content compared to Col-2 ecotype after inoculation of *Fusarium oxysporum* (Epple et al., 1997). This study supports the relationship between thionins and chlorophyll content in leaves. A future study that focuses on *THI2.2* under abiotic stress, particularly iron deficiency, may reveal a novel function of, such as maintaining chlorophyll content in the leaves under iron deficiency. Among the listed genes in Table 3.7, *FDB29* (AT4G22060), *FDA16* (AT2G26160), *FDB1* (AT1G10110), *FDA11* (AT2G17030), and *FDA1* (AT1G44080) belong to F-box protein family and encode F-box proteins. They are involved in various cellular processes, including protein ubiquitination and degradation, which eventually influence chlorophyll biosynthesis and breakdown. They were also known to play important roles in abiotic stress responses. For example, in previous studies, overexpression of the wheat *TaFBA1* gene, which belongs to the F-box protein family, improved the photosynthetic capacity of plants under salt, heat, and drought stresses (Q. Li et al., 2018; Zhao et al., 2017; S. Zhou et al., 2014). The overexpression lines exhibited increased tolerance to oxidative stress, as evidenced by reduced accumulation of reactive oxygen species and lower levels of malondialdehyde (S.M. Zhou et al., 2015). Therefore, a study investigating other genes may identify a novel function of an F-box protein in chlorophyll biosynthesis under iron deficiency. For root dry weight trait, *NGA1, NGATHA1*, (AT2G46870) plays a role in auxin-mediated developmental processes, including root development. Their role in regulating genes associated with auxin responses makes them critical for root growth and biomass accumulation, directly influencing root dry weight. For example, in a previous study, overexpression of *BrNGA1* resulted in reduced organ growth, including both lateral organs and root growth (Kwon et al., 2009). Typically, reduced root growth would likely result in lower root biomass, which could potentially correlate with decreased root dry weight. To establish a direct correlation between them, experimental data measuring both variables is required. Another gene, *DLO1, DMR6-Like Oxygenase 1*, involves oxidative stress response, and it was revealed that they negatively regulate defense responses against

pathogens (Zeilmaker et al., 2015). Likewise, in our study, this gene may reduce root dry weight under iron deficiency by negatively affecting the oxidative stress responses. Further investigation into the gene expression patterns of this gene under conditions of iron deficiency could provide additional insights into its function and regulatory mechanisms. For root fresh weight trait, *DJ1C, DJ-1 HOMOLOG C*, (AT4G34020) gene was listed. It was known that DJ-1 homologs are involved in stress responses as the transgenic plants with elevated AtDJ-1a levels exhibited enhanced tolerance against environmental stress conditions (Xu et al., 2010). Therefore, this gene may have a role in tolerance to iron deficiency and affect root biomass. Another gene, *CPN60B, CHAPERONIN 60 BETA*, (AT1G55490) encodes chaperonin protein, which is crucial for protein folding and assembly. Since proper protein folding is essential for functioning many cellular processes, including cell division, elongation, and differentiation, chaperonins might indirectly influence root growth by ensuring the correct folding and functionality of proteins involved in these processes. However, direct evidence for this relationship would require further research and experimentation. For Ferric Chelate Reductase activity in roots, *BLH4*, *BEL1-LIKE HOMEODOMAIN 4,* (AT2G23760) gene encodes BEL1-like homeodomain proteins, which are transcription factors that regulate developmental processes (R. Kumar et al., 2007). Even though the role of *BHL4* in root architecture and development is not known, our study suggests that there might be a relationship between *BHL4* and root metabolic activities. These metabolic activities may involve ferric chelate reductase activity. Another gene, *LECRK-IX.1, L-TYPE LECTIN RECEPTOR KINASE IX.1,* (AT5G10530) encodes L-type lectin receptor kinases that are involved in signaling pathways that mediate plant development and abiotic and biotic stress responses (Vaid et al., 2013). In a previous study, rice lectin-type RLK *OsCORK1* was investigated for its function in copper stress response, where overexpression of *OsCORK1* was exhibited tolerance (K. Wang et al., 2023). Therefore, the *LECRK-IX.1* gene may have a potential for iron deficiency tolerance by encoding a kinase that upregulates the *FRO2* gene, eventually will increase FCR activity in roots (Vasconcelos et al., 2006). Lastly, *DUF617,* (AT1G76610) gene

encodes MIZU-KUSSEI-like protein and was thought to be important for FCR activity. Its role in lateral root development by maintaining auxin levels was known. The over-expression of *MIZ1*, encodes MIZU-KUSSEI 1 protein in roots, which showed a reduction in lateral root formation (Moriwaki et al., 2011). A reduction in lateral root development may also have positive or negative effects on FCR activity. Some genes have been found to be important to mention for total root area and volume traits. *CRK10, CYSTEINE-RICH RLK (RECEPTOR-LIKE PROTEIN KINASE) 10,* (AT4G23180) gene encodes receptor-like protein kinases that often play diverse roles in plant growth and development. Therefore, it's possible that this gene could indirectly influence root development through its involvement in signaling pathways related to stress responses or hormonal regulation. *IAA13, AUXIN-INDUCED PROTEIN 13,* (AT2G33310) gene is involved in the auxin signaling pathway, which is crucial in regulating root growth and development. Auxin is a key hormone involved in processes such as cell elongation, division, and differentiation, all of which are critical for root development. Therefore, IAA13 likely influences root area and volume through its role in auxin signaling. Moreover, the *NAKR3, SODIUM POTASSIUM ROOT DEFECTIVE 3,* (AT3G53530) gene is involved in the regulation of sodium and potassium ion homeostasis in plants. Proper ion balance is crucial for various physiological processes, including root growth and development. Mutations in the NAKR1 gene have been associated with defects in root architecture, indicating its importance in maintaining root structure and function (H. Tian et al., 2011). Therefore, NAKR3 may have also influenced the root area and volume through its role in ion homeostasis and root physiology. Lastly, *KAB1, POTASSIUM CHANNEL BETA SUBUNIT 1*, (AT1G04690) gene encodes KAB1, which is involved in regulating potassium channels. Potassium channels play a critical role in regulating ion transport and maintaining cellular ion homeostasis, which is essential for various physiological processes in plants, including root growth and development. This encoded protein can modulate the channel's activity, affecting how potassium ions are transported within the plant cells. Given the importance of potassium in cell turgor, enzyme activation, and overall plant

nutrition, KAB1 likely influences root development by regulating potassium ion transport and homeostasis. For maximum root length trait, two genes stand out: *PME12, PECTIN METHYLESTERASE 12*, (AT2G26440) and *UBC33, UBIQUITIN-CONJUGATING ENZYME 33* (AT5G50430). *PME12* encodes pectin methylesterases involved in modifying the cell wall pectins, which play crucial roles in cell adhesion, expansion, and growth (Kohli et al., 2015). Therefore, it could be related to increased root length as well. On the other hand, the *UBC33* gene involves ubiquitin-mediated protein degradation pathways (Feng et al., 2020). Even though there isn't direct evidence linking this gene to root development, ubiquitin-mediated protein degradation pathways are known to regulate various aspects of plant development, including root growth. Therefore, this gene likely influences root development.

Besides the individual investigation of these candidate genes, gene ontology results can further help reveal relationships between the candidate genes and the related traits. The gene ontology analysis of CHL trait indicates the importance of a complex network of regulatory mechanisms such as jasmonic acid mediated signaling pathway and response to salicylic acid. Plants with efficient salicylic and jasmonic acid signaling pathways can better manage stress and enhance overall plant health and chlorophyll content. Likewise, lateral root development finding can be associated with CHL, as the enhanced root growth results in better nutrient and water uptake and eventually increases chlorophyll content. For RDW, it was seen that this trait is influenced by both growth-related processes and environmental stress responses. Regarding FCR, those functions highlight the role of FCR in morphological development, and adaptive stress responses in roots. The analysis for TRA and TRV indicates that these traits are governed by a wide range of metabolic activities and environmental response mechanisms. For instance, unidimensional cell growth refers to elongation along one axis, which is critical for root elongation and branching. Genes involved in this process may contribute to root length and overall root system architecture, directly impacting root area and volume. For RFW, those associations underscore the importance of protein homeostasis, stress

responses, and metabolic regulation in determining root biomass. For example, efficient stress management can lead to healthier roots and increase in root fresh weight. Lastly for MRL trait, the results suggest that root elongation is tightly regulated by structural modifications, defense mechanisms, and responses to water availability. For example, genes promoting root hair cell differentiation can enhance root length by increasing the absorptive capacity and growth potential of the root system.

Overall, this comprehensive gene ontology analysis highlights the diverse and complex genetic regulatory networks underlying important physiological and biochemical traits in plants. It reflects a broad array of metabolic, developmental, and stress response pathways, aiding in understanding the molecular basis of these traits and potentially guiding future research and breeding programs aimed at improving plant performance.

CHAPTER 5

CONCLUSION

In this study, we investigated the physiological and biochemical responses of 123 durum wheat genotypes *(Triticum durum)* under iron deficiency, focusing on understanding the genetic basis of these responses. We applied iron deficiency treatments and measured various traits associated with plant growth and iron uptake strategies. The significant findings of this study can be listed as:

1. Iron deficiency has significantly impacted various physiological and biochemical traits in durum wheat, including increased FCR enzyme activity in roots, rhizosphere acidification, and maximum root number traits. It decreases in all the other investigated traits.
2. Importantly, this study also supported the idea of utilization of two iron uptake strategies, Strategy I and II, by wheat to absorb Fe in soil.
3. Genetic analysis identified seven markers associated with total chlorophyll concentration, FCR enzyme activity in roots, root fresh and dry weights, maximum root length, total root area and volume traits; and 63 candidate genes in *Triticum durum* and their orthologs in *Arabidopsis thaliana*.
4. Analysis of genotype responses revealed distinct patterns of sensitivity and tolerance to iron deficiency, where Turkish landraces, TR56128-Eskişehir, TR54977-Yozgat, TR56135-Eskişehir and other candidate tolerant genotypes demonstrated tolerance, and Turkish cultivars, Gap, Ceylan-95, Tunca-79 and other candidate sensitive genotypes demonstrated sensitivity.

In conclusion, our study contributes to understanding durum wheat's response to iron deficiency and provides valuable insights into the genetic basis of trait variation.

Identifying candidate genotypes and genetic markers associated with tolerance to iron deficiency can be used as resources for targeted breeding efforts aimed at developing durum wheat varieties with improved tolerance to iron deficiency. Future research could focus on validating the functional significance of identified genetic markers and elucidating the underlying molecular mechanisms of plant responses to iron deficiency, ultimately enhancing agricultural productivity and food security.

REFERENCES

Ahmed, A. A. M., Mohamed, E. A., Hussein, M. Y., & Sallam, A. (2021). Genomic regions associated with leaf wilting traits under drought stress in spring wheat at the seedling stage revealed by GWAS. *Environmental and Experimental Botany*, *184*, 104393. https://doi.org/10.1016/j.envexpbot.2021.104393

Akbari, M., Wenzl, P., Caig, V., Carling, J., Xia, L., Yang, S., Uszynski, G., Mohler, V., Lehmensiek, A., Kuchel, H., Hayden, M. J., Howes, N., Sharp, P., Vaughan, P., Rathmell, B., Huttner, E., & Kilian, A. (2006). Diversity arrays technology (DArT) for high-throughput profiling of the hexaploid wheat genome. *Theoretical and Applied Genetics*, *113*(8), 1409–1420. https://doi.org/10.1007/s00122-006-0365-4

Akram, S., Arif, M. A. R., & Hameed, A. (2021). A GBS-based GWAS analysis of adaptability and yield traits in bread wheat (Triticum aestivum L.). *Journal of Applied Genetics*, *62*(1), 27–41. https://doi.org/10.1007/s13353-020-00593-1

Aksoy, E., & Koiwa, H. (2013). Determination of Ferric Chelate Reductase Activity in the Arabidopsis thaliana Root. *BIO-PROTOCOL*, *3*(15). https://doi.org/10.21769/BioProtoc.843

Aksoy, E., Maqbool, A., & Abudureyimu, B. (2020). Arpa Nikotinamin Sentaz1 (HvNAS1) Genini Yüksek Seviyede İfade Eden Arabidopsis thaliana Bitkileri Demir Eksikliğine Dayanıklılık Gösterir. *Turkish Journal of Agriculture - Food Science and Technology*, *8*, 70–79. https://doi.org/10.24925/turjaf.v8isp1.70-79.3974

Alemu, A., Feyissa, T., Tuberosa, R., Maccaferri, M., Sciara, G., Letta, T., & Abeyo, B. (2020). Genome-wide association mapping for grain shape and color traits in Ethiopian durum wheat (Triticum turgidum ssp. durum). *The Crop Journal*, *8*(5), 757–768. https://doi.org/10.1016/j.cj.2020.01.001

Alsaleh, A., Baloch, F. S., Derya, M., Azrak, M., Kilian, B., Özkan, H., & Nachit, M. (2015). Genetic Linkage Map of Anatolian Durum Wheat Derived from a

Cross of Kunduru-1149 × Cham1. *Plant Molecular Biology Reporter*, *33*(2), 209–220. https://doi.org/10.1007/s11105-014-0749-6

Alsaleh, A., Bektas, H., Baloch, F. S., Nadeem, M. A., & Özkan, H. (2022). Turkish durum wheat conserved ex-situ and in situ unveils a new hotspot of unexplored genetic diversity. *Crop Science*, *62*(3), 1200–1212. https://doi.org/10.1002/csc2.20723

Altschul, S. F., Gish, W., Miller, W., Myers, E. W., & Lipman, D. J. (1990). Basic local alignment search tool. *Journal of Molecular Biology*, *215*(3), 403–410. https://doi.org/10.1016/S0022-2836(05)80360-2

Amir, R., Hacham, Y., & Galili, G. (2002). Cystathionine γ-synthase and threonine synthase operate in concert to regulate carbon flow towards methionine in plants. *Trends in Plant Science*, *7*(4), 153–156. https://doi.org/10.1016/S1360-1385(02)02227-6

Anjum, N. A., Umar, S., Singh, S., Nazar, R., & Khan, N. A. (2008). Sulfur Assimilation and Cadmium Tolerance in Plants. In *Sulfur Assimilation and Abiotic Stress in Plants* (pp. 271–302). Springer Berlin Heidelberg. https://doi.org/10.1007/978-3-540-76326-0_13

Aoyama, T., Kobayashi, T., Takahashi, M., Nagasaka, S., Usuda, K., Kakei, Y., Ishimaru, Y., Nakanishi, H., Mori, S., & Nishizawa, N. K. (2009). OsYSL18 is a rice iron (III)–deoxymugineic acid transporter specifically expressed in reproductive organs and phloem of lamina joints. *Plant Molecular Biology*, *70*(6), 681–692. https://doi.org/10.1007/s11103-009-9500-3

Baloch, F. S., Alsaleh, A., Shahid, M. Q., Çiftçi, V., E. Sáenz de Miera, L., Aasim, M., Nadeem, M. A., Aktaş, H., Özkan, H., & Hatipoğlu, R. (2017). A Whole Genome DArTseq and SNP Analysis for Genetic Diversity Assessment in Durum Wheat from Central Fertile Crescent. *PLOS ONE*, *12*(1), e0167821. https://doi.org/10.1371/journal.pone.0167821

Barberon, M. (2017). The endodermis as a checkpoint for nutrients. *New Phytologist*, *213*(4), 1604–1610. https://doi.org/10.1111/nph.14140

Barberon, M., Dubeaux, G., Kolb, C., Isono, E., Zelazny, E., & Vert, G. (2014). Polarization of IRON-REGULATED TRANSPORTER 1 (IRT1) to the plant-soil interface plays crucial role in metal homeostasis. *Proceedings of the National Academy of Sciences*, *111*(22), 8293–8298. https://doi.org/10.1073/pnas.1402262111

Barutçular, C., El Sabagh, A., Koc, M., & Ratnasekera, D. (2017). Relationships Between Grain Yield and Physiological Traits Of Durum Wheat Varieties Under Drought And High Temperature Stress In Mediterranean Environments. *FRESENIUS ENVIRONMENTAL BULLETIN*, *26*(6), 4282–4291.

Bashir, K., Inoue, H., Nagasaka, S., Takahashi, M., Nakanishi, H., Mori, S., & Nishizawa, N. K. (2006). Cloning and Characterization of Deoxymugineic Acid Synthase Genes from Graminaceous Plants. *Journal of Biological Chemistry*, *281*(43), 32395–32402. https://doi.org/10.1074/jbc.M604133200

Bashir, K., & Nishizawa, N. K. (2006). Deoxymugineic Acid Synthase. *Plant Signaling & Behavior*, *1*(6), 290–292. https://doi.org/10.4161/psb.1.6.3590

Beasley, J. T., Bonneau, J. P., & Johnson, A. A. T. (2017). Characterisation of the nicotianamine aminotransferase and deoxymugineic acid synthase genes essential to Strategy II iron uptake in bread wheat (Triticum aestivum L.). *PLOS ONE*, *12*(5), e0177061. https://doi.org/10.1371/journal.pone.0177061

Beyer, S., Daba, S., Tyagi, P., Bockelman, H., Brown-Guedira, G., & Mohammadi, M. (2019). Loci and candidate genes controlling root traits in wheat seedlings—a wheat root GWAS. *Functional & Integrative Genomics*, *19*(1), 91–107. https://doi.org/10.1007/s10142-018-0630-z

Blair, M. W., Knewtson, S. J., Astudillo, C., Li, C.-M., Fernandez, A. C., & Grusak, M. A. (2010). Variation and inheritance of iron reductase activity in the roots of common bean (Phaseolus vulgaris L.) and association with seed iron

accumulation QTL. *BMC Plant Biology*, *10*(1), 215. https://doi.org/10.1186/1471-2229-10-215

Bocchini, M., Bartucca, M. L., Ciancaleoni, S., Mimmo, T., Cesco, S., Pii, Y., Albertini, E., & Del Buono, D. (2015). Iron deficiency in barley plants: phytosiderophore release, iron translocation, and DNA methylation. *Frontiers in Plant Science*, *6*. https://doi.org/10.3389/fpls.2015.00514

Bonneau, J., Baumann, U., Beasley, J., Li, Y., & Johnson, A. A. T. (2016). Identification and molecular characterization of the nicotianamine synthase gene family in bread wheat. *Plant Biotechnology Journal*, *14*(12), 2228–2239. https://doi.org/10.1111/pbi.12577

Budak, K., Aktaş, H., & Çevik, S. (2022). Morphological and physiological variation in drought tolerance of wheat landraces originated from southeast Türkiye. *Mediterranean Agricultural Sciences*, *35*(2), 91–95. https://doi.org/10.29136/mediterranean.1085160

Cheng, L., Wang, F., Shou, H., Huang, F., Zheng, L., He, F., Li, J., Zhao, F.-J., Ueno, D., Ma, J. F., & Wu, P. (2007). Mutation in Nicotianamine Aminotransferase Stimulated the Fe (II) Acquisition System and Led to Iron Accumulation in Rice. *Plant Physiology*, *145*(4), 1647–1657. https://doi.org/10.1104/pp.107.107912

Clark, R. B., Williams, E. P., Ross, W. M., Herron, G. M., & Witt, M. D. (1988). Effect of iron deficiency chlorosis on growth and yield component traits of sorghum [1]. *Journal of Plant Nutrition*, *11*(6–11), 747–754. https://doi.org/10.1080/01904168809363839

Connolly, E. L., Campbell, N. H., Grotz, N., Prichard, C. L., & Guerinot, M. Lou. (2003). Overexpression of the FRO2 Ferric Chelate Reductase Confers Tolerance to Growth on Low Iron and Uncovers Posttranscriptional Control. *Plant Physiology*, *133*(3), 1102–1110. https://doi.org/10.1104/pp.103.025122

Connolly, E. L., Fett, J. P., & Guerinot, M. Lou. (2002). Expression of the IRT1 Metal Transporter Is Controlled by Metals at the Levels of Transcript and Protein Accumulation. *The Plant Cell*, *14*(6), 1347–1357. https://doi.org/10.1105/tpc.001263

Curie, C., Cassin, G., Couch, D., Divol, F., Higuchi, K., Le Jean, M., Misson, J., Schikora, A., Czernic, P., & Mari, S. (2009). Metal movement within the plant: contribution of nicotianamine and yellow stripe 1-like transporters. *Annals of Botany*, *103*(1), 1–11. https://doi.org/10.1093/aob/mcn207

Curie, C., Panaviene, Z., Loulergue, C., Dellaporta, S. L., Briat, J.-F., & Walker, E. L. (2001). Maize yellow stripe1 encodes a membrane protein directly involved in Fe (III) uptake. *Nature*, *409*(6818), 346–349. https://doi.org/10.1038/35053080

DiDonato, R. J., Roberts, L. A., Sanderson, T., Eisley, R. B., & Walker, E. L. (2004). Arabidopsis Yellow Stripe-Like2 (YSL2): a metal-regulated gene encoding a plasma membrane transporter of nicotianamine–metal complexes. *The Plant Journal*, *39*(3), 403–414. https://doi.org/10.1111/j.1365-313X.2004.02128.x

Dong, Y., Wan, Y., Liu, F., & Zhuge, Y. (2019). Effects of exogenous SA supplied with different approaches on growth, chlorophyll content and antioxidant enzymes of peanut growing on calcareous soil. *Journal of Plant Nutrition*, *42*(16), 1869–1883. https://doi.org/10.1080/01904167.2019.1648679

Dubeaux, G., Zelazny, E., & Vert, G. (2015). Getting to the root of plant iron uptake and cell-cell transport: Polarity matters! *Communicative & Integrative Biology*, *8*(3), e1038441. https://doi.org/10.1080/19420889.2015.1038441

Easlon, H. M., & Bloom, A. J. (2014). Easy Leaf Area: Automated digital image analysis for rapid and accurate measurement of leaf area. *Applications in Plant Sciences*, *2*(7). https://doi.org/10.3732/apps.1400033

Eide, D., Broderius, M., Fett, J., & Guerinot, M. L. (1996). A novel iron-regulated metal transporter from plants identified by functional expression in yeast.

Proceedings of the National Academy of Sciences, *93*(11), 5624–5628. https://doi.org/10.1073/pnas.93.11.5624

Feng, H., Wang, S., Dong, D., Zhou, R., & Wang, H. (2020). Arabidopsis Ubiquitin-Conjugating Enzymes UBC7, UBC13, and UBC14 Are Required in Plant Responses to Multiple Stress Conditions. *Plants*, *9*(6), 723. https://doi.org/10.3390/plants9060723

Fernández, V., Eichert, T., Del Río, V., López-Casado, G., Heredia-Guerrero, J. A., Abadía, A., Heredia, A., & Abadía, J. (2008). Leaf structural changes associated with iron deficiency chlorosis in field-grown pear and peach: physiological implications. *Plant and Soil*, *311*(1–2), 161–172. https://doi.org/10.1007/s11104-008-9667-4

FAOSTAT (2023). https://www.fao.org/faostat/en/#data/QCL.

Ganal, M. W., Altmann, T., & Röder, M. S. (2009). SNP identification in crop plants. *Current Opinion in Plant Biology*, *12*(2), 211–217. https://doi.org/10.1016/j.pbi.2008.12.009

Garcia-Oliveira, A. L., Chander, S., Ortiz, R., Menkir, A., & Gedil, M. (2018). Genetic Basis and Breeding Perspectives of Grain Iron and Zinc Enrichment in Cereals. *Frontiers in Plant Science*, *9*. https://doi.org/10.3389/fpls.2018.00937

Green, L. S., & Rogers, E. E. (2004). FRD3 Controls Iron Localization in Arabidopsis. *Plant Physiology*, *136*(1), 2523–2531. https://doi.org/10.1104/pp.104.045633

Guo, Z., Du, N., Li, Y., Zheng, S., Shen, S., & Piao, F. (2020). Gamma-aminobutyric acid enhances tolerance to iron deficiency by stimulating auxin signaling in cucumber (Cucumis sativusL.). *Ecotoxicology and Environmental Safety*, *192*, 110285. https://doi.org/10.1016/j.ecoenv.2020.110285

Hell, R., & Stephan, U. W. (2003). Iron uptake, trafficking and homeostasis in plants. *Planta*, *216*(4), 541–551. https://doi.org/10.1007/s00425-002-0920-4

Higuchi, K., Watanabe, S., Takahashi, M., Kawasaki, S., Nakanishi, H., Nishizawa, N. K., & Mori, S. (2001). Nicotianamine synthase gene expression differs in barley and rice under Fe-deficient conditions. *The Plant Journal*, *25*(2), 159–167. https://doi.org/10.1111/j.1365-313X.2001.00951.x

Hiremath, P. J., Kumar, A., Penmetsa, R. V., Farmer, A., Schlueter, J. A., Chamarthi, S. K., Whaley, A. M., Carrasquilla-Garcia, N., Gaur, P. M., Upadhyaya, H. D., Kavi Kishor, P. B., Shah, T. M., Cook, D. R., & Varshney, R. K. (2012). Large-scale development of cost-effective SNP marker assays for diversity assessment and genetic mapping in chickpea and comparative mapping in legumes. *Plant Biotechnology Journal*, *10*(6), 716–732. https://doi.org/10.1111/j.1467-7652.2012.00710.x

Hoagland, D. R., & Arnon, D. I. (1950). The Water-Culture Method for Growing Plants without Soil. *California Agricultural Experiment Station*, *Circular*(347).

Hoang, G. T., Gantet, P., Nguyen, K. H., Phung, N. T. P., Ha, L. T., Nguyen, T. T., Lebrun, M., Courtois, B., & Pham, X. H. (2019). Genome-wide association mapping of leaf mass traits in a Vietnamese rice landrace panel. *PLOS ONE*, *14*(7), e0219274. https://doi.org/10.1371/journal.pone.0219274

Hocaoğlu, O., Akçura, M., & Kaplan, M. (2020). Changes in the Grain Element Contents of Durum Wheat Varieties of Turkey Registered between 1967–2010. *Communications in Soil Science and Plant Analysis*, *51*(4), 431–439. https://doi.org/10.1080/00103624.2019.1709487

Hua, Y., Wang, Y., Zhou, T., Huang, J., & Yue, C. (2022). Combined morpho-physiological, ionomic and transcriptomic analyses reveal adaptive responses of allohexaploid wheat (Triticum aestivum L.) to iron deficiency. *BMC Plant Biology*, *22*(1), 234. https://doi.org/10.1186/s12870-022-03627-4

Huang, M., Liu, X., Zhou, Y., Summers, R. M., & Zhang, Z. (2019). BLINK: a package for the next level of genome-wide association studies with both

individuals and markers in the millions. *GigaScience*, *8*(2). https://doi.org/10.1093/gigascience/giy154

Inoue, H., Higuchi, K., Takahashi, M., Nakanishi, H., Mori, S., & Nishizawa, N. K. (2003). Three rice nicotianamine synthase genes, *OsNAS1*, *OsNAS2* , and *OsNAS3* are expressed in cells involved in long-distance transport of iron and differentially regulated by iron. *The Plant Journal*, *36*(3), 366–381. https://doi.org/10.1046/j.1365-313X.2003.01878.x

Inoue, H., Kobayashi, T., Nozoye, T., Takahashi, M., Kakei, Y., Suzuki, K., Nakazono, M., Nakanishi, H., Mori, S., & Nishizawa, N. K. (2009). Rice OsYSL15 Is an Iron-regulated Iron (III)-Deoxymugineic Acid Transporter Expressed in the Roots and Is Essential for Iron Uptake in Early Growth of the Seedlings. *Journal of Biological Chemistry*, *284*(6), 3470–3479. https://doi.org/10.1074/jbc.M806042200

Inoue, H., Takahashi, M., Kobayashi, T., Suzuki, M., Nakanishi, H., Mori, S., & Nishizawa, N. K. (2008). Identification and localisation of the rice nicotianamine aminotransferase gene OsNAAT1 expression suggests the site of phytosiderophore synthesis in rice. *Plant Molecular Biology*, *66*(1–2), 193–203. https://doi.org/10.1007/s11103-007-9262-8

Ishimaru, Y., Kakei, Y., Shimo, H., Bashir, K., Sato, Y., Sato, Y., Uozumi, N., Nakanishi, H., & Nishizawa, N. K. (2011). A Rice Phenolic Efflux Transporter Is Essential for Solubilizing Precipitated Apoplasmic Iron in the Plant Stele. *Journal of Biological Chemistry*, *286*(28), 24649–24655. https://doi.org/10.1074/jbc.M111.221168

Ishimaru, Y., Suzuki, M., Tsukamoto, T., Suzuki, K., Nakazono, M., Kobayashi, T., Wada, Y., Watanabe, S., Matsuhashi, S., Takahashi, M., Nakanishi, H., Mori, S., & Nishizawa, N. K. (2006). Rice plants take up iron as an Fe3+-phytosiderophore and as Fe2+. *The Plant Journal*, *45*(3), 335–346. https://doi.org/10.1111/j.1365-313X.2005.02624.x

Jaccoud, D. (2001). Diversity Arrays: a solid state technology for sequence information independent genotyping. *Nucleic Acids Research*, *29*(4), 25e–225. https://doi.org/10.1093/nar/29.4.e25

Jean, M. Le, Schikora, A., Mari, S., Briat, J., & Curie, C. (2005). A loss-of-function mutation in AtYSL1 reveals its role in iron and nicotianamine seed loading. *The Plant Journal*, *44*(5), 769–782. https://doi.org/10.1111/j.1365-313X.2005.02569.x

Jeong, J., & Connolly, E. L. (2009). Iron uptake mechanisms in plants: Functions of the FRO family of ferric reductases. *Plant Science*, *176*(6), 709–714. https://doi.org/10.1016/j.plantsci.2009.02.011

Jiménez, M. R., Casanova, L., Saavedra, T., Gama, F., Suárez, M. P., Correia, P. J., & Pestana, M. (2019). Responses of tomato (Solanum lycopersicum L.) plants to iron deficiency in the root zone. *Folia Horticulturae*, *31*(1), 223–234. https://doi.org/10.2478/fhort-2019-0017

Jiménez, S., Pinochet, J., Abadía, A., Moreno, M. Á., & Gogorcena, Y. (2008). Tolerance Response to Iron Chlorosis of Prunus Selections as Rootstocks. *HortScience*, *43*(2), 304–309. https://doi.org/10.21273/HORTSCI.43.2.304

Jin, Y., Li, D., Liu, M., Cui, Z., Sun, D., Li, C., Zhang, A., Cao, H., & Ruan, Y. (2023). Genome-Wide Association Study Identified Novel SNPs Associated with Chlorophyll Content in Maize. *Genes*, *14*(5), 1010. https://doi.org/10.3390/genes14051010

Jose, A., Mahey, R., Sharma, J. B., Bhatla, N., Saxena, R., Kalaivani, M., & Kriplani, A. (2019). Comparison of ferric Carboxymaltose and iron sucrose complex for treatment of iron deficiency anemia in pregnancy- randomised controlled trial. *BMC Pregnancy and Childbirth*, *19*(1), 54. https://doi.org/10.1186/s12884-019-2200-3

Kakei, Y., Ishimaru, Y., Kobayashi, T., Yamakawa, T., Nakanishi, H., & Nishizawa, N. K. (2012). OsYSL16 plays a role in the allocation of iron. *Plant Molecular Biology*, *79*(6), 583–594. https://doi.org/10.1007/s11103-012-9930-1

Karaman, M., Kendal, E., Aktaş, H., Tekdal, S., & Altıkat A. (2012). Kalite Parametreleri Yönünden Yerli ve Yabancı Bazı Ekmeklik Buğday Çeşitlerinin Değerlendirilmesi. *Tarım Bilimleri Araştırma Dergisi*, *2*, 29–32.

Karim, S., Alezzawi, M., Garcia-Petit, C., Solymosi, K., Khan, N. Z., Lindquist, E., Dahl, P., Hohmann, S., & Aronsson, H. (2014). A novel chloroplast localized Rab GTPase protein CPRabA5e is involved in stress, development, thylakoid biogenesis and vesicle transport in Arabidopsis. *Plant Molecular Biology*, *84*(6), 675–692. https://doi.org/10.1007/s11103-013-0161-x

Kawakami, Y., & Bhullar, N. K. (2021). Delineating the future of iron biofortification studies in rice: challenges and future perspectives. *Journal of Experimental Botany*, *72*(6), 2099–2113. https://doi.org/10.1093/jxb/eraa446

Khan, Mohd. K., Pandey, A., Choudhary, S., Hakki, E. E., Akkaya, M. S., & Thomas, G. (2014). From RFLP to DArT: molecular tools for wheat (Triticum spp.) diversity analysis. *Genetic Resources and Crop Evolution*, *61*(5), 1001–1032. https://doi.org/10.1007/s10722-014-0114-5

Kim, S. A., & Guerinot, M. Lou. (2007). Mining iron: Iron uptake and transport in plants. *FEBS Letters*, *581*(12), 2273–2280. https://doi.org/10.1016/j.febslet.2007.04.043

Kim, S. A., Punshon, T., Lanzirotti, A., Li, L., Alonso, J. M., Ecker, J. R., Kaplan, J., & Guerinot, M. Lou. (2006). Localization of Iron in Arabidopsis Seed Requires the Vacuolar Membrane Transporter VIT1. *Science*, *314*(5803), 1295–1298. https://doi.org/10.1126/science.1132563

Kinsella, R. J., Kahari, A., Haider, S., Zamora, J., Proctor, G., Spudich, G., Almeida-King, J., Staines, D., Derwent, P., Kerhornou, A., Kersey, P., & Flicek, P.

(2011). Ensembl BioMarts: a hub for data retrieval across taxonomic space. *Database*, *2011*(0), bar030–bar030. https://doi.org/10.1093/database/bar030

Kılıç H., Kendal, E., Aktaş H., & Tekdal, S. (2014). İleri Kademe Ekmeklik Buğday Hatlarının Farklı Çevrelerde Tane Verimi ve Bazı Kalite Özellikleri Yönünden Değerlendirilmesi. *Journal of the Institute of Science and Technology*, *4*(4), 87–95.

Klatte, M., Schuler, M., Wirtz, M., Fink-Straube, C., Hell, R., & Bauer, P. (2009). The Analysis of Arabidopsis Nicotianamine Synthase Mutants Reveals Functions for Nicotianamine in Seed Iron Loading and Iron Deficiency Responses. *Plant Physiology*, *150*(1), 257–271. https://doi.org/10.1104/pp.109.136374

Kobayashi, T., Nakanishi, H., Takahashi, M., Kawasaki, S., Nishizawa, N.-K., & Mori, S. (2001). In vivo evidence that Ids3 from Hordeum vulgare encodes a dioxygenase that converts 2′-deoxymugineic acid to mugineic acid in transgenic rice. *Planta*, *212*(5–6), 864–871. https://doi.org/10.1007/s004250000453

Kobayashi, T., Nakanishi Itai, R., & Nishizawa, N. K. (2014). Iron deficiency responses in rice roots. *Rice*, *7*(1), 27. https://doi.org/10.1186/s12284-014-0027-0

Kobayashi, T., & Nishizawa, N. K. (2012). Iron Uptake, Translocation, and Regulation in Higher Plants. *Annual Review of Plant Biology*, *63*(1), 131–152. https://doi.org/10.1146/annurev-arplant-042811-105522

Kobayashi, T., Ogo, Y., Itai, R. N., Nakanishi, H., Takahashi, M., Mori, S., & Nishizawa, N. K. (2007). The transcription factor IDEF1 regulates the response to and tolerance of iron deficiency in plants. *Proceedings of the National Academy of Sciences*, *104*(48), 19150–19155. https://doi.org/10.1073/pnas.0707010104

Koike, S., Inoue, H., Mizuno, D., Takahashi, M., Nakanishi, H., Mori, S., & Nishizawa, N. K. (2004). OsYSL2 is a rice metal-nicotianamine transporter that

is regulated by iron and expressed in the phloem. *The Plant Journal*, *39*(3), 415–424. https://doi.org/10.1111/j.1365-313X.2004.02146.x

Kujur, A., Bajaj, D., Upadhyaya, H. D., Das, S., Ranjan, R., Shree, T., Saxena, M. S., Badoni, S., Kumar, V., Tripathi, S., Gowda, C. L. L., Sharma, S., Singh, S., Tyagi, A. K., & Parida, S. K. (2015). Employing genome-wide SNP discovery and genotyping strategy to extrapolate the natural allelic diversity and domestication patterns in chickpea. *Frontiers in Plant Science*, *6*. https://doi.org/10.3389/fpls.2015.00162

Kumar, A., Kaur, G., Goel, P., Bhati, K. K., Kaur, M., Shukla, V., & Pandey, A. K. (2019). Genome-wide analysis of oligopeptide transporters and detailed characterization of yellow stripe transporter genes in hexaploid wheat. *Functional & Integrative Genomics*, *19*(1), 75–90. https://doi.org/10.1007/s10142-018-0629-5

Kumar, R., Kushalappa, K., Godt, D., Pidkowich, M. S., Pastorelli, S., Hepworth, S. R., & Haughn, G. W. (2007). The Arabidopsis BEL1-LIKE HOMEODOMAIN Proteins SAW1 and SAW2 Act Redundantly to Regulate KNOX Expression Spatially in Leaf Margins. *The Plant Cell*, *19*(9), 2719–2735. https://doi.org/10.1105/tpc.106.048769

Kwon, S. H., Lee, B. H., Kim, E. Y., Seo, Y. S., Lee, S., Kim, W. T., Song, J. T., & Kim, J. H. (2009). Overexpression of a Brassica rapa NGATHA Gene in Arabidopsis thaliana Negatively Affects Cell Proliferation During Lateral Organ and Root Growth. *Plant and Cell Physiology*, *50*(12), 2162–2173. https://doi.org/10.1093/pcp/pcp150

Kyriacou, B., Moore, K. L., Paterson, D., de Jonge, M. D., Howard, D. L., Stangoulis, J., Tester, M., Lombi, E., & Johnson, A. A. T. (2014). Localization of iron in rice grain using synchrotron X-ray fluorescence microscopy and high resolution secondary ion mass spectrometry. *Journal of Cereal Science*, *59*(2), 173–180. https://doi.org/10.1016/j.jcs.2013.12.006

Lanquar, V., Lelièvre, F., Bolte, S., Hamès, C., Alcon, C., Neumann, D., Vansuyt, G., Curie, C., Schröder, A., Krämer, U., Barbier-Brygoo, H., & Thomine, S. (2005). Mobilization of vacuolar iron by AtNRAMP3 and AtNRAMP4 is essential for seed germination on low iron. *The EMBO Journal*, *24*(23), 4041–4051. https://doi.org/10.1038/sj.emboj.7600864

Levy, A. A., Galili, G., & Feldman, M. (1988). Polymorphism and genetic control of high molecular weight glutenin subunits in wild tetraploid wheat Triticum turgidum var. dicoccoides. *Heredity*, *61*(1), 63–72. https://doi.org/10.1038/hdy.1988.91

Li, J., Cao, X., Jia, X., Liu, L., Cao, H., Qin, W., & Li, M. (2021). Iron Deficiency Leads to Chlorosis Through Impacting Chlorophyll Synthesis and Nitrogen Metabolism in Areca catechu L. *Frontiers in Plant Science*, *12*. https://doi.org/10.3389/fpls.2021.710093

Li, Q., Wang, W., Wang, W., Zhang, G., Liu, Y., Wang, Y., & Wang, W. (2018). Wheat F-Box Protein Gene TaFBA1 Is Involved in Plant Tolerance to Heat Stress. *Frontiers in Plant Science*, *9*. https://doi.org/10.3389/fpls.2018.00521

Li, S., Song, Z., Liu, X., Zhou, X., Yang, W., Chen, J., & Chen, R. (2022). Mediation of Zinc and Iron Accumulation in Maize by ZmIRT2, a Novel Iron-Regulated Transporter. *Plant and Cell Physiology*, *63*(4), 521–534. https://doi.org/10.1093/pcp/pcab177

Li, S., Zhou, X., Chen, J., & Chen, R. (2018). Is there a strategy I iron uptake mechanism in maize? *Plant Signaling & Behavior*, *13*(4), e1161877. https://doi.org/10.1080/15592324.2016.1161877

Li, S., Zhou, X., Huang, Y., Zhu, L., Zhang, S., Zhao, Y., Guo, J., Chen, J., & Chen, R. (2013). Identification and characterization of the zinc-regulated transporters, iron-regulated transporter-like protein (ZIP) gene family in maize. *BMC Plant Biology*, *13*(1), 114. https://doi.org/10.1186/1471-2229-13-114

Li, S., Zhou, X., Li, H., Liu, Y., Zhu, L., Guo, J., Liu, X., Fan, Y., Chen, J., & Chen, R. (2015). Overexpression of ZmIRT1 and ZmZIP3 Enhances Iron and Zinc Accumulation in Transgenic Arabidopsis. *PLOS ONE*, *10*(8), e0136647. https://doi.org/10.1371/journal.pone.0136647

Li, S., Zhou, X., Zhao, Y., Li, H., Liu, Y., Zhu, L., Guo, J., Huang, Y., Yang, W., Fan, Y., Chen, J., & Chen, R. (2016). Constitutive expression of the ZmZIP7 in Arabidopsis alters metal homeostasis and increases Fe and Zn content. *Plant Physiology and Biochemistry*, *106*, 1–10. https://doi.org/10.1016/j.plaphy.2016.04.044

Li, Y., Zeng, H., Xu, F., Yan, F., & Xu, W. (2022). H+-ATPases in Plant Growth and Stress Responses. *Annual Review of Plant Biology*, *73*(1), 495–521. https://doi.org/10.1146/annurev-arplant-102820-114551

Liang, G., Zhang, H., Li, Y., Pu, M., Yang, Y., Li, C., Lu, C., Xu, P., & Yu, D. (2020). Oryza sativa FER-LIKE FE DEFICIENCY-INDUCED TRANSCRIPTION FACTOR (OsFIT/OsbHLH156) interacts with OsIRO2 to regulate iron homeostasis. *Journal of Integrative Plant Biology*, *62*(5), 668–689. https://doi.org/10.1111/jipb.12933

LICHTENTHALER, H. K., & WELLBURN, A. R. (1983). Determinations of total carotenoids and chlorophylls *a* and *b* of leaf extracts in different solvents. *Biochemical Society Transactions*, *11*(5), 591–592. https://doi.org/10.1042/bst0110591

Liu, Y., Lin, Y., Gao, S., Li, Z., Ma, J., Deng, M., Chen, G., Wei, Y., & Zheng, Y. (2017). A genome-wide association study of 23 agronomic traits in Chinese wheat landraces. *The Plant Journal*, *91*(5), 861–873. https://doi.org/10.1111/tpj.13614

Llosa, M. J., Bermejo, A., Cano, A., Quiñones, A., & Forner-Giner, M. A. (2009). The citrus rootstocks Cleopatra mandarin, Poncirus trifoliata, Forner-Alcaide 5

and Forner-Alcaide 13 vary in susceptibility to iron deficiency chlorosis. *Journal of the American Pomological Society*, *63*(4), 160–167.

Long, W., Li, Q., Wan, N., Feng, D., Kong, F., Zhou, Y., & Yuan, J. (2020). Root morphological and physiological characteristics in maize seedlings adapted to low iron stress. *PLOS ONE*, *15*(9), e0239075. https://doi.org/10.1371/journal.pone.0239075

Ma, J. F., Taketa, S., Chang, Y.-C., Takeda, K., & Matsumoto, H. (1999). Biosynthesis of phytosiderophores in several Triticeae species with different genomes. *Journal of Experimental Botany*, *50*(334), 723–726. https://doi.org/10.1093/jxb/50.334.723

Mary, V., Schnell Ramos, M., Gillet, C., Socha, A. L., Giraudat, J., Agorio, A., Merlot, S., Clairet, C., Kim, S. A., Punshon, T., Guerinot, M. Lou, & Thomine, S. (2015). Bypassing Iron Storage in Endodermal Vacuoles Rescues the Iron Mobilization Defect in the *natural resistance associated-macrophage protein3natural resistance associated-macrophage protein4* Double Mutant. *Plant Physiology*, *169*(1), 748–759. https://doi.org/10.1104/pp.15.00380

Mathpal, P., Kumar, U., Kumar, A., Kumar, S., Malik, S., Kumar, N., Dhaliwal, H. S., & Kumar, S. (2018). Identification, expression analysis, and molecular modeling of Iron-deficiency-specific clone 3 (Ids3)-like gene in hexaploid wheat. *3 Biotech*, *8*(4), 219. https://doi.org/10.1007/s13205-018-1230-2

Matsuoka, Y. (2011). Evolution of Polyploid Triticum Wheats under Cultivation: The Role of Domestication, Natural Hybridization and Allopolyploid Speciation in their Diversification. *Plant and Cell Physiology*, *52*(5), 750–764. https://doi.org/10.1093/pcp/pcr018

Mendoza-Cózatl, D. G., Xie, Q., Akmakjian, G. Z., Jobe, T. O., Patel, A., Stacey, M. G., Song, L., Demoin, D. W., Jurisson, S. S., Stacey, G., & Schroeder, J. I. (2014). OPT3 Is a Component of the Iron-Signaling Network between Leaves and Roots and Misregulation of OPT3 Leads to an Over-Accumulation of

Cadmium in Seeds. *Molecular Plant*, *7*(9), 1455–1469. https://doi.org/10.1093/mp/ssu067

Mizuno, D., Higuchi, K., Sakamoto, T., Nakanishi, H., Mori, S., & Nishizawa, N. K. (2003). Three Nicotianamine Synthase Genes Isolated from Maize Are Differentially Regulated by Iron Nutritional Status. *Plant Physiology*, *132*(4), 1989–1997. https://doi.org/10.1104/pp.102.019869

Molassiotis, A., Tanou, G., Diamantidis, G., Patakas, A., & Therios, I. (2006). Effects of 4-month Fe deficiency exposure on Fe reduction mechanism, photosynthetic gas exchange, chlorophyll fluorescence and antioxidant defense in two peach rootstocks differing in Fe deficiency tolerance. *Journal of Plant Physiology*, *163*(2), 176–185. https://doi.org/10.1016/j.jplph.2004.11.016

Møller, I. M., Jensen, P. E., & Hansson, A. (2007). Oxidative modifications to cellular components in plants. *Annual Review of Plant Biology*, *58*, 459–481. https://doi.org/10.1146/annurev.arplant.58.032806.103946

Mori, S., Nishizawa, N., Kawai, S., Sato, Y., & Takagi, S. (1987). Dynamic state of mugineic acid and analogous phytosiderophores in Fe-deficient barley. *Journal of Plant Nutrition*, *10*(9), 1003–1011. https://doi.org/10.1080/01904168709363628

Moriwaki, T., Miyazawa, Y., Kobayashi, A., Uchida, M., Watanabe, C., Fujii, N., & Takahashi, H. (2011). Hormonal Regulation of Lateral Root Development in Arabidopsis Modulated by *MIZ1* and Requirement of GNOM Activity for *MIZ1* Function. *Plant Physiology*, *157*(3), 1209–1220. https://doi.org/10.1104/pp.111.186270

Morrissey, J., Baxter, I. R., Lee, J., Li, L., Lahner, B., Grotz, N., Kaplan, J., Salt, D. E., & Guerinot, M. Lou. (2009). The Ferroportin Metal Efflux Proteins Function in Iron and Cobalt Homeostasis in *Arabidopsis*. *The Plant Cell*, *21*(10), 3326–3338. https://doi.org/10.1105/tpc.109.069401

Mouchel, C. F., Osmont, K. S., & Hardtke, C. S. (2006). BRX mediates feedback between brassinosteroid levels and auxin signalling in root growth. *Nature*, *443*(7110), 458–461. https://doi.org/10.1038/nature05130

Murata, Y., Ma, J. F., Yamaji, N., Ueno, D., Nomoto, K., & Iwashita, T. (2006). A specific transporter for iron (III)–phytosiderophore in barley roots. *The Plant Journal*, *46*(4), 563–572. https://doi.org/10.1111/j.1365-313X.2006.02714.x

Nachit, M. M., Elouafi, I., Pagnotta, A., El Saleh, A., Iacono, E., Labhilili, M., Asbati, A., Azrak, M., Hazzam, H., Benscher, D., Khairallah, M., Ribaut, J.-M., Tanzarella, O. A., Porceddu, E., & Sorrells, M. E. (2001). Molecular linkage map for an intraspecific recombinant inbred population of durum wheat (Triticum turgidum L. var. durum). *Theoretical and Applied Genetics*, *102*(2–3), 177–186. https://doi.org/10.1007/s001220051633

Nakanishi, H., Ogawa, I., Ishimaru, Y., Mori, S., & Nishizawa, N. K. (2006). Iron deficiency enhances cadmium uptake and translocation mediated by the Fe^{2+} transporters OsIRT1 and OsIRT2 in rice. *Soil Science and Plant Nutrition*, *52*(4), 464–469. https://doi.org/10.1111/j.1747-0765.2006.00055.x

Nakanishi, H., Yamaguchi, H., Sasakuma, T., Nishizawa, N. K., & Mori, S. (2000). Two dioxygenase genes, Ids3 and Ids2, from Hordeum vulgare are involved in the biosynthesis of mugineic acid family phytosiderophores. *Plant Molecular Biology*, *44*(2), 199–207. https://doi.org/10.1023/A:1006491521586

Nenova, V. R. (2009). Growth and photosynthesis of pea plants under different iron supply. *Acta Physiologiae Plantarum*, *31*(2), 385–391. https://doi.org/10.1007/s11738-008-0247-2

Now 8 billion and counting: Where the world's population has grown most and why that matters (2022). https://unctad.org/data-visualization/now-8-billion-and-counting-where-worlds-population-has-grown-most-and-why.

Nozoye, T., Nagasaka, S., Kobayashi, T., Sato, Y., Uozumi, N., Nakanishi, H., & Nishizawa, N. K. (2015). The Phytosiderophore Efflux Transporter TOM2 Is

Involved in Metal Transport in Rice. *Journal of Biological Chemistry*, *290*(46), 27688–27699. https://doi.org/10.1074/jbc.M114.635193

Nozoye, T., Nagasaka, S., Kobayashi, T., Takahashi, M., Sato, Y., Sato, Y., Uozumi, N., Nakanishi, H., & Nishizawa, N. K. (2011). Phytosiderophore Efflux Transporters Are Crucial for Iron Acquisition in Graminaceous Plants. *Journal of Biological Chemistry*, *286*(7), 5446–5454. https://doi.org/10.1074/jbc.M110.180026

Ogo, Y. (2006). Isolation and characterization of IRO2, a novel iron-regulated bHLH transcription factor in graminaceous plants. *Journal of Experimental Botany*, *57*(11), 2867–2878. https://doi.org/10.1093/jxb/erl054

Ogo, Y., Kobayashi, T., Nakanishi Itai, R., Nakanishi, H., Kakei, Y., Takahashi, M., Toki, S., Mori, S., & Nishizawa, N. K. (2008). A Novel NAC Transcription Factor, IDEF2, That Recognizes the Iron Deficiency-responsive Element 2 Regulates the Genes Involved in Iron Homeostasis in Plants. *Journal of Biological Chemistry*, *283*(19), 13407–13417. https://doi.org/10.1074/jbc.M708732200

Palmer, C. M., & Guerinot, M. Lou. (2009). Facing the challenges of Cu, Fe and Zn homeostasis in plants. *Nature Chemical Biology*, *5*(5), 333–340. https://doi.org/10.1038/nchembio.166

Pao, S. S., Paulsen, I. T., & Saier, M. H. (1998). Major Facilitator Superfamily. *Microbiology and Molecular Biology Reviews*, *62*(1), 1–34. https://doi.org/10.1128/MMBR.62.1.1-34.1998

Pearce, S., Tabbita, F., Cantu, D., Buffalo, V., Avni, R., Vazquez-Gross, H., Zhao, R., Conley, C. J., Distelfeld, A., & Dubcovksy, J. (2014). Regulation of Zn and Fe transporters by the GPC1gene during early wheat monocarpic senescence. *BMC Plant Biology*, *14*(1), 368. https://doi.org/10.1186/s12870-014-0368-2

Peng, J. H., Sun, D., & Nevo, E. (2011). Domestication evolution, genetics and genomics in wheat. *Molecular Breeding*, *28*(3), 281–301. https://doi.org/10.1007/s11032-011-9608-4

Pizzio, G., Regmi, K., & Gaxiola, R. (2015). Rhizosphere Acidification Assay. *BIO-PROTOCOL*, *5*(23). https://doi.org/10.21769/BioProtoc.1676

Poland, J. A., Brown, P. J., Sorrells, M. E., & Jannink, J.-L. (2012). Development of High-Density Genetic Maps for Barley and Wheat Using a Novel Two-Enzyme Genotyping-by-Sequencing Approach. *PLoS ONE*, *7*(2), e32253. https://doi.org/10.1371/journal.pone.0032253

Pooja Kohli, Manmohit Kalia, & Reena Gupta. (2015). Pectin Methylesterases: A Review. *Journal of Bioprocessing & Biotechniques*, *05*(05). https://doi.org/10.4172/2155-9821.1000227

Ravanel, S., Ruffet, M.-L., & Douce, R. (1995). Cloning of an Arabidopsis thaliana cDNA encoding cystathionine-lyase by functional complementation in Escherichia coli. *Plant Molecular Biology*, *29*(4), 875–882. https://doi.org/10.1007/BF00041177

Rellán-Álvarez, R., Giner-Martínez-Sierra, J., Orduna, J., Orera, I., Rodríguez-Castrillón, J. Á., García-Alonso, J. I., Abadía, J., & Álvarez-Fernández, A. (2010). Identification of a Tri-Iron (III), Tri-Citrate Complex in the Xylem Sap of Iron-Deficient Tomato Resupplied with Iron: New Insights into Plant Iron Long-Distance Transport. *Plant and Cell Physiology*, *51*(1), 91–102. https://doi.org/10.1093/pcp/pcp170

Ren, J., Sun, D., Chen, L., You, F., Wang, J., Peng, Y., Nevo, E., Sun, D., Luo, M.-C., & Peng, J. (2013). Genetic Diversity Revealed by Single Nucleotide Polymorphism Markers in a Worldwide Germplasm Collection of Durum Wheat. *International Journal of Molecular Sciences*, *14*(4), 7061–7088. https://doi.org/10.3390/ijms14047061

Robinson, N. J., Procter, C. M., Connolly, E. L., & Guerinot, M. Lou. (1999). A ferric-chelate reductase for iron uptake from soils. *Nature*, *397*(6721), 694–697. https://doi.org/10.1038/17800

Roschzttardtz, H., Conéjéro, G., Curie, C., & Mari, S. (2009). Identification of the Endodermal Vacuole as the Iron Storage Compartment in the Arabidopsis Embryo. *Plant Physiology*, *151*(3), 1329–1338. https://doi.org/10.1104/pp.109.144444

Roschzttardtz, H., Séguéla-Arnaud, M., Briat, J.-F., Vert, G., & Curie, C. (2011). The FRD3 Citrate Effluxer Promotes Iron Nutrition between Symplastically Disconnected Tissues throughout *Arabidopsis* Development. *The Plant Cell*, *23*(7), 2725–2737. https://doi.org/10.1105/tpc.111.088088

Satbhai, S. B., Setzer, C., Freynschlag, F., Slovak, R., Kerdaffrec, E., & Busch, W. (2017). Natural allelic variation of FRO2 modulates Arabidopsis root growth under iron deficiency. *Nature Communications*, *8*(1), 15603. https://doi.org/10.1038/ncomms15603

Schaaf, G., Ludewig, U., Erenoglu, B. E., Mori, S., Kitahara, T., & von Wirén, N. (2004). ZmYS1 Functions as a Proton-coupled Symporter for Phytosiderophore- and Nicotianamine-chelated Metals. *Journal of Biological Chemistry*, *279*(10), 9091–9096. https://doi.org/10.1074/jbc.M311799200

Schmiedeberg, L., Krüger, C., Stephan, U. W., Bäumlein, H., & Hell, R. (2003). Synthesis and proof-of-function of a [^{14}C]-labelled form of the plant iron chelator nicotianamine using recombinant nicotianamine synthase from barley. *Physiologia Plantarum*, *118*(3), 430–438. https://doi.org/10.1034/j.1399-3054.2003.00128.x

Scholz, G., Becker, R., Pich, A., & Stephan, U. W. (1992). Nicotianamine - a common constituent of strategies I and II of iron acquisition by plants: A review. *Journal of Plant Nutrition*, *15*(10), 1647–1665. https://doi.org/10.1080/01904169209364428

Seethepalli, A., Dhakal, K., Griffiths, M., Guo, H., Freschet, G. T., & York, L. M. (2021). RhizoVision Explorer: open-source software for root image analysis and measurement standardization. *AoB PLANTS*, *13*(6). https://doi.org/10.1093/aobpla/plab056

Sharma, S., Kaur, G., Kumar, A., Meena, V., Ram, H., Kaur, J., & Pandey, A. K. (2020). Gene Expression Pattern of Vacuolar-Iron Transporter-Like (VTL) Genes in Hexaploid Wheat during Metal Stress. *Plants*, *9*(2), 229. https://doi.org/10.3390/plants9020229

Shewry, P. R. (2009). Wheat. *Journal of Experimental Botany*, *60*(6), 1537–1553. https://doi.org/10.1093/jxb/erp058

Shojima, S., Nishizawa, N.-K., Fushiya, S., Nozoe, S., Irifune, T., & Mori, S. (1990). Biosynthesis of Phytosiderophores. *Plant Physiology*, *93*(4), 1497–1503. https://doi.org/10.1104/pp.93.4.1497

Singh, S., Gupta, M., Pandher, S., Kaur, G., Goel, N., Rathore, P., & Palli, S. R. (2019). RNA sequencing, selection of reference genes and demonstration of feeding RNAi in Thrips tabaci (Lind.) (Thysanoptera: Thripidae). *BMC Molecular Biology*, *20*(1), 6. https://doi.org/10.1186/s12867-019-0123-1

Stec, B. (2006). Plant thionins – the structural perspective. *Cellular and Molecular Life Sciences*, *63*(12), 1370–1385. https://doi.org/10.1007/s00018-005-5574-5

Sukumaran, S., Reynolds, M. P., & Sansaloni, C. (2018). Genome-Wide Association Analyses Identify QTL Hotspots for Yield and Component Traits in Durum Wheat Grown under Yield Potential, Drought, and Heat Stress Environments. *Frontiers in Plant Science*, *9*. https://doi.org/10.3389/fpls.2018.00081

Sun, Q., Zhai, L., Zhao, D., Gao, M., Wu, Y., Wu, T., Zhang, X., Xu, X., Han, Z., & Wang, Y. (2023). Kinase MxMPK4-1 and calmodulin-binding protein MxIQM3 enhance apple root acidification during Fe deficiency. *Plant Physiology*, *191*(3), 1968–1984. https://doi.org/10.1093/plphys/kiac587

Suzuki, K., Higuchi, K., Nakanishi, H., Nishizawa, N. K., & Mori, S. (1999). Cloning of nicotianamine synthase genes from *Arabidopsis thaliana*. *Soil Science and Plant Nutrition*, *45*(4), 993–1002. https://doi.org/10.1080/00380768.1999.10414350

Tadesse, W., Ogbonnaya, F. C., Jighly, A., Sanchez-Garcia, M., Sohail, Q., Rajaram, S., & Baum, M. (2015). Genome-Wide Association Mapping of Yield and Grain Quality Traits in Winter Wheat Genotypes. *PLOS ONE*, *10*(10), e0141339. https://doi.org/10.1371/journal.pone.0141339

Takagi, S. (1976). Naturally occurring iron-chelating compounds in oat- and rice-root washings. *Soil Science and Plant Nutrition*, *22*(4), 423–433. https://doi.org/10.1080/00380768.1976.10433004

Takagi, S., Nomoto, K., & Takemoto, T. (1984). Physiological aspect of mugineic acid, a possible phytosiderophore of graminaceous plants. *Journal of Plant Nutrition*, *7*(1–5), 469–477. https://doi.org/10.1080/01904168409363213

Takahashi, M., Yamaguchi, H., Nakanishi, H., Shioiri, T., Nishizawa, N.-K., & Mori, S. (1999). Cloning Two Genes for Nicotianamine Aminotransferase, a Critical Enzyme in Iron Acquisition (Strategy II) in Graminaceous Plants. *Plant Physiology*, *121*(3), 947–956. https://doi.org/10.1104/pp.121.3.947

Tamuk, P., Pandey, R., Purakayastha, T. J., Barman, M., Chakraborty, D., Gurung, B., Choudhury, S., Trivedi, A., & Singh, B. (2024). Grain and shoot iron (Fe) content and root phytosiderophore release are the major determinants of Fe-deficiency tolerance index (FeDTI) and the reliable screening markers to breed Fe-efficient rice (*Oryza sativa* L.). *Journal of Plant Nutrition*, 1–25. https://doi.org/10.1080/01904167.2024.2320212

Thomine, S., & Vert, G. (2013). Iron transport in plants: better be safe than sorry. *Current Opinion in Plant Biology*, *16*(3), 322–327. https://doi.org/10.1016/j.pbi.2013.01.003

Tian, H., Baxter, I. R., Lahner, B., Reinders, A., Salt, D. E., & Ward, J. M. (2011). Arabidopsis NPCC6/NaKR1 Is a Phloem Mobile Metal Binding Protein Necessary for Phloem Function and Root Meristem Maintenance. *The Plant Cell*, *22*(12), 3963–3979. https://doi.org/10.1105/tpc.110.080010

Tian, Q., Zhang, X., Yang, A., Wang, T., & Zhang, W.-H. (2016). CIPK23 is involved in iron acquisition of Arabidopsis by affecting ferric chelate reductase activity. *Plant Science*, *246*, 70–79. https://doi.org/10.1016/j.plantsci.2016.01.010

Trebbi, D., Ravi, S., Broccanello, C., Chiodi, C., Francis, G., Oliver, J., Mulpuri, S., Srinivasan, S., & Stevanato, P. (2019). Identification and validation of SNP markers linked to seed toxicity in Jatropha curcas L. *Scientific Reports*, *9*(1), 10220. https://doi.org/10.1038/s41598-019-46698-4

Tripathy, M. K., Deswal, R., & Sopory, S. K. (2021). Plant RABs: Role in Development and in Abiotic and Biotic Stress Responses. *Current Genomics*, *22*(1), 26–40. https://doi.org/10.2174/1389202922666210114102743

Tyrka, M., Krajewski, P., Bednarek, P. T., Rączka, K., Drzazga, T., Matysik, P., Martofel, R., Woźna-Pawlak, U., Jasińska, D., Niewińska, M., Ługowska, B., Ratajczak, D., Sikora, T., Witkowski, E., Dorczyk, A., & Tyrka, D. (2023). Genome-wide association mapping in elite winter wheat breeding for yield improvement. *Journal of Applied Genetics*, *64*(3), 377–391. https://doi.org/10.1007/s13353-023-00758-8

TÜİK (2023a). https://data.tuik.gov.tr/Kategori/GetKategori?p=Tarim-111.

TÜİK (2023b). https://biruni.tuik.gov.tr/medas/?kn=92&locale=tr.

Ueno, D., Rombolà, A. D., Iwashita, T., Nomoto, K., & Ma, J. F. (2007). Identification of two novel phytosiderophores secreted by perennial grasses. *New Phytologist*, *174*(2), 304–310. https://doi.org/10.1111/j.1469-8137.2007.02056.x

Vaid, N., Macovei, A., & Tuteja, N. (2013). Knights in Action: Lectin Receptor-Like Kinases in Plant Development and Stress Responses. *Molecular Plant*, *6*(5), 1405–1418. https://doi.org/10.1093/mp/sst033

Vasconcelos, M., Eckert, H., Arahana, V., Graef, G., Grusak, M. A., & Clemente, T. (2006). Molecular and phenotypic characterization of transgenic soybean expressing the Arabidopsis ferric chelate reductase gene, FRO2. *Planta*, *224*(5), 1116–1128. https://doi.org/10.1007/s00425-006-0293-1

Vatansever, R., Filiz, E., & Eroglu, S. (2017). Genome-wide exploration of metal tolerance protein (MTP) genes in common wheat (Triticum aestivum): insights into metal homeostasis and biofortification. *BioMetals*, *30*(2), 217–235. https://doi.org/10.1007/s10534-017-9997-x

Vert, G., Grotz, N., Dédaldéchamp, F., Gaymard, F., Guerinot, M. Lou, Briat, J.-F., & Curie, C. (2002). IRT1, an Arabidopsis Transporter Essential for Iron Uptake from the Soil and for Plant Growth. *The Plant Cell*, *14*(6), 1223–1233. https://doi.org/10.1105/tpc.001388

Walker, E. L., & Connolly, E. L. (2008). Time to pump iron: iron-deficiency-signaling mechanisms of higher plants. *Current Opinion in Plant Biology*, *11*(5), 530–535. https://doi.org/10.1016/j.pbi.2008.06.013

Walter, A., Pich, A., Scholz, G., Marschner, H., & Römheld, V. (1995). Diurnal Variations in Release of Phytosiderophores and in Concentrations of Phytosiderophores and Nicotianamine in Roots and Shoots of Barley. *Journal of Plant Physiology*, *147*(2), 191–196. https://doi.org/10.1016/S0176-1617(11)81505-1

Wang, J., & Zhang, Z. (2021). GAPIT Version 3: Boosting Power and Accuracy for Genomic Association and Prediction. *Genomics, Proteomics & Bioinformatics*, *19*(4), 629–640. https://doi.org/10.1016/j.gpb.2021.08.005

Wang, K., Li, S., Yang, Z., Chen, C., Fu, Y., Du, H., Sun, H., Li, J., Zhao, Q., & Du, C. (2023). L-type lectin receptor-like kinase OsCORK1 as an important

negative regulator confers copper stress tolerance in rice. *Journal of Hazardous Materials*, *459*, 132214. https://doi.org/10.1016/j.jhazmat.2023.132214

Wang, M., Gong, J., & Bhullar, N. K. (2020). Iron deficiency triggered transcriptome changes in bread wheat. *Computational and Structural Biotechnology Journal*, *18*, 2709–2722. https://doi.org/10.1016/j.csbj.2020.09.009

Wang, M., Kawakami, Y., & Bhullar, N. K. (2019). Molecular Analysis of Iron Deficiency Response in Hexaploid Wheat. *Frontiers in Sustainable Food Systems*, *3*. https://doi.org/10.3389/fsufs.2019.00067

Wang, S., Li, L., Ying, Y., Wang, J., Shao, J. F., Yamaji, N., Whelan, J., Ma, J. F., & Shou, H. (2020). A transcription factor OsbHLH156 regulates Strategy II iron acquisition through localising IRO2 to the nucleus in rice. *New Phytologist*, *225*(3), 1247–1260. https://doi.org/10.1111/nph.16232

Wang, S., Xu, S., Chao, S., Sun, Q., Liu, S., & Xia, G. (2019). A Genome-Wide Association Study of Highly Heritable Agronomic Traits in Durum Wheat. *Frontiers in Plant Science*, *10*. https://doi.org/10.3389/fpls.2019.00919

Wang, W., Ye, J., Ma, Y., Wang, T., Shou, H., & Zheng, L. (2020). OsIRO3 Plays an Essential Role in Iron Deficiency Responses and Regulates Iron Homeostasis in Rice. *Plants*, *9*(9), 1095. https://doi.org/10.3390/plants9091095

Wang, Y., Xu, X., Hao, Y., Zhang, Y., Liu, Y., Pu, Z., Tian, Y., Xu, D., Xia, X., He, Z., & Zhang, Y. (2021). QTL Mapping for Grain Zinc and Iron Concentrations in Bread Wheat. *Frontiers in Nutrition*, *8*. https://doi.org/10.3389/fnut.2021.680391

White, P. J., & Brown, P. H. (2010). Plant nutrition for sustainable development and global health. *Annals of Botany*, *105*(7), 1073–1080. https://doi.org/10.1093/aob/mcq085

XLSTAT, A. (2021). *A complete statistical add-in for Microsoft Excel*.

Xu, X. M., Lin, H., Maple, J., Björkblom, B., Alves, G., Larsen, J. P., & Møller, S. G. (2010). The Arabidopsis DJ-1a protein confers stress protection through cytosolic SOD activation. *Journal of Cell Science*, *123*(10), 1644–1651. https://doi.org/10.1242/jcs.063222

Yan, X., Liao, H., Beebe, S. E., Blair, M. W., & Lynch, J. P. (2004). QTL mapping of root hair and acid exudation traits and their relationship to phosphorus uptake in common bean. *Plant and Soil*, *265*(1–2), 17–29. https://doi.org/10.1007/s11104-005-0693-1

Yao, E., Blake, V. C., Cooper, L., Wight, C. P., Michel, S., Cagirici, H. B., Lazo, G. R., Birkett, C. L., Waring, D. J., Jannink, J.-L., Holmes, I., Waters, A. J., Eickholt, D. P., & Sen, T. Z. (2022). GrainGenes: a data-rich repository for small grains genetics and genomics. *Database*, *2022*. https://doi.org/10.1093/database/baac034

Yorgancılar, M., Yakışır, E., & Tanur Erkoyuncu, M. (2016). Moleküler Markörlerin Bitki Islahında Kullanımı. *Bahri Dağdaş Bitkisel Araştırma Dergisi*, *4*(2), 1–12.

Zeilmaker, T., Ludwig, N. R., Elberse, J., Seidl, M. F., Berke, L., Van Doorn, A., Schuurink, R. C., Snel, B., & Van den Ackerveken, G. (2015). DOWNY MILDEW RESISTANT 6 and DMR 6- LIKE OXYGENASE 1 are partially redundant but distinct suppressors of immunity in Arabidopsis. *The Plant Journal*, *81*(2), 210–222. https://doi.org/10.1111/tpj.12719

Zhai, Z., Gayomba, S. R., Jung, H., Vimalakumari, N. K., Piñeros, M., Craft, E., Rutzke, M. A., Danku, J., Lahner, B., Punshon, T., Guerinot, M. Lou, Salt, D. E., Kochian, L. V., & Vatamaniuk, O. K. (2014). OPT3 Is a Phloem-Specific Iron Transporter That Is Essential for Systemic Iron Signaling and Redistribution of Iron and Cadmium in *Arabidopsis* . *The Plant Cell*, *26*(5), 2249–2264. https://doi.org/10.1105/tpc.114.123737

Zhang, C., Lu, W., Yang, Y., Shen, Z., Ma, J. F., & Zheng, L. (2018). OsYSL16 is Required for Preferential Cu Distribution to Floral Organs in Rice. *Plant and Cell Physiology*, *59*(10), 2039–2051. https://doi.org/10.1093/pcp/pcy124

Zhang, Z., Xie, Q., Jobe, T. O., Kau, A. R., Wang, C., Li, Y., Qiu, B., Wang, Q., Mendoza-Cózatl, D. G., & Schroeder, J. I. (2016). Identification of AtOPT4 as a Plant Glutathione Transporter. *Molecular Plant*, *9*(3), 481–484. https://doi.org/10.1016/j.molp.2015.07.013

Zhao, Z., Zhang, G., Zhou, S., Ren, Y., & Wang, W. (2017). The improvement of salt tolerance in transgenic tobacco by overexpression of wheat F-box gene TaFBA1. *Plant Science*, *259*, 71–85. https://doi.org/10.1016/j.plantsci.2017.03.010

Zhou, S., Sun, X., Yin, S., Kong, X., Zhou, S., Xu, Y., Luo, Y., & Wang, W. (2014). The role of the F-box gene TaFBA1 from wheat (Triticum aestivum L.) in drought tolerance. *Plant Physiology and Biochemistry*, *84*, 213–223. https://doi.org/10.1016/j.plaphy.2014.09.017

Zhou, S.-M., Kong, X.-Z., Kang, H.-H., Sun, X.-D., & Wang, W. (2015). The Involvement of Wheat F-Box Protein Gene TaFBA1 in the Oxidative Stress Tolerance of Plants. *PLOS ONE*, *10*(4), e0122117. https://doi.org/10.1371/journal.pone.0122117

Zhou, X., Li, S., Zhao, Q., Liu, X., Zhang, S., Sun, C., Fan, Y., Zhang, C., & Chen, R. (2013). Genome-wide identification, classification and expression profiling of nicotianamine synthase (NAS) gene family in maize. *BMC Genomics*, *14*(1), 238. https://doi.org/10.1186/1471-2164-14-238

Zielińska-Dawidziak, M. (2015). Plant Ferritin—A Source of Iron to Prevent Its Deficiency. *Nutrients*, *7*(2), 1184–1201. https://doi.org/10.3390/nu7021184

Zocchi, G., De Nisi, P., Dell'Orto, M., Espen, L., & Gallina, P. M. (2007). Iron deficiency differently affects metabolic responses in soybean roots. *Journal of Experimental Botany*, *58*(5), 993–1000. https://doi.org/10.1093/jxb/erl259

APPENDICES

A. Plant Material

Names, registered country, and year of the durum wheat genotypes used in the study.

No	Name	Country - Year	No	Name	Country - Year
1	Kunduru-1149	TR - 1967	**63**	Creco	IT - 1974
2	Çeşit-1252	TR - 1999	**64**	Irıde	IT - 1996
3	Yılmaz-98	TR - 1998	**65**	Dylan	IT - 2002
4	Yelken-2000	TR - 2000	**66**	Ofanto	IT - 1990
5	Altın	TR - 1998	**67**	Cham-1	SY - 1984
6	Meram-2002	TR - 2002	**68**	Cham-9	SY - 2010
7	Dumlupınar	TR - 2006	**69**	TR 32090 - Ankara	TR - NA
8	Şölen-2002	TR - 2002	**70**	TR 53861 - Yozgat	TR - NA
9	Altıntoprak-98	TR - 1998	**71**	TR 80984 - Eskişehir	TR - NA
10	Çakmak-79	TR - 1979	**72**	TR 72025 - Konya	TR - NA
11	Eminbey	TR - 2007	**73**	TR 81249 - Elazığ	TR - NA
12	Kümbet-2000	TR - 2000	**74**	TR 81371 - Niğde	TR - NA
13	İmren	TR - 2009	**75**	TR 71914 - Konya	TR - NA
14	Balcalı-2000	TR - 2000	**76**	TR 81356 - Konya	TR - NA
15	Sham-1	TR - 1984	**77**	TR 81381 - Sivas	TR - NA
16	Ankara-98	TR - 1998	**78**	TR 45305 - Yozgat	TR - NA
17	Balcalı-85	TR - 1985	**79**	TR 46881 - Erzincan	TR - NA
18	Fuatbey-2000	TR - 2000	**80**	TR 81259 - Malatya	TR - NA
19	Akbaşak-073144	TR - 1970	**81**	TR 81273 - Ankara	TR - NA
20	Artuklu	TR - 2008	**82**	TR 47949 - Kars	TR - NA
21	Mirzabey-2000	TR - 2000	**83**	TR 54969 - Yozgat	TR - NA
22	Aydın-93	TR - 1993	**84**	TR 63315 - Konya	TR - NA
23	Diyarbakır-81	TR - 1981	**85**	TR 81238 - Erzincan	TR - NA
24	Eyyubi	TR - 2008	**86**	TR 56206 - Eskişehir	TR - NA
25	Selçuklu-97	TR - 1997	**87**	TR 56128 - Eskişehir	TR - NA
26	Fatasel-185/1	TR - 1964	**88**	TR 54977 - Yozgat	TR - NA
27	Altınbaç-95	TR - 1995	**89**	TR 54973 - Yozgat	TR - NA
28	Harran-95	TR - 1995	**90**	TR 53860 - Yozgat	TR - NA
29	Sarıçanak-98	TR - 1998	**91**	TR 56135 - Eskişehir	TR - NA
30	Tüten-2002	TR - 2002	**92**	TR 32015 - Malatya	TR - NA
31	Turabi	TR - 2004	**93**	TR 31930 - Malatya	TR - NA
32	Ege-88	TR - 1988	**94**	TR 32167 - Yozgat	TR - NA
33	Şahinbey	TR - 2008	**95**	TR 35150 - Yozgat	TR - NA
34	Zühre	TR - 2011	**96**	TR 31887 - Elâzığ	TR - NA
35	Gündaş	TR - 2012	**97**	TR 31902 - Malatya	TR - NA
36	Akçakale-2000	TR - 2002	**98**	TR 31893 - Malatya	TR - NA
37	Gökgöl-79	TR - 1979	**99**	TR 35148 - Yozgat	TR - NA
38	Amanos 97	TR - 1997	**100**	TR 81277 - Ankara	TR - NA
39	Kızıltan-91	TR - 1991	**101**	TR 81283 - Ankara	TR - NA
40	Özberk	TR - 2005	**102**	TR 81284 - Ankara	TR - NA

41	Urfa-2005	TR - 2005	**103**	TR 81367 - Konya	TR - NA
42	Ceylan-95	TR - 1995	**104**	TR 81374 - Konya	TR - NA
43	Salihli-92	TR - 1992	**105**	TR 81258 - Malatya	TR - NA
44	Gap	TR - 2004	**106**	TR 81278 - Ankara	TR - NA
45	Soylu	TR - 2012	**107**	TR 81323 - Ankara	TR - NA
46	Ali baba	TR - 2010	**108**	TR 81369 - Niğde	TR - NA
47	Tunca-79	TR - 1979	**109**	TR 81550 - Niğde	TR - NA
48	Şarıbaşak	TR - 1970	**110**	TR 81544 - Niğde	TR - NA
49	Vatan	TJ - 1978	**111**	Bağacak	TR - NA
50	Zenit	IT - 1992	**112**	Menceki	TR - NA
51	Saragolıa	IT - 2004	**113**	Mersiniye	TR - NA
52	Svevo	IT - 1996	**114**	Sivaslan	TR - NA
53	Clavdio	IT - 2011	**115**	Şırnak Alkaya	TR - NA
54	Baio	IT - 1998	**116**	Kurtulan	TR - NA
55	UI- Darwin	USA - 2006	**117**	Karadere	TR - NA
56	UC1113	USA - 2005	**118**	Hacıhalil	TR - NA
57	AC-Pathfinder	CA - 1999	**119**	Hevidi	TR - NA
58	AC-Nevigator	CA - 1999	**120**	Beyaziye	TR - NA
59	Floradur	AU - 2003	**121**	Mısrı	TR - NA
60	C9	IL - NA	**122**	İskenderiye	TR - NA
61	C43	IL - NA	**123**	Havrani	TR - 1970
62	Inbar	IL - 1978			

TR, Türkiye; TJ, Tajikistan; USA, United States of America; CA, Canada; AU, Austria; IL, Israel; IT, Italy; SY, Syria; NA, not available.

B. Leaf Scans

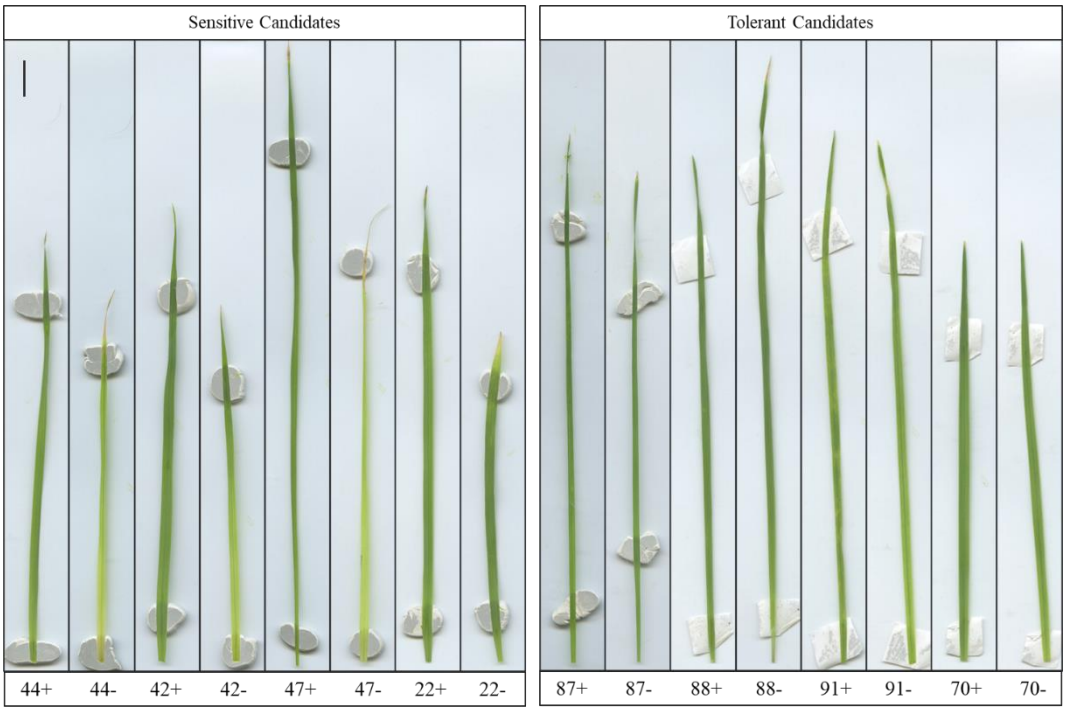

Leaf scans of the candidate sensitive and tolerant genotypes. The numbers correspond to the genotype numbers in Appendix A and Table 3.6, whereas '+' and '-' refer to control and Fe deficient conditions, respectively. The scale bar corresponds to 1 centimeter.

C. Root Scans

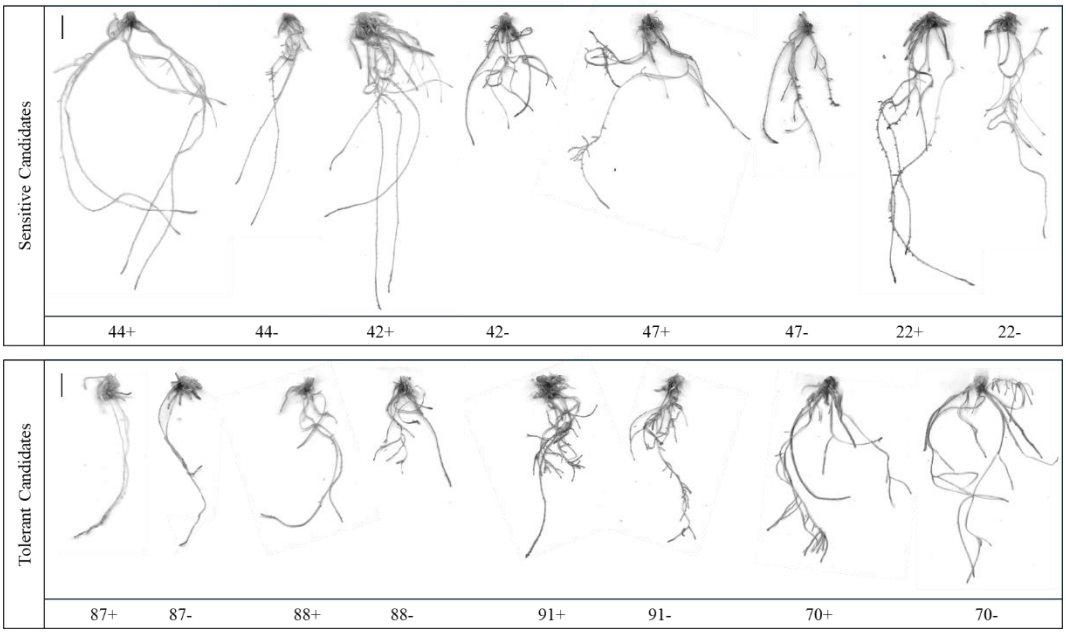

Root scans of the candidate sensitive and tolerant genotypes in the upper and lower sections, respectively. The numbers correspond to the genotype numbers in Appendix A and Table 3.6, whereas '+' and '-' refer to control and Fe deficient conditions, respectively. The scale bar corresponds to 1 centimeter.

D. Normality Test and Distribution Graphs

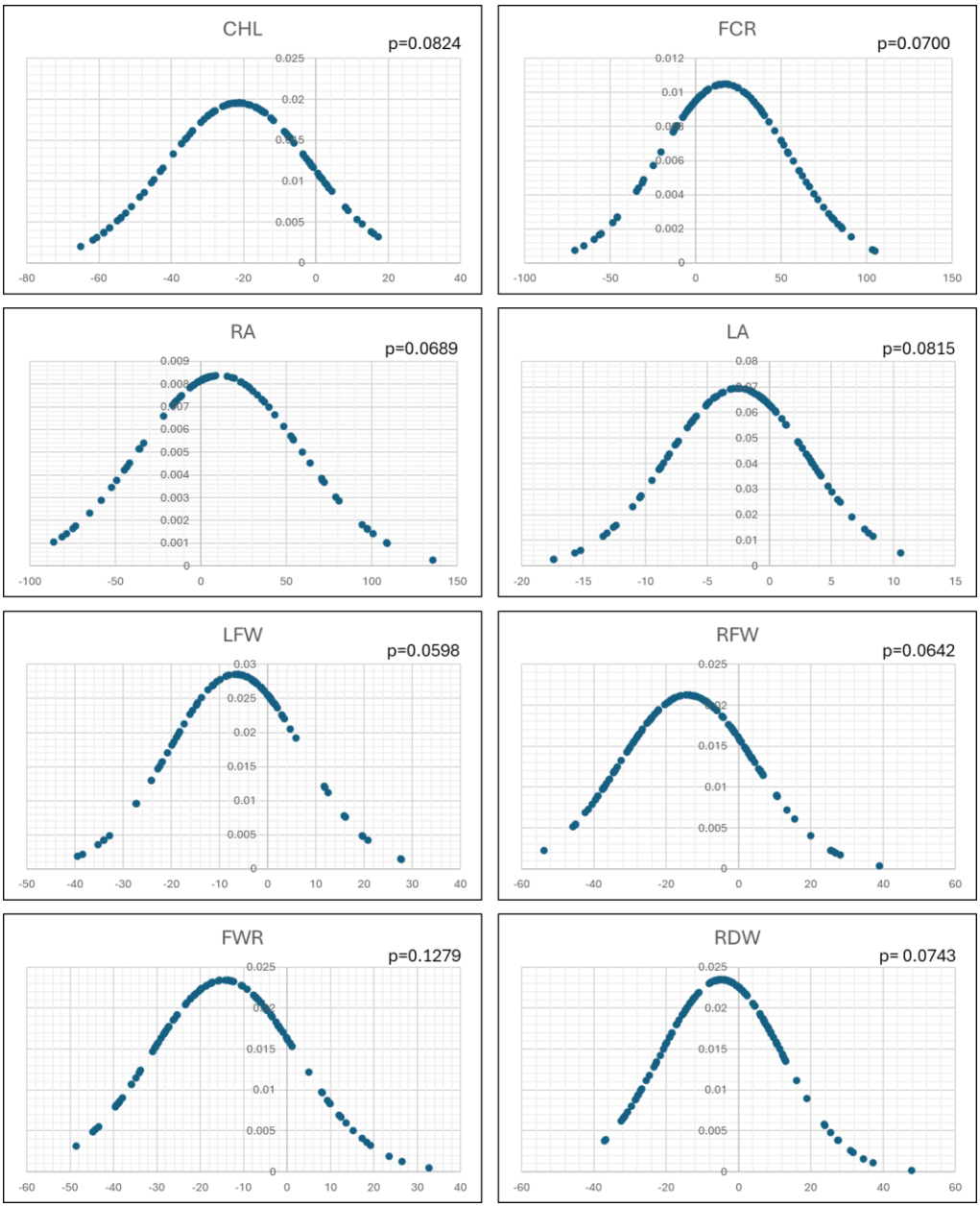

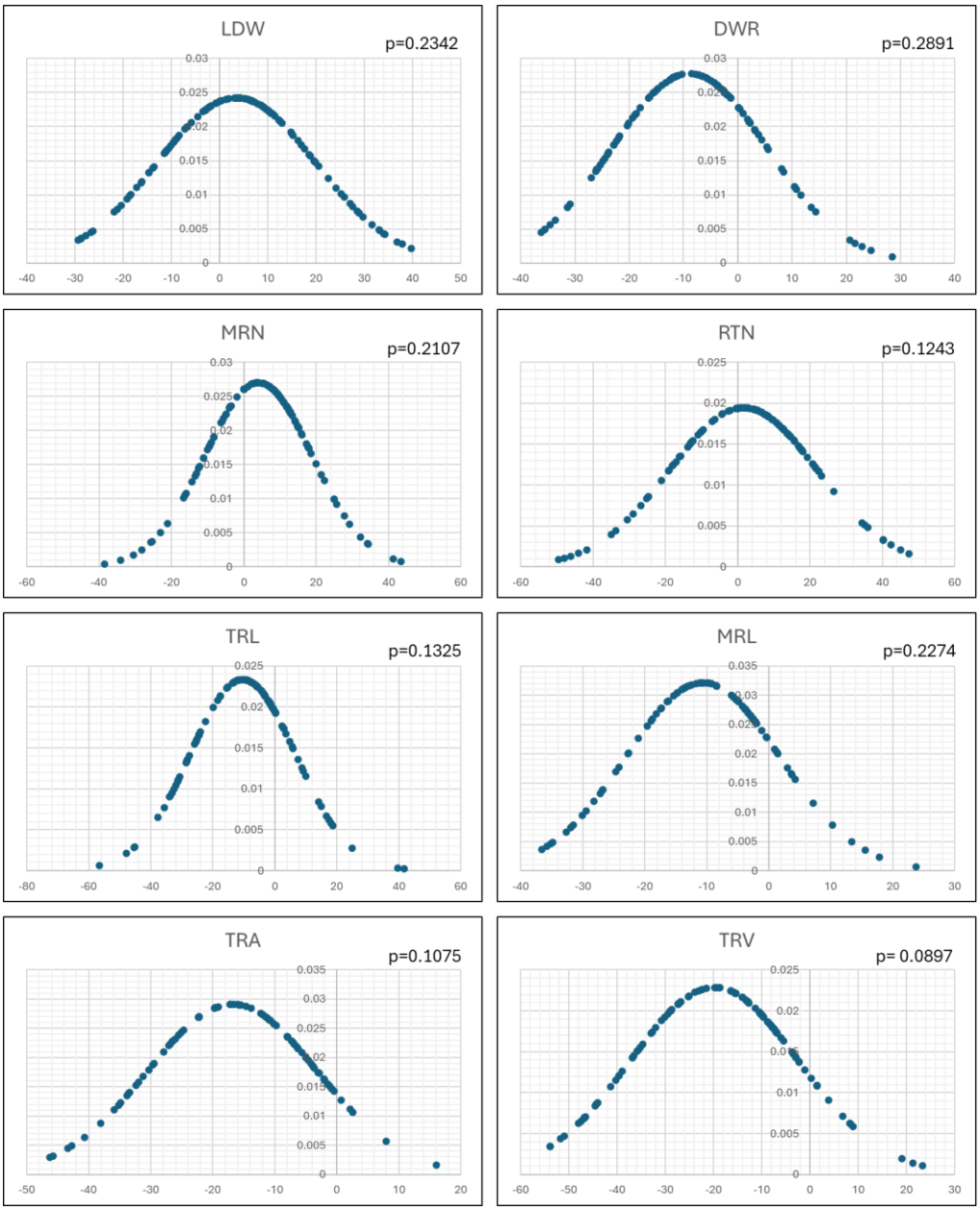

The distribution graphs of the relative changes of investigated traits. The p-value results of Shapiro-Wilk normality tests are indicated in the top right corner of each graph. CHL, total chlorophyll concentration; FCR, ferric chelate reductase enzyme activity; RA, rhizosphere acidification; LA, leaf area; LFW, second leaf fresh weight; RFW, root fresh weight; FWR, root fresh weight/second leaf fresh weight ratio; RDW, root dry weight; LDW, second leaf dry weight; DWR, root dry weight/second leaf dry weight ratio; MRN, maximum root number; RTN, root tip number; TRL, total root length; MRL, maximum root length; TRA, total root area; TRV, total root volume